AFCRL-71-0571

ANALYSES AND TESTS OF MYLAR FALLING SPHERES

by

Frederick F. Fischbach, Harold F. Allen, Fred L. Bartman

The University of Michigan
High Altitude Engineering Laboratory
Ann Arbor, Michigan 48105

Contract No. F19628-70-C-0245

Project No. 6682
Task No. 668202
Work Unit No. 66820201

FINAL REPORT

Period Covered: 15 April 1970 - 15 December 1971

Date of Report: 15 December 1971

Contract Monitor: John B. Wright
Meteorology Laboratory

Prepared for

AIR FORCE CAMBRIDGE RESEARCH LABORATORIES
AIR FORCE SYSTEMS COMMAND
UNITED STATES AIR FORCE
BEDFORD, MASSACHUSETTS 01730

Unclassified

Security Classification

DOCUMENT CONTROL DATA - R & D

(Security classification of title, body of abstract and indexing annotation must be entered when the overall report is classified)

1. ORIGINATING ACTIVITY *(Corporate author)*

University of Michigan
High Altitude Engineering Laboratory
Ann Arbor, Michigan 48105

2a. REPORT SECURITY CLASSIFICATION

unclassified

2b. GROUP

3. REPORT TITLE

ANALYSES AND TESTS OF MYLAR FALLING SPHERES

4. DESCRIPTIVE NOTES *(Type of report and inclusive dates)*

Scientific - Final 15 April 1970 - 15 December 1971

Approved
25 April 1972

5. AUTHOR(S) *(First name, middle initial, last name)*

Frederick F. Fischbach
Harold F. Allen
Fred L. Bartman

6. REPORT DATE	7a. TOTAL NO. OF PAGES	7b. NO. OF REFS
15 December 1971	167	174

8a. CONTRACT OR GRANT NO.	9a. ORIGINATOR'S REPORT NUMBER(S)
F 19628-70-C-0245	036140-1-F
b. PROJECT NO. Task, Work Unit Nos. 6682-02-01	
c. DoD Element 65710F	9b. OTHER REPORT NO(S) *(Any other numbers that may be assigned this report)*
d. DoD Subelement 676682	AFCRL-71-0571

10. DISTRIBUTION STATEMENT

A - Approved for public release; distribution unlimited.

11. SUPPLEMENTARY NOTES	12. SPONSORING MILITARY ACTIVITY
TECH, OTHER	Air Force Cambridge Research Laboratories (LY) L. G. Hanscom Field Bedford, Massachusetts 01730

13. ABSTRACT

The analysis and tests of mylar falling spheres described herein contain results on several theoretical and experimental factors related to the success of the falling sphere program. A careful study of the literature and experimental methods used to obtain sphere drag coefficients has led to recommended tables of sphere drag coefficients. Studies of flight experience and theoretical studies of initial sphere temperatures, isopentane evaporation, radiation effects, convective heat transfer to the atmosphere, heat transfer within the sphere and chemical reaction on the sphere surface provide information which may possibly be used in future work to compute a realistic reliable temperature-time history of falling spheres. The results of the "radiation effects" calculation suggests that an aluminized sphere has great radiant energy absorption characteristics in daytime for evaporation of the isopentane used for inflation. There is no evidence to indicate that sphere failures are due to insufficient heat for evaporation, however. The results of the Viper-Dart sphere test program suggest that thermal problems during the rocket ascent or during sphere ejection and inflation may be the principal cause of flight failures of falling spheres. Remedies are suggested. Component improvement recommendations are made for existing and future Viper-Dart-Robin payloads. Recommendations are made for improvement of the 1970 data analysis program.

DD FORM 1 NOV 65 1473

unclassified

Security Classification

14. KEY WORDS	LINK A		LINK B		LINK C	
	ROLE	WT	ROLE	WT	ROLE	WT
Passive Sphere						
Density						
Wind						
Aerodynamic Heating						
Radiative Equilibrium Temperature						
Isopentane						
Temperature						
Pressure						
Data Analysis						

Unclassified

Security Classification

DOCUMENT CONTROL DATA - R & D

(Security classification of title, body of abstract and indexing annotation must be entered when the overall report is classified)

1. ORIGINATING ACTIVITY *(Corporate author)*

University of Michigan
High Altitude Engineering Laboratory
Ann Arbor, Michigan 48105

2a. REPORT SECURITY CLASSIFICATION

unclassified

2b. GROUP

3. REPORT TITLE

ANALYSES AND TESTS OF MYLAR FALLING SPHERES

4. DESCRIPTIVE NOTES *(Type of report and inclusive dates)*

Scientific - Final 15 April 1970 - 15 December 1971

Approved
25 April 1972

5. AUTHOR(S) *(First name, middle initial, last name)*

Frederick F. Fischbach
Harold F. Allen
Fred L. Bartman

6. REPORT DATE	7a. TOTAL NO. OF PAGES	7b. NO. OF REFS
15 December 1971	167	174

8a. CONTRACT OR GRANT NO.	9a. ORIGINATOR'S REPORT NUMBER(S)
F 19628-70-C-0245	036140-1-F
b. PROJECT NO. Task, Work Unit Nos. 6682-02-01	
c. DoD Element 65710F	9b. OTHER REPORT NO(S) *(Any other numbers that may be assigned this report)*
d. DoD Subelement 676682	AFCRL-71-0571

10. DISTRIBUTION STATEMENT

A - Approved for public release; distribution unlimited.

11. SUPPLEMENTARY NOTES	12. SPONSORING MILITARY ACTIVITY
TECH, OTHER	Air Force Cambridge Research Laboratories (LY) L. G. Hanscom Field Bedford, Massachusetts 01730

13. ABSTRACT

The analysis and tests of mylar falling spheres described herein contain results on several theoretical and experimental factors related to the success of the falling sphere program. A careful study of the literature and experimental methods used to obtain sphere drag coefficients has led to recommended tables of sphere drag coefficients. Studies of flight experience and theoretical studies of initial sphere temperatures, isopentane evaporation, radiation effects, convective heat transfer to the atmosphere, heat transfer within the sphere and chemical reaction on the sphere surface provide information which may possibly be used in future work to compute a realistic reliable temperature-time history of falling spheres. The results of the "radiation effects" calculation suggests that an aluminized sphere has great radiant energy absorption characteristics in daytime for evaporation of the isopentane used for inflation. There is no evidence to indicate that sphere failures are due to insufficient heat for evaporation, however. The results of the Viper-Dart sphere test program suggest that thermal problems during the rocket ascent or during sphere ejection and inflation may be the principal cause of flight failures of falling spheres. Remedies are suggested. Component improvement recommendations are made for existing and future Viper-Dart-Robin payloads. Recommendations are made for improvement of the 1970 data analysis program.

DD FORM 1 NOV 65 1473

unclassified

Security Classification

14. KEY WORDS	LINK A		LINK B		LINK C	
	ROLE	WT	ROLE	WT	ROLE	WT
Passive Sphere						
Density						
Wind						
Aerodynamic Heating						
Radiative Equilibrium Temperature						
Isopentane						
Temperature						
Pressure						
Data Analysis						

AFCRL-71-0571

ANALYSES AND TESTS OF MYLAR FALLING SPHERES

by

Frederick F. Fischbach, Harold F. Allen, Fred L. Bartman

University of Michigan
High Altitude Engineering Laboratory
Ann Arbor, Michigan 48105

Contract No. F19628-70-C-0245
Project No. 6682
Task No. 668202
Work Unit No. 66820201

FINAL REPORT

Period Covered: 15 April 1970 - 15 December 1971

Date of Report: 15 December 1971

Contract Monitor: John B. Wright
Meteorology Laboratory

Prepared for

AIR FORCE CAMBRIDGE RESEARCH LATORATORIES
AIR FORCE SYSTEMS COMMAND
UNITED STATES AIR FORCE
BEDFORD, MASSACHUSETTS 01730

PREFACE

This report on the "Analysis and Tests of Mylar Falling Spheres" was primarily the work of F. F. Fischbach. Dr. H. F. Allen assisted Mr. Fischbach with the "Viper-Dart Sphere Test Program. F. L. Bartman assisted in the calculations and writing of some parts of the section "Thermal Studies of Falling Spheres" and edited the report in Mr. Fischbach's absence.

ABSTRACT

The analysis and tests of mylar falling spheres described herein contain results on several theoretical and experimental factors related to the success of the falling sphere program. A careful study of the literature and experimental methods used to obtain sphere drag coefficients has led to recommended tables of sphere drag coefficients. Studies of flight experience and theoretical studies of initial sphere temperatures, isopentane evaporation, radiation effects, convective heat transfer to the atmosphere, heat transfer within the sphere and chemical reaction on the sphere surface provide information which may possibly be used in future work to compute a realistic reliable temperature-time history of falling spheres. The results of the "radiation effects" calculation suggests that an aluminized sphere has greater radiant energy absorption characteristics in daytime for evaporation of the isopentane used for inflation. There is no evidence to indicate that sphere failures are due to insufficient heat for evaporation, however. The results of the Viper-Dart sphere test program suggest that thermal problems during the rocket ascent or during sphere ejection and inflation may be the principal cause of flight failures of falling spheres. Remedies are suggested. Component improvement recommendations are made for existing and future Viper-Dart-Robin payloads. Recommendations are made for improvement of the 1970 data analysis program.

TABLE OF CONTENTS

List of Tables

List of Figures

Symbols

A = area, cm^2

C = orifice coefficient

C_f = orifice discharge coefficient (empirically determined)

$C_{f\infty}$ = local friction coefficient

C_p, C_v = specific heats at constant pressure and constant volume, respectively

$C_{H\infty}$ = the Stanton number

d = sphere diameter, cm or meters

da_1 = an element of area on the earth's surface

da_2 = an element of area on the mylar sphere

$dq_\lambda(1-2)$ = the rate of energy transfer from an element of area da_1 on earth to an element of area da_2 on the mylar sphere

e = strain of mylar

E = Young's Modulus of mylar, $550 \cdot 10^3$ psi

f = frequency of points

F = shredding frequency, cps.

g = acceleration of gravity, $cm. sec.^{-2}$

G_r = Grashof number

H = altitude of mylar sphere above the earth's surface

$H_{E\lambda}$ = flux of radiation leaving the earth, $watts \cdot cm^2 \cdot \mu m^{-1}$

$H_{S\lambda}$ = the spectral solar irradiance, $watts \cdot cm^{-2} \cdot \mu m^{-1}$

$H_{T\lambda}$ = flux of thermal radiation emitted by the earth, $watts \cdot cm^{-2} \cdot \mu m^{-1}$

h = heat transfer coefficient

h = parameter used to define portion of area of falling sphere which is contiguous to the boundary layer

$I_{E\lambda}$ = the spectral intensity of radiation leaving the earth, $watts \cdot cm^{-2} \cdot ster^{-1} \cdot \mu m^{-1}$

$I_{T\lambda}$ = the spectral intensity of thermal radiation leaving the earth, watts $cm^{-2} \cdot ster^{-1} \cdot \mu m^{-1}$

K = absorption coefficient

k = the thermal conductivity of a fluid

$\dot{m}$ = mass flow rate, gr. sec^{-1}

M = Mach number

M = number of points

n = number density, cm^{-3}.

N = number of points

N_u = Nusselt number = nx/k

P = pressure, mb.

Pr = the Prandtl number

q, Q = the rate of heat flow

q_w = the rate of heat flow at the wall

q_λ = rate of transfer radiant energy at wavelength λ

R = Reynolds number (also Re)

R = radius of mylar sphere, cm.

R = gas constant for a perfect gas, ergs. $^oK^{-1} \cdot mol.^{-1}$

r_{1-2} = distance from earth to mylar sphere

R_1 = radius of the earth

S = hoop stress

Sr = Strouhal number (Fd/V_∞)

t = time, sec.

T = temperature, ^oK

$\bar{T}$ = mean temperature (time average) for a brief period

T_g = initial isopentane temperature

T_r = recovery temperature

T_s = initial mylar temperature

T_w = mean wall temperature

$T_{w_{ins}}$ = mean insulated wall temperature

T_∞ = free stream (local) temperature

V = volume, cm^3

v = velocity

$\bar{v}$ = mean velocity (time average) for a brief period

v_∞ = free stream velocity

$W_{\lambda(T)}$ = The radiant emittance of the mylar material at mean temperature T.

x = coordinate along surface in direction of free stream

X = dimensionless time ratio

Y = "unaccomplished" temperature change

z = coefficient in viscosity power law

Z = altitude

$\alpha_\lambda, \epsilon_\lambda, r_\lambda, \tau_\lambda$ = spectral absorptivity, emissivity, reflectivity and transmissivity, respectively

α, β = integration constants

β = the solid angle of the earth as viewed from the sphere, steradians

$\gamma = \frac{C_p}{C_v}$ = ratio of specific heats

δ = thickness of layer of liquid isopentane, cm.

ΔT = temperature increment, ^oK

θ_1 = zenith angle of a ray at the earth

θ_2 = zenith angle of a ray at the mylar sphere

λ = wavelength, μm.

μ = the viscosity of a fluid

ρ = density, gr cm^{-3}

ρ_λ = bi-directional reflectance of earth's surface

ρ_∞ = free stream mass density

σ = variance

τ = mylar thickness

τ_X = transmissivity of mylar of thickness X

τ_w = the shear stress

INTRODUCTION

The passive inflatable falling-sphere technique has been one of the most reliable, economical and accurate methods of measurement of upper atmosphere structure. In this experiment a sphere made of very light material, inflated after ejection from a small inexpensive rocket, is passively tracked by radar to determine drag acceleration and thus the atmospheric structure parameters density temperature, pressure and wind.

Present designs have been frequently subject to a type of failure in which the sphere has collapsed before reaching the design deflation altitude.

The purpose of the present investigation has been to consider and analyze the sum total of accumulated flight experience, ground testing and physical theory applicable to the falling-sphere technique in order to possibly obtain an explanation for these failures.

In addition a complete review and evaluation of sphere drag coefficient data available up to but not including ballistic range data obtained at the Arnold Engineering Development Center in 1970 has been carried out.

This report on the results of the study is presented in two parts plus three Appendices. Conclusions and recommendations are presented at the end of each part or appendix.

The survey of sphere drag coefficient data is presented in Part I. The scope of the investigation and method of data available are described. Recommended drag coefficient data are given in tables at the end of this part of the report. Comparisons with other sets of drag coefficient data previously used with the falling-sphere experiment are made on pages 4 and 5.

The "Inflation Analysis of Mylar Falling Spheres" is contained in Part II. In separate sections an introduction is provided, and flight experience, ground test experience, thermal studies, the suitability of isopentane as inflatant and a sphere leak analysis are considered. A summary of the logical analysis, results and conclusions are contained in the last section of this part on pages 113 to 117.

Appendix A contains a complete description of ground tests and altitude-chamber tests of the Viper-Dart Sphere test program carried out as a part of this study. The conclusions obtained as a result of this test program are given on pages 142 to 144.

In appendix B recommendations for balloon system component improvements are made for Viper-Dart-Robin payloads now in inventory, for future procurements and for a new design.

An appraisal of the 1970 program for Robin sphere data processing is given in Appendix C. Results and conclusions of this study are given on pages 157 to 167.

PART 1 - A PRELIMINARY SURVEY OF THE DRAG COEFFICIENT OF SPHERES AS APPLICABLE TO THE FALLING-SPHERE TECHNIQUE FOR ATMOSPHERIC DENSITY

(F. F. Fischbach)

I. Introduction

The drag coefficient of a falling sphere has been investigated for the purpose of determining the applicability of the many experimental data to the Viper-Dart-Robin technique.

The bulk of the historical data is confined to the incompressible flow region. These data are important because a considerable portion of the falling-sphere trajectory lies in the region of low Mach number.

For the portions of a typical flight which have transonic and supersonic velocities the drag coefficient is determined from a comparatively small number of experimental results. Fortunately, the experimental results have been relatively consistent.

This study has been largely an attempt to assess all results to date, and to evaluate the merits of different experimental methods in terms of their applicability to the inflated mylar sphere technique.

II. Scope of Investigation

The incompressible flow regime suffers no shortage of experimental results. The drag coefficient of a sphere in low-speed flow was one of the classic investigations of aerodynamic theory and occupied the attention of such investigators as Sir Isaac Newton, Lord Kelvin, Prof. G. Eiffel, and Prof. Prandtl. As such, one might assume the investigations to have been fully definitive in the sense of determining a unique drag coefficient function. Such was not the case. Experimental errors obscured the free flight drag function and as of today they are not completely resolved.

The original efforts between 1900 and 1932 were based entirely on wind tunneling or from free drops from towers, airplanes, or in water (or other liquid). Recent measurements made in ballistic ranges have overcome many inherent difficulties of the earlier techniques. The present results include some but not all of the current ballistic range measurements.

The compressible flow regime between low Mach numbers and Mach 1 is covered by adequate measurements. At Mach 1 measurements are almost entirely lacking. At speeds above Mach 1 and below Mach 2.5 more measurements are required. Above Mach 2.5 very little Mach dependence is seen.

The present investigation has developed an interim drag coefficient recommendation based upon all measurements from 1900 through 1969. In the low-speed regime the ninety-six references listed below furnish the basis for the table. For the high-speed regime the table is based upon fourteen references, also listed below.

A large number of experimental results have been obtained by a variety of methods, by many investigators, over a period exceeding 250 years for the drag coefficient of falling spheres. It has not been possible to find an objective method for synthesizing this data. Considerable subjectivity is required in the preparation of a single empirical function to describe the drag coefficient data. We will describe the method of attack utilized by the investigators:

1. Considerable effort was put forth to obtain an absolutely complete set of original references cited in the world's scientific literature. Specifically avoided was the utilization of data ascribed by one author to a prior

author. All papers and reports were examined in their original form with the exception of Russian and German papers translated and published by the U. S. N. A. C. A. Even in these cases the datum points themselves (not the accompanying descriptions) were checked in detail.

The present investigators failed to obtain the following original papers:

Costanzi 6, 7

Loukianot 45

Data ascribed to these three references by Prandtl, Wieselsberger, and Riabovchinsky have been utilized but viewed with considerable reservation.

2. All investigators' data were placed in comparable parametric context. This involved recomputing the Reynolds' Number in many cases, where the original papers used a different parameter (usually associated with a different basis of characteristic length).

3. Those data found to be in error due to experimental problems completely and satisfactorily explained by subsequent investigations were given almost no weight.

4. Summaries, surveys, and reviews were found often to contain plotting errors, translation errors, and parametric errors. Even more disturbing was the usual perpetuation of such errors from one review to another, even by otherwise very careful investigators. Accordingly such summaries were accorded little weight. This was the raison d'etre for examination of only original documents.

5. Being thus left with a lesser number of fully credited datum points, these points were weighted according to a subjective formula appraising these particulars:

a) Consistency between investigators using different methods

b) Consistency (internal) between investigations by same method

c) Applicability of experimental method to free-falling spheres

d) Consistency with other investigations at slight overlap or slight extrapolation of Reynolds Number

e) Internal random error as evidenced by standard deviations reported

Attacking the problem in this manner, the most decisive investigations for our purposes were those of Allen, Lunnon, Shakespear, Riabovchinsky Goin & Lawrence, Flachsbart, Wieselsberger, Aroesty and Ashkenas. However, in no way was consideration limited only to those data.

The recommended drag coefficients given here take into account all evidence available at the beginning of the contract period. These exclude the bulk of the ballistic range data gathered by AEDC in 1970.

These recommended coefficients are generally within 2% of values used by University of Michigan programs subsequent to 1968. They are generally with 4% of values used by University of Michigan investigators in 1967 and current ROBIN programs. They are generally within 1 to 2% of values published in 1970 by AEDC. They are in serious disagreement, (from 5% to 10%) at speeds of Mach 9 and above, near Mach 1 and also at low Reynolds Numbers, with values used by the ROBIN program of 1965 and the University of Michigan investigations of 1965 and 1966. These latter two programs used drag coefficients based on the Heinrich experiments 21, 22 now believed to have suffered from considerable experimental error, particularly in trends regarding variation with Mach Number only and Reynolds number

only. Accordingly, temperatures in the rapid deceleration regions and at low altitudes were more detrimentally affected than density alone.

The meeting of falling sphere investigators at NASA Langley Research Center in September 1970 resulted in the adoption of AEDC ballistic range data by the presently experimenting scientific community. Australia was not represented but is expected to join the agreement.

The present investigators note that while exhibiting excellent internal consistency, small standard deviations, and great Mach Number resolution near Mach 1, no proof of the absence of systematic error in the AEDC data is possible. In this regard, comparison to other methods, notably Allen and Flachsbart - Wieselsberger at low Mach Numbers, and Aeroesty & Ashkenas at High Mach Numbers, indicate that important systematic errors are improbable. The Allen work, done 70 years prior, nevertheless suggests that in free flight in the upper atmosphere drag coefficients could be generally lower by about 1%. A repetition of Allen's method would be most interesting and certainly not expensive.

III. Interim Drag Coefficient Value Recommendations - Supersonic

Reynolds Number	Mach Number							
	1.0	1.2	1.4	1.6	1.8	2.0	2.5	3.0
200	1.150	1.193	1.232	1.264	1.290	1.310	1.340	
300	1.083	1.133	1.172	1.204	1.230	1.250	1.280	
500	1.017	1.067	1.106	1.138	1.164	1.184	1.214	
700	.956	1.031	1.070	1.102	1.128	1.148	1.178	
900	.906	1.006	1.045	1.077	1.103	1.123	1.153	
1,000	.899	.996	1.035	1.067	1.093	1.113	1.143	
1,500	.872	.960	.999	1.031	1.057	1.077	1.107	
2,000	.853	.933	.972	1.004	1.030	1.050	1.080	
3,000	.827	.903	.942	.974	1.000	1.020	1.050	
4,000	.817	.883	.922	.954	.980	1.000	1.030	
5,000	.806	.870	.909	.941	.967	.987	1.017	
6,000	.800	.859	.898	.930	.956	.976	1.006	
7,000	.794	.852	.891	.923	.949	.969	.999	
8,000	.790	.843	.882	.914	.940	.960	.990	
9,000	.780	.838	.877	.909	.935	.955	.985	
10,000	.774	.833	.872	.904	.930	.950	.980	
15,000	.774	.833	.870	.889	.915	.935	.965	
20,000	.778	.835	.871	.890	.913	.920	.950	
30,000	.782	.837	.873	.891	.911	.920	.950	
40,000	.786	.839	.876	.891	.910	.920	.950	
50,000	.794	.842	.880	.891	.910	.920	.950	

IV. Interim Drag Coefficient Value Recommendations - Subsonic

Reynolds	Mach Number									
Number	0	.20	.33	.46	.60	.75	.79	.84	.89	.93	.98
200	.680										1.144
300	.590										1.077
500	.510										1.011
700	.490										.950
900	.460	.480	.485	.507	.545	.606	.624	.662	.725	.785	.900
1,000	.444	.460	.473	.494	.532	.593	.610	.649	.710	.790	.893
1,500	.412	.422	.436	.454	.491	.546	.565	.599	.658	.730	.866
2,000	.392	.400	.417	.435	.469	.523	.543	.579	.642	.716	.848
3,000	.374	.380	.400	.418	.449	.502	.522	.560	.624	.696	.822
4,000	.370	.374	.393	.413	.441	.493	.513	.552	.616	.688	.812
5,000	.367	.373	.393	.412	.440	.492	.512	.550	.615	.687	.802
6,000	.364	.373	.394	.415	.440	.492	.512	.550	.614	.684	.796
7,000	.367	.378	.398	.419	.443	.494	.513	.551	.613	.681	.790
8,000	.370	.381	.402	.425	.446	.497	.516	.553	.612	.676	.784
9,000	.376	.387	.408	.432	.451	.500	.518	.554	.611	.671	.776
10,000	.382	.395	.412	.437	.457	.503	.520	.555	.610	.666	.770
15,000	.390	.405	.425	.448	.464	.515	.527	.569	.612	.666	.770
20,000	.398	.413	.433	.454	.474	.519	.539	.579	.614	.669	.774
30,000	.406	.419	.438	.460	.484	.524	.548	.585	.618	.672	.778
40,000	.418	.434	.458	.476	.500	.529	.567	.597	.631	.688	.782
50,000	.430	.448	.472	.491	.516	.533	.588	.609	.648	.708	.790

V. Sphere Drag Coefficient References Low Speed Regime

1. Allen, H. S. The motion of a sphere in a viscous fluid. Phil. Mag. (5) 50, 323 and 519, 1900.

2. Arnold, H. D. Limitations imposed by slip and inertia terms upon Stokes[1] law for the motion of spheres through liquids. Phil. Mag. (6) 22, 755, 1911.

3. Bacon, D. L. and E. G. Reid The resistance of spheres in windtunnels and in air. NACA Rpt. No. 185, 1924.

4. Castleman, R. A. The resistance to the steady motion of small spheres in fluids. NACA TN 231, 1926.

5. Cook, Gilbert An experimental determination of the inertia of a sphere moving in a fluid. Phil Mag (6) 39, 350, 1920.

6. Costanzi, G. Alcune esperienze di idrodinamica, Rendiconti delle esperiennze e studi nello stab. di esp. e costr. aeronautiche del genio, II Jahrg. Nr. 4, 169, Rome, Oct. 1912.
   Perhaps:
   Italy, Ministerio dell aeronautico, Rendiconti tecnici

7. Costanzi, G. Rassegna aero-Marittima, Apr. 1914.

8. Cowley, W. L. and H. Levy On the effect of accelerations on the resistance of a body. Gt. Britain A. C. A. R & M. 612, 1918.

9. Dryden, H. L. and A. M. Kuethe Effect of turbulence in wind tunnel measurements. NACA TR 342, 1929.

10. Dryden, H. L. et al Measurements of the intensity and scale of wind tunnel turbulence and their relation to the critical Reynolds numbers of spheres. NACA TR 581, 1937.

11. Eiffel, G. La resistance de l'air et l'aviation, Paris, 1910. Eng. Trans. by Jerome C. Hunsaker, Houghton-Mifflin, Boston & New York, 1913.

12. Eiffel, G. Sur la resistance des spheres dans l'air en movement. Comptes Rendus, 155, Nr. 27, 1597, 1912.

13. Eiffel, G. Nouvelles recherches sur la resistance de l'air. Paris Librairie Aeronautique, 1914.

14. Faxen, H. Der Widerstand gegen die Bewegung einer starren Kugel in einer zähen Flüssigkeit, die swischen swei parallen ebenen Wänden iengeschlossen ist. Annalen der Physik, 68, 89, 1922.

15. Fage, A. Experiments on a sphere at critical Reynolds numbers. Gt. Britain A. R. C. R & M 1766, 1936.

16. Flachsbart, O. Neue Untersuchungen uber den Luftwiderstand von Kugeln. Phys. Z. S., 28, 461, 1927. (Trans. N. A. C. A. TM 475, 1928)

17. Flachsbart, O. Der Widerstand von Kugeln in der Ungebung der Kritischen Reynoldschen Zahl, Ergebnisse der Aero V. A. zu Gottingen. IV Lieferung. Ed. by Prandtl & Betz, Oldenbourg, Munchen and Berlin, 1932.

18. Föppl, O. Ergebnisse der Aerodynamischen Versuchsanstalt von Eiffel, verlichen mit den Gottingen Resultaten. ZS fur Flugtechnik und Motorluftschiffahrt, 3, 118, 1912.

19. Goin, K. L. & W. R. Lawrence Subsonic drag of spheres at Reynolds numbers from 200 to 10, 000. AIAA J. , 6, 961, 1968.

20. Goldstein, S. Modern developments in fluid dynamics. 1st Ed., Vol. II, 491, Oxford Univ. Press, London, 1938.

21. Heinrich, H. G., E. L. Haak, & R. J. Niccum Drag coefficient of a sphere corresponding to a "one meter Robin sphere" descending from 260, 000 ft altitude (Reynolds Nos. 789 to 23, 448, Mach Nos. 0. 056 to 0. 90) Univ. of Minn. Report Contract AF 19(604)-8-34, May 1963.

22. Heinrich, H. G., et al. Modification of the Robin meteorological balloon. Vol. II. Drag evaluations. Air Force Off. of Aerospace Res. Rpt. AFCRL-65-734(II), 30 Sep. 1965.

23. Heinrich, H. G. and R. A. Noreen An assessment of sphere drag coefficient data. Pp 93-110 in NASA SP-219, 1969.

24. Hesselburg, T. & B. J. Birkeland Steigegeschwindigkeit der Pilotballone, Physik der Freich Atmosphäre IV Band, 196, 1912.

25. Hirsch, Paul Über die Bewegung der Kugeln in ruhenden Flussigkeiten, ZS für angewandte Mathematik und Mechanik, 3, 93, 1923.

26. Hoerner, S. Tests of spheres with reference to Reynolds number, turbulence, and surface roughness. NASA TM 777, 1935. (From Luftfahrtforschung, XII, No. 1, 1935.)

27. Hoerner, S. Fluid-dynamic drag. Pub. by author. 1958.

28. Homann, F. The effect of high viscosity on the flow around a cylinder and around a sphere. NACA TM 1334, 1952. (Trans. of "Der Einfluss grosser Zahigkeit bei der Stronung um den Zylinder und um die Kugel." ZAMM, 16, No. 3, 1936.)

29. Ingebo, R. D. Drag coefficients for droplets and solid spheres in clouds accelerating in airstreams. NACA TN 3762, 1956.

30. Jacobs, E. N. Sphere drag tests in the variable density wind tunnel. NACA TN 312, 1929.

31. Jones, O. G. The viscosity of liquids. Phil. Mag. (5) 37, 451, 1894.

32. Kelvin, Lord On the stability of steady and of periodic fluid motion. Phil. Mag. (5) 23, 459 and 529, 1887.

33. Kelvin, Lord Stability of motion. Phil. Mag. (5), 24, 272, 1887.

34. Kelvin, Lord On the propagation of laminar motion through a turbulently moving inviseid liquid. Phil. Mag (5)., 24, 342, 1887.

35. Knibbs, G. H. On the steady flow of water in uniform pipes and channels J. Roy. Soc. New S. Wales, 31, 314, 1897.

36. Krey, H. Widerstand von Sandkornern und Kugeln bei der Bewegung in Wasser. Mitt. Vers.-Anst. Wasserbau Schiffbau, Berlin, 1921.

37. Kuethe, A. M. and J. D. Schetzer Foundations of aerodynamics. 290-291, Wiley, 1950.

38. Ladenburg, R. Über den Einfluss von Wänden auf die Bewegung einer Kugel in einer reibenden Flussigkeit. Ann der Physik, 23, 447, 1907.

39. Ladenburg, R. Über die innere Reibung zäher Flüssigkeiten und ihre Abhängigkeit vom Druck. Ann. der Physik, 22, 287, 1907.

40. Lamb, H. On the uniform motion of a sphere through a viscous fluid. Phil. Mag. (6), 21, 112, 1911.

41. Lemin, C. E. On the motion of a sphere through a viscous fluid. Phil. Mag. (7), 12, 589, 1931.

42. Liebster, H. Uber den Widerstand von Kugeln. Ann d Physik (4), 82, 541, 1927.

43. Liebster, H. & L. Schiller Kinematographische Messungen der Fallbewegung von Kugeln in zäher Flussigkeit, auch in nächster Nähe einer Wand. Phys. ZS, 25, 670, 1924.

44. Littlewood, J. E. Trajectories of small horizontal velocity in a resisting medium. Proc. Camb. Phil. Soc., 22, Part III, 217, 1924.

45. Loukianof L'Ecole Imperial Technique de Moscow, 1914.

46. Lunon, R. G. The resistance of the air to falling spheres. Phil. Mag. (6) 47, 173, 1924.

47. Lunnon, R. G. Fluid resistance to moving spheres. Roy. Soc. Proc. A, 110 302, 1926.

48. Lunnon, R. G. Fluid resistance to moving spheres Roy. Soc. Proc. A, 118, 680, 1928.

49. Lyon, H. M. Effect of turbulence on drag of airship models. Gt. Britain A. R. C. R & M 1511, 1933.

50. LeClair, B. P., A. E. Hamielec, & H. R. Pruppacher, A numerical study of the drag on a sphere at low and intermediate reynolds numbers. J. A. S., 27, 308, 1970.

51. Maurain, C. Action d'un courant d'air sur des spheres. Bull. de l'institut aerotechnique de l'Univ. Paris, 3, 76, 1913.

52. Millikan, C. B. & A. L. Klein The effect of turbulence. Aircraft Engineering, p 169, Aug. 1933.

53. Möller, Hydrodynamic experiments on the sphere. Physikalische ZS., 39 57, 1938.

54. Muttray, H. Der Widerstand von Kugeln, IV Kapitel, (Section) 13, pp. 291-307 of Wien-Harms Handbuch der Experimentalphysik, Band IV, Hydro-und Aero Dynamik, 2. Teil, Ed. by L. Schiller, Akademische Verlagsegesellschaft M. B. H., Leipzig, 1932.

55. Newton, Sir Isaac Principia, Book II, Sect. VII, Prop. XL, Excerpts 1-14, 1719.

56. Maxworthy, T. Accurate measurements of sphere drag at low Reynolds numbers. J. Fl. Mech. (Gt. Br.) 23, part 2, 369, 1965.

57. Manning, W. P. & W. H. Gauvin Heat and Mass Transfer to decelerating finely atomized sprays Amer. Inst. Chem Eng. J., 6, 184, 1960.

58. Pannell, J. R. Experiments on the resistance of spheres. Gt. Britain A. C. A. R & M. 190, 1916.

59. Platt, R. C. Turbulence factors of N. A. C. A. wind tunnels as determined by sphere tests. N. A. C. A. Rpt. 558, 1935.

60. Prandtl, L. Der Widerstand von Kugeln. Nachrichten d. Kgl. Gesellschaft der Wissenschaften zu Göttingen, Math. Phys. Klasse, 177, 1914.

61. Pasternak, I. S. & W. H. Gauvin Turbulent convective heat and mass transfer from accelerating particles. Amer. Inst. Chem Eng. J. 7, 254, 1961.

62. Rayleigh, Lord On the question of the satbility of the flow of fluids. Phil. Mag. (5), 34, 59, 1892.

63. Rayleigh, Lord On the flow of viscous fluids, Phil. Mag. (5), 36, , 1893.

64. Relf, E. F. & L. F. G. Simmons The frequency of the eddies generated by the motion of circular cylinders through a fluid. A. R. C. R & M 917, 1924.

65. Reynolds, O. An experimental investigation of the circumstances which determine whether the motion of water shall be direct or sinuous, and of the law of resistance in parallel channels. Phil. Trans. 174, Part 3, 935, 1883.

66. Riabouchinsky, D. P. On the resistance of spheres and ellipsoids in wind tunnels. Bull. de l'institut Aerodynamique de Koutchino, Fascicule V, 73, 1914 (N. A. C. A. TN 44).

67. Richardson, L. F. The aerodynamic resistance of spheres, shot upward to measure the wind. Phy. Soc. Lon. 36, 67, 1923.

68. Richardson, L. F. Theory of the measurement of wind by shooting spheres upward. Phil. Trans. 223, A, 351, 1923.

69. Sauerwein, R. T. Sphere drag determined by coasting through still air. J. Aero. Sci. 147, July 1934.

70. Schiller, L. Fallversuche mit Kugeln und Scheiben. Wien-Harms Handbuch der Experimental physik, Band IV, Hydro-und Aero-Dynamik, 2 Teil, 337-387.

71. Schiller, L. & H. Schmiedel Widerstandsmessungen an Kugel und Scheibe bei Kleinen Reynoldsschen Zahlen. ZS. F. M., 19, 497, 1928.

72. Schlicting, H. Boundary Layer Theory, Translated by J. Kestin, 4th Ed. McGraw Hill, 1960.

73. Schmidt, F. S. Zur beschleunigten Bewegung kugelformiger Korper in widersthenden Mitteln. Leipziger Dissertation, 1919. Auch. Ann. d. Phy (4), 61, 633, 1920.

74. Schmiedel, J. Experimentelle Untersuchungen uber die Fallbewegung von Kugeln und Scheiben in reibenden Flussigkeiten. Dissertation Leipzig 1928. Auch: Phys. 25, 29, 593, 1928.

75. Schrenk, O. Versuche an einer Kugel mit Grenzschichtabsangung. ZS. F. M. 17, 366. 1926. NACA. Tm 388, 1926.

76. Selberg, B. P. Shock tube determination of the drag coefficient of small spherical particles. NASA Cr-418, 1966.

77. Serby, J. E. & M. B. Morgan Turbulence measurements in flight. Gt. Britain A. R. C. R. & M. 1725, 1936.

78. Shakespear, G. A. Experiments on the resistance of the air to falling spheres. Phil. Mag. (6), 28, 728, 1914.

79. Sivier, K. R. & J. A. Nicholls Subsonic sphere drag measurements at intermediate Reynolds numbers. N. A. S. A. CR-1392, 1969.

80. Torobin, L. B. and W. H. Gauvin The drag coefficients of single spheres moving in steady and accelerated motion in a turbulent fluid. A. I. Ch. E. J., 7, 615, 1961.

81. Toussaint, Capt. & Lt. Hayer The resistance of spheres of small diameter in an airstream of high velocity. Aerotechnical Institute of Saint Cyr. TN 45, 1921.

82. Westgren, A. Uber die Bewegung einer Kugel in einem von zwei parallelen Wanden begrentzen zahen Medium. Ann d Phys., 52, 308, 1917.

83. Whetham, W. C. D. On the alleged slipping at the boundary of a liquid in motion. Phil. Trans. Roy. Soc., A. 181, 559, 1890.

84. Wieselsberger, C. Der Luftwiderstand von Kugeln. ZS. F. M., 5, 140, 1914.

85. Wieselsberger, C. 1921

86. Wieselsberger, C. Further information on the laws of fluid resistance. Phys ZS, 23, 219. 1922. N. A. C. A. TN 121, 1922.

87. Wieselsberger, C. Uber die Verbesserung der Stromung in Windkanalen, J. Soc. Mech. Engineers (Japan), 28, Nr. 98, June, 1925; N. A. C. A. TM 470, 1928.

88. Wieselsberger, C., A. Betz, & L. Prnadtl Der Widerstand von Kugeln, Ellipsoiden und Scheiben. Ergebnisse der Aerodynamischen Versuchsanstalt zu Gottingen, II Lieferung, 28, Oldenburg, Munchen & Berlin, 1923.

89. Wenger, R. Die Steigegeschwindigkeit der Gummiballone und die Turbulence in der Atmosphëre. Ann. d. Hydrographic, 45, 121, 1917.

90. Williams, W. E. On the motion of a sphere in a viscous fluid. Phil. Mag. (6), 29, 529, 1915.

91. Winny, H. F. The vortex system generated behind a sphere moving through a viscous fluid. Gt. Britain. A. R. C. R & M 1531, 1932.

92. Wiselius, I. S. I. Drag and pressure measurements with plaster spheres in Windtunnel 3 and 4 of the National Aeronautical Research Institute. Verslagen en Verhandelingen A. 950, National Luchtvaart laboratorium, XIII-1947, Amsterdam.

93. Woodward, R. S. Results of experiments on metallic spheres falling in water. Note on paper in Trans. N. Y. Acad. Sci. 15, 2, 1895.

94. Zarin, N. A. Measurement of non-continuum and turbulence effects on subsonic sphere drag. Univ. of Michigan Dissertation, 1969.

95. Zeleny, J. & L. W. McKeehan Die Endgeschwindigkeit des Falles kleiner Kugeln in Luft. Phys. Z. S., 11, 78, 1910.

96. Zahm, A. F. Flow and drag formulas for simple quadrics. N. A. C. A. Rpt. 253, 1926.

VI. Sphere Drag Coefficient References High Speed Regime

1. Aroesty, J. Sphere drag in low density supersonic flow, Univ. of California Tech. Rpt. HE-150-192, Berkeley, 1962.

2. Ashkenas, H. Sphere drag at low Reynolds numbers and supersonic speeds, J. P. L. Research Summary No. 36-12, 1, Jan. 1962.

3. Bailey, A. B. Private communication, Oct. 1969.

4. Charters, A. C. & R. N. Thomas The aerodynamic performance of small spheres from supersonic to high supersonic velocities, J. Aeron. Sci. 12, 10, 1945.

5. Clark, A. B. J. & F. T. Harris Free flight air-drag measurement technique, J. Aeron. Sci. 20, 9, 1953.

6. Hodges, A. J. The drag coefficient of very high velocity spheres, J. Aeron. Sci. 24, 10, 1957.

7. Jensen, N. A. Suplementary data on sphere drag tests, Part 2, Rept HE-150-92, Univ. of California, Berkeley, 1962.

8. Kane, E. D. Sphere drag data at supersonic speeds and low Reynolds number, J. Aeron. Sci. 18, 4, 1951.

9. May, A. Supersonic drag of spheres at low reynolds number in free flight, NAVORD Rept. 4392, 1956.

10. May, A. & W. R. Witt, Jr. Free-flight determinations of the drag coefficients of spheres, J. Aeron. Sci. 20, 9, 1953.

11. Schaaf, S. A. & P. L. Chambre Flow of rarefied gases, Princeton Aeronautical Paperbacks, Princeton Univ. Press, 1961.

12. Sherman, F. S. Note on sphere drag data, J. Aeron. Sci. 18, 8, 1951.

13. S reekanth, A. K. drag measurements on circular cylinders and spheres in the transition regime at Mach number of 2, Univ. of Toronto, Inst. of Aerophysics, Rept. 74, 1961.

14. Wegener, P. P. & H. Ashkenas Wind tunnel measurements of sphere drag at supersonic speeds and low Reynolds numbers, J. Fluid Mech. 10, (Part 4), 1961.

PART 2 - INFLATION ANALYSIS OF MYLAR FALLING SPHERES

by F. F. Fischbach

I. Introduction

A. Background

The falling-sphere technique has long been employed to determine atmospheric density through the measurement of drag acceleration. Presently, the most important designs are those in which an inflatable sphere is made of very light material, inflated after ejection from a rocket, and passively tracked by radar to determine drag acceleration.

There are three fully-developed designs for inflated sphere systems. One is launched on a routine operational basis. The other two are not used routinely but have been flown enough to provide considerable performance data.

Inflation of the sphere in all systems is caused by the evaporation of isopentane which is carried in a small aluminum capsule within the sphere. At the time of ejection the capsule is opened and subjected to a very low pressure. This causes evaporation and consequent pressure within the sphere on the order of 15 mb. Once the sphere has fallen to an altitude where the ambient pressure equals the internal pressure, the sphere collapses rather quickly with respect to altitude, say 1 km., and presents a much higher drag shape to the atmosphere.

The present systems while accumulating much experience have been subject frequently to a certain type of failure, namely, that the sphere has collapsed before reaching the design deflation altitude.

At first this type of failure was considered merely annoying because it was assumed that only the lowest few kilometers of atmospheric data would be unavailable. However, further analysis showed that the type of failure was important to all of the data, thus if the inflatant compound were all or partly missing at the time of launch, or if some leaked out of the sphere during the fall, not only would the sphere collapse too high but the mass assumed in the drag calculation would be incorrect at all altitudes. Since the mass is directly proportional to the calculated density, the size of the potential error is seen to be up to 16%.

There are many potential explanations for early deflation other than one involving mass loss, therefore, it is urgently required to analyze the sum total of flight experience, ground testing and theory for possible, probable, or certain explanations.

B. Method of Analysis

The question of inflation of the Arcas-Robin was the subject of a former analysis (Ref. 1). This together with the design and development analyses of the Judi-Dart-Robin and the Viper-Dart-Robin (Refs. 2 through 8) furnish valuable bases and background, particularly with regard to ground and chamber tests.

Flight experience with the Arcas-Robin will be used as well as that from the Judi- and Viper-Dart-Robins, the University of Michigan 66 cm spheres, and the Australian Weapons Research Establishment 2-meter spheres (Refs. 9 through 19). Fortunately the flight experience with each system was markedly different, and since certain elements of design were common a number of logical conclusions will be drawn.

The theory is taken from a large number of references which will be noted later, and consists largely of thermodynamic considerations.

A final logical analysis is presented summing up the present state of development, giving the logical conclusions, and recommending the tests required and changes to the present system which will increase the inflation reliability.

II. Pertinent Flight Experience

A. Description of the Systems

Although many of the systems have gone through a variety of configurations the flight experience available for this analysis has been obtained largely with four: Arcas - Robin and Viper - Dart Robin, developed by the Air Force, the 66 cm. aluminized sphere designed by the University of Michigan, and a 2 meter aluminized sphere developed at the Australian Weapons Research Establishment. The Robin is a 1-meter sphere with internal radar corner reflector which has been used in several rockets. The reason for distinguishing between Arcas and Viper-Dart Robins is that almost all components (inflation capsule, packaging, ejection, trajectory, data reduction) are entirely different, the one remaining more or less the same being the sphere itself.

Table 1 is a summary of the features of each system. For cases where designs have been changed data pertaining to the largest number of flights are given unless the change has a direct bearing on this investigation.

TABLE 1

SUMMARY OF FEATURES - INFLATED SPHERE SYSTEMS

Feature	Arcas-Robin	Viper-Dart Robin	Univ. of Mich.	Aust. W. K. E.
SPHERE:				
Diameter	1.00M.	1.00M	66 cm.	2.00M.
Material	Mylar A	Mylar A	Mylar A	Melinex
Thickness	.0005 in.	.0005 in.	.0005 in.	.0005 in.
Outer surface aluminized?	no	no	yes	yes
Internal corner refl'r?	yes	yes	no	no
Corner reflector mat'l.	1/4 mylar aluminized both sides		--	--
Reflector attachment	6-.012 Piano wire springs		--	--
Weight of skin	68g	72g±2	34g.	397 g.
Weight of reflector	14g	14g±1	--	--
Total wt. incl. capsule	113 g nom.	113±4 g	50g.	(594g) 1.31±.05lb.
CAPSULE:				
Material	aluminum	aluminum	aluminum	aluminum
Weight empty	8g	8.4±2.0g	8g.	122g.
Shape	cylinder	cylinder	cylinder	hemisphere
Actuated by	expanding pillow & rubber seal	piston with hollow needle	G-actuated conical punch	timer
No. of orifices	two	one	two	one
Dia. of orifice	.0135	.025 in.	0.13 in.	.040
Weight of isopentane	21.7g	18.6g	8.0g.	74.6g
PACKING:				
Vol. of sphere assy.	6 in^3	6 in^3	4 in^3	30 in^3
Vol. inside staves/can	(some 25 in^3) 81 in^3	30 in^3	20 in^3	150 in^3
Packing fraction	(24%) 7.5 %	20%	20%	20%
Folded by hand?	yes	yes	yes	yes
Vacuum bagged?	no	yes	no	?
Protective wrap?	yes	yes	yes	yes
Ablative coating?	no	no	no	no
Insulation?	--	yes	yes	heavy wall
Air Gap?	--	yes	no	no

TABLE 1 (cont.)

Feature	Arcas-Robin	Viper-Dart Robin	Univ. of Mich	Aust. W. K. E.
EJECTION:				
Acceleration	small	small	500g(max)	small
Sealed ejection charge:	later models	yes	yes	pneumatic
Direction	aft	forward	angled forward or aft	aft
Time	128	166 sec	70 sec	120 sec
Altitude	65 KM	130 KM	85 KM	364, 000 ft
Initiated by	pyro delay	pyro. delay	timer	timer
ROCKET:				
Max. acceleration		134 g		30 g
Max. deceleration		6. 9 g		5 g
Stages	one	one+dart	two	two
Time 1st burnout		3. 0sec	3. 4 sec	3 sec
Time 2nd ignition	--	--	21 sec	21 sec
Time 2nd burnout	--	--	24 sec	24 sec
Predicted apogee	75 KM	130 KM	150 KM	(218 KM) 420, 000
Time to apogee	128 sec	166 sec	186 sec	172 sec
OPERATIONAL:				
Tracked by	FPS-16	FPS-16 (Beacon option)	FPQ-6 (some FPS-16)	FPS-16 (some FPQ-6)
Primary Acquisition	skin	skin	skin	Beacon (lighted)
Secondary acquisition		--	optical	optical
Density Data Begun	70 KM	100KM	125KM(upleg) 100 KM(down)	100 KM
Upleg data?	no	no	yes	no

In addition to the summary in Table 1, the pertinent details regarding routine inspection and testing are worthy of discussion.

The Arcas-Robin configuration went through many modifications and the results of the ground and chamber tests that constituted the development program are discussed in the next section. The current Military Specification; Balloon, Radar Target, Meteorological ML-568/AM, MIL-B-27373A of 20 January 1964 provides the following routine tests for the Robin:

Capsule: Filled, weighed to ±. 0005 gram. Exposed to temperature cycle of -40° C to +50° C in 5 hours, stored at 20° C for 24 hours, reweighing must indicate loss of less than . 005 gram.

Pressure integrity: At atmospheric pressure the balloon is pressurized to 10 mb over atmospheric. In 30 min it shall lose less than 0. 5 mb pressure.

Capsule actuation: Must not open at more than 300 mb. Must open at 50 mb or more.

Shape: At 10 mb overpressure, 3 mutually perpendicular diameters shall be 1±. 005 meter. Same test to be repeated at 5 mb and 2 mb.

Weight: Total weight shall be less than 125 grams and be recorded.

The Robin under procurement for the Viper-Dart system is tested similarly. We believe the balloon tests are the same. The capsules are handled thus:

1. Capsules filled and weighed and temperature cycled -40° C to +50° C at the manufacturing source in Arizona. The weight is rechecked

in one week and again in one month. A loss of . 012 grams is cause for rejection.

2. The filled capsules are shipped to the balloon manufacture facility in Minnesota. The weight is checked upon arrival inspection. About 2% have been rejected at this time. After storage which is generally not lengthy, the weight is rechecked prior to insertion in the balloon. None have been rejected at this time.

3. The total weight of the sphere assembly in staves, taped, including tape is recorded. The taped assembly is then transshipped to the Dart manufacturer in Arizona. No further weighing is done. The tape is removed and the staves inserted into the Dart which is sealed and shipped to the purchaser.

The above procedure was reported by the manufacturer. We do not hold a copy of the formal purchase specifications.

The Australian Department of Supply, Weapons Research Establishment 2-meter sphere system is procured under specifications which are not available to us.

The University of Michigan procurement of 66 cm. sphere systems has been under similar specifications as the Robin. The balloon is overpressured 15 mb. and measured. Three mutually perpendicular diameters are recorded and must be ±1/2%. The capsule is filled, weighed, stored, and reweighed. After insertion in the balloon, the sphere assembly is weighed for data reduction purposes, then inserted in staves for storage until flight. No further weighing is done.

Procurement of the Michigan system by other agencies, notably Sandia Corp., has been done independently and possibly with different test procedures.

B. Test Flight Data

The flight data have been assembled from the following sources: Robin systems - references 1 through 8, 20 and recent private communications, Australian system - references 9 through 19, Michigan system - our files, reference 21, and Sandia Corp. data.

Certain flights were conducted utilizing hardware components on a trial basis or for testing rocket parameters, and some failed under circumstances not germane to the present investigation. Accordingly, these flights are not included. For example, 2 early Michigan flights at Kwajalein, Marshall Is., failed probably because of the capsule design. The test series was stopped until a redesigned capsule was available. No further failures of that type were encountered. Since no conclusions concerning the remainder of the system could be made, these flights are not considered.

It is unfortunate that a majority of the Arcas - Robin flight data falls into this category because the balloon proper has many of the same features as the Viper-Dart-Robin under investigation. However, the crucial present determination, that of deflation altitude, was not satisfactorily made with the former data reduction procedure. The deflation altitudes determined by means of the λ-check were not reliable, but not because of the principle of the λ-check. The major problem was the smoothing interval which was too short. With the current Robin data process procedure both a fall rate criterion and the λ-check are used to determine deflation altitude; meanwhile, the smoothing interval has been greatly increased. The λ-check now agrees pretty well with the fall-rate criterion (which is done perhaps too approximately

using a 5-km layer). The purpose in pointing this out is to ensure that no one will assume that, because the λ-check is presently reliable, it was also reliable when utilized with the former smoothing interval.

Table 2 summarizes the Australian flights and gives all details which are germane to sphere inflation. Table 3 does the same for the Michigan 66 cm. system. Table 4 summarizes the Viper-Dart-Robin and other Dart-Robins when pertinent to the current Robin design. The latter table includes flights up to the present date and the data while very preliminary are adequate for this investigation.

TABLE 2

SUMMARY OF INFLATION DATA - FLIGHTS OF AUSTRALIAN 2 - METER SPHERE SYSTEM

ALL THE FOLLOWING FLIGHTS AT WOOMERA, SO. AUSTRALIA
LAT. 31°S., FPS-16 RADAR

HAD#	Date	Local Time	Deflation Alt. (KM)	Surface Temp. (F)	Cloud Cover	Remarks
129	15-4-64	1832	43	68	0	
126	14-5-64	1807	44	66	3/8	
128	11-6-64	1801	41	58	3/8	
141	9-7-64	1809	44	57	0	
135	20-8-64	1832	72	66	0	"Possibly due to non-release of C_5H_{12}"
144	17-9-64	1847	38	62	0	
146	15-10-64	1906	40	72	1/8	
145	11-11-64	1929	no inflation	84	7/8	"Premature Ejection"
157	12-11-64	1930	41	87	1/8	
130	13-7-64	1234	58	60	8/8	"Collapsed Prematurely"
131	14-7-64	1200	43	58	7/8	
133	15-7-64	1219	43	N/A	7/8	
134	16-7-64	1213	38	N/A	0	
159	8-12-64	1956	43	79	4/8	
161	10-12-64	1956	40	72	1/8	
152	2-3-65	1927	41	92	1/8	
153	30-3-65	1900	70	81	0	"Probably due to non-release of C_5H_{12}"
160	11-5-65	0839	47	61	2/8	"Collapsed slightly prematurely"
172	8-6-65	1807	no inflation	60	1/8	"Sphere apparently burst on ejection & descended at abnormal high speed"
171	9-6-65	1801	72	58	3/8	"Prob. due to non-release of C_5H_{12}"
174	7-7-65	1807	44	62	7/8	"Collapsed in normal fashion"
177	3-8-65	1822	73	56	5/8	"Prob. due to non-release of C_5H_{12}"
105	29-3-62	1858	unknown	N/A	0	Only used supersonic data
178	5-10-65	1857	67	83	0	"Prob. due to non-release of C_5H_{12}"
179	9-11-65	1928	56	61	2/8	"Unknown reason"
151	6-12-65	1954	43	75	1/8	
176	26-1-66	2002	41	99	3/8	
186	23-2-66	1936	47	78	0	
181	22-3-66	1908	38	66	1/8	
188	17-5-66	1812	41	69	6/8	
185	15-6-66	1805	40	56	2/8	
187	19-7-66	1818	41	56	3/8	
189	23-8-66	1834	41	54	4/8	
190	27-9-66	1852	44	76	0	
191	1-11-66	1918	38	68	0	

TABLE 2 (cont.)

ALL THE FOLLOWING FLIGHTS FROM CARNARVON, W. AUST.

LAT. 25°S, FPQ - 6 RADAR

Had#	Date	Local Time	Deflation Alt. (KM)	Surface Temp. (F)	Cloud Cover	Remarks
132	14-7-64	--	--	--	--	2nd stage failed to ignite
135	15-7-64	--	unknown	--	--	2nd stage failed to ignite
136	16-7-64	1330	49	N/A	3/8	"Sphere split prob. owing to heating by solar radiation"
137	17-7-64	1315	53	N/A	5/8	"Again the sphere split"
142	22-10-64	--	--	--	--	"Sphere apparently not ejected"
140	22-10-64	0512	41	N/A	0	
148	22-10-64	1903	52	N/A	N/A	"Sphere apparently split"
143	22-10-64	--	--	--	--	2nd stage failed to ignite

TABLE 3

SUMMARY OF INFLATION DATA - FLIGHTS OF UNIVERSITY OF MICHIGAN 66 CM SPHERE SYSTEM

ALL THE FOLLOWING FLIGHTS AT WALLOPS IS., VA:

NASA#	DATE	GMT	DEFLATION ALT. (KM)	REMARKS
10.254	24-7-68	1845	30	Sphere 1
10.254	24-7-68	1845	100+	Sphere 2
10.265	24-7-68	1020	40.5	
10.266	24-7-68	2155	36	
10.169	8-8-65	0340	35	
			Below	FPS-16 Track Ends at 38
10.154	7-8-65	1830	38	FPQ-6 Track Ends at 47
10.157	26-1-66	0152	30	
10.253	24-7-68	0500	33.5	Sphere 1
10.253	24-7-68	0500	28	Sphere 2
14.386	19-11-68	2005	29.5	
10.143	4-2-66	0154	"Early"	Sphere 1 (no data)
10.143	4-2-66	0154	28	Sphere 2
10.264	1-2-68	1853	29	
10.159	3-2-66	1831	28	
10.158	26-1-66	0152	29	
10.175	23-10-65	1614	31	
10.174	19-10-65	2310	32	
			Below	
10.129	13-10-65	1651	41	Track ended

TABLE 3 (cont.)

ALL THE FOLLOWING FLIGHTS AT KAUAI, HAWAII

OCTOBER 1964 THROUGH JUNE 1969

Local Time	Deflation Alt. (km)
1930	35
2206	31
2000	30
2007	29
0745	28
1350	30
2000	39
0515	30
1900	30
2318	30
2025	30
2045	37
2100	29
1000	36
0015	35
1530	29
0600	32
1200	45
2145	30

TWO FLIGHTS FROM TONOPAH, NEV.

LT	KM
0515	34
1645	31

Two additional flights failed due to early ejection.

Three additional flights failed due to non-or no inflation.

These inflation capsules were the first of a new procurement, many of which were found to have leaked in storage.

Four out of four flights have subsequently failed after refilling and resealing the defective capsules.

TABLE 3 (cont.)

ALL THE FOLLOWING FLIGHTS AT KWAJALEIN, MARSHALL IS.

Date	Flt#	Local Time (GMT + 11.5 hrs)	Deflation Alt. (km)	Remarks
18-6-63	3	1458	32	
20-6-63	4	1430	32	
4-11-63	5	2201	39	
4-11-63	6	2356	31	
10-11-63	7	0356	Below 36	Data recorder failed 34.4 km.
15-11-63	8	0228	31	
24-1-64	11	0655	32	
14-3-64	12	0650	31	
12-5-64	13	2255	Below 36	Data recorder failed 35.1 km.
17-6-64	14	1231	31	
18-6-64	15	1349	31	
19-6-64	16	0500	31	

On 3 of the above flights a different sphere was tracked ascending.

On all flights 3 spheres per rocket were flown.

There were two flights in which no acquisition was made of any sphere. (This had to be either a problem with radar or the ejection timer. Flights 9 and 10.)

On the first two flights, 26-3-63, not listed, both failed to inflate but both carried pneumatic capsules which were replaced with the current design on all subsequent flights.

TABLE 4

SUMMARY OF INFLATION DATA - FLIGHTS OF VIPER-DART-ROBIN

The first 17 development flights were at Eglin AFB.

The primary emphasis was on vehicle development.

The results relating to inflation are as follows:

1	Vehicle failure
5	No radar acquisition of vehicle or sphere
1	"Bad Robin"
1	"Questionable Robin"
9	"Good Robin"

"Good Robin" implies a successful ejection and initial rigid inflation. Deflation was not calculated. Although 9 "Good Robins" were reported, data has been reported from only 1 of these flights. It gave density to 42 km. 35 cc of Isopentane was used on all flights.

The next 14 Viper-Dart-Robin flights were part of a series of 19 vehicle development tests. A secondary objective was to lower the Robin deflation altitude. The launch site was Cape Kennedy, Daytime, November 1968 to October 1969.

Results were as follows:

5	Vehicle failed - no payload test
1	No data on payload
1	Failed to eject sphere
7	Reported "Good Payload Performance"

Data from these 7:

Isopentane	Deflation Alt. (KM)
30cc	38
35cc	50
30cc	30
30cc	No Report
30cc	42
30cc	67
30cc	67

TABLE 4 (cont.)

The next 18 development rounds have been reported as preliminary data. All carry 30cc Isopentane. All were daytime launches. Pertinent inflation data:

Launch Site	Year	Deflation Altitude (km)
Eglin	1969	36
Eglin	1969	37
Eglin	1969	34
Eglin	1969	42
Eglin	1969	70
Eglin	1969	40
Eglin	1969	70
Wallops	1969	43
Wallops	1969	31
Wallops	1969	37
Pt. Mugu	1969	30
Pt. Mugu	1969	35 or 55
Eglin	1970	36
Eglin	1970	57
Eglin	1970	45
Pt. Mugu	1970	No inflation
Pt. Mugu	1970	32

TABLE 4 (cont.)

The first 30 flights of production procurement payloads have had deflation data reported as preliminary information. All carry 30 cc Isopentane. Flights in August, September, October 1970, all at local noon:

Launch Site	Deflation Alt. (km)	Launch Site	Deflation Alt. (km)
Barking Sands	57	Cape Kennedy	No inflation
" "	54	"	60 - 70
Point Mugu	No acquisition	"	60 - 70
" "	39	"	60 - 70
" "	70	"	60 - 70
" "	35	"	60 - 70
" "	50	"	55 - 60
Cape Kennedy and	55 - 60	"	50 - 55
Ascension Island	40 - 45	"	Above 70
" "	45 - 50	"	Above 70
" "	30 - 35	"	"Good"
" "	50 - 55	"	"Good"
" "	50 - 55	"	"Good"
" "	45 - 50		
" "	50 - 55		
" "	40 - 45		
" "	55 - 60		

C. Summary

The tests are categorized and grouped for correlative analysis below:

N = No. of flights

D = Design deflation altitude

Group	Deflation Altitude							
	D to D+3 km		D+3 to D+10 km		D+10 to 65 km		Above 65 km	
	N	%	N	%	N	%	N	%
All Flights								
V-D Robin (1m)	8	16%	15	29%	16	31%	12	24%
Univ-Mich(. 66m)	33	72%	10	22%	2	4%	1	2%
Australia (2m)	4	11%	20	54%	7	19%	6	16%
V-D-Robin								
Development	7	32%	8	36%	4	18%	3	14%
Production	1	3%	7	24%	12	41%	9	31%
AMR	1	4%	5	22%	9	39%	8	35%
PMR	0	0%	2	33%	3	50%	1	17%
Univ-Mich								
Wallops Is.	10	66%	3	20%	1	7%	1	7%
Kwajalein I.	9	90%	1	10%	0	0%	0	0%
Kauai I.	14	66%	6	29%	1	5%	0	0%
Australia								
Carnarvon	0	0%	1	25%	3	75%	0	0%
Woomera	4	12%	19	58%	4	12%	6	18%

III. Pertinent Ground Test Experience

Ground tests of spheres are reported in references 1 through 8. Positive results which are pertinent to the Viper-Dart-Robin sphere system are limited to:

1. Type of inflatant
2. Amount of inflatant
3. Activation of the capsule
4. Post-ejection integrity of the sphere

The use of isopentane as an inflatant was tested repeatedly in the Arcas-Robin program. Nothing was discovered in these tests which was not already known about the chemicals. Use of other chemicals was not found to be advantageous.

The amount of isopentane was varied several times in the development program. The employment of 30 cc (18.6 grams) was finally adopted. The use of more isopentane (to prevent early deflation in flight tests) was tried and concluded to make no difference.

The capsule was activated in 10 out of 10 Viper-Dart-Robin tests at Wright-Patterson AFB as reported in reference 7. In these tests 10 spheres were ejected at a simulated altitude of 150,000 feet. Six of the ten were ejected at chamber ambient temperature and four were heated to 150°C. All inflated sufficiently to be rigid but only the four heated spheres inflated to "full pressure". It was reported further that "some" of the spheres were damaged and that the damage was considered to be the result of collision with the staves protruding from the backstop. Since no test details were reported in reference 7, particularly the time-pressure history of the chamber and the collapse pressure, it is not possible to conclude that even one sphere had post-ejection integrity nor that even one sphere failed to have integrity.

The integrity of the sphere when tested in the Arcas-Robin program would be pertinent to the present design since the sphere, corner reflector, and springs are identical. However, the full scale vacuum chamber tests of twenty Arcas-Robin payloads encountered many difficulties almost all of which left the sphere damaged or improperly inflated. This resulted in little information about post-ejection integrity which pertains to the Viper-Dart-Robin design.

IV. Thermal Studies Of Mylar Falling Spheres

A. Introduction (by F. L. Bartman)

When the work on the "Inflation Analysis of Mylar Falling Spheres" was begun it was planned to carry out a complete analysis of the thermal history of mylar falling spheres. During the course of the work, it became obvious that such a study, complete and reliable in all aspects, could not be carried out with the funds and manpower allocated to this project. In several areas, assumptions would have to be made, whose reliabiability might be so poor that the results could not be depended upon.

Thus, although a beginning has been made on such a thermal history, the final result desired, reliable temperature vs time curves for falling spheres has not been produced.

It is hoped that additional funds can be provided so that in the near future such a study could be completed.

B. Initial Temperatures

The temperature of the sphere and capsule at the time of ejection is a function of the temperature at launch and the aerodynamic heating. The temperature-time history for each type of sphere will be calculated on the basis of the warmest and coldest extremes and also on the most probable conditions covering the majority of actual flights conducted.

Spheres have not been launched in cold climates but may in the future. Considering this possibility, the launch temperature extremes are taken to be $-40^{\circ}F$. ($-40^{\circ}C$.) and $+122^{\circ}F$ ($+50^{\circ}C$). The most probable temperature at launch is taken to be $65^{\circ}F$ (about $18^{\circ}C$).

Aerodynamic heating may be negligible as in the 3-sphere University of Michigan Nike-Cajun payload or extreme as in the Viper-Dart-Robin system. The most probable aerodynamic heating for the Viper-Dart-Robin is taken as $100^{\circ}C$.; for the University of Michigan (Strap-on, Nike Apache) $40^{\circ}C$.; for the Australian system $20^{\circ}C$.

It is assumed that the maximum temperature at which Mylar retains its strength is about $150^{\circ}C$.

From the above considerations, the possible range of ejection temperatures (ejection at 130 km) will lie between the values of the lowest launch temperature plus the minimum heating ($-40^{\circ}C + 20^{\circ}C = -20^{\circ}C$) and the maximum launch temperature plus maximum heating ($50^{\circ}C + 100^{\circ}C = 150^{\circ}C$). The average condition for the Viper-Dart-Robin system would be average launch temperature plus Viper-Dart-Robin heating ($18^{\circ}C + 100^{\circ}C = 118^{\circ}C$). In summary, we have:

Cold extreme (all sphere systems)	$-20^{\circ}C$
Average Viper-Dart Robin	$118^{\circ}C$
Hot extreme (all sphere systems)	$150^{\circ}C$

C. Isopentane Evaporation (F. F. Fischbach and F. L. Bartman)

The capsule containing isopentane must be properly scaled to prevent evaporation in storage and must not leak during the rocket flight. At ejection or shortly thereafter the capsule is opened to its ambient pressure which is nearly a total vacuum. The pressure seen is the pressure created within the sphere by entrapped air and may be expected to be on the order of 0.1 mb.

If the orientation of the capsule is such that the drag force opposes the direction of the orifice in the capsule, the capsule will certainly release all of the isopentane into the sphere, mostly in liquid form, in a matter of a few seconds after drag on the order of a fraction of a g is encountered. This has been proved by the several ground tests and the performance of the Australian system in which the capsule is so oriented.

If the orientation of the capsule is such that the orifice is directed essentially sidewise to the drag, as in the Robin and the University of Michigan systems, at least 55% of the isopentane will be expelled in liquid form shortly after any appreciable drag is encountered, probably before. However the remaining 45% will in the worst case (meaning most slowly, which is conservative from the evaporation standpoint) issue from the orifice in vapor form. Whatever "sloshing" or vigorous boiling occurs will increase the percentage expelled as liquid, but for now let us assume none. During the daytime radiation will aid the evaporation significantly (note daytime equilibrium temperature of 282.3 to 301.0^{o}K on p. 63) while at night it may not, (note night overcast equilibrium temperatures of 217.7-219.8^{o}K). Aerodynamic heating may also assist the evaporation somewhat.

The pressure inside the sphere cannot be greater than the vapor pressure over liquid corresponding to the equilibrium temperature of the sphere. If the temperature is sufficiently high the vapor pressure will also be. The balloon will expand, all of the isopentane will be vaporized and the internal pressure of the completely inflated sphere will be determined by the gas law.

$$p = \frac{\rho RT}{M}$$

The isopentane vapor pressure and the completely inflated sphere pressure if all isopentane were evaporated are shown below for the equilibrium radiation temperatures summarized on page 63.

Conditions	Equilibrium Temperature ^{o}K	Vapor Pressure mb	Inflated Sphere Pressure mb
Clear sky - day	282.3	500	11.5
Clear sky - night	234.5	50	9.5
Overcast - day	298.9	910	12.0
Overcast - night	217.7	15	8.7

In all cases the vapor pressure is sufficiently high to insure evaporation and sphere inflation. The situation is summarized in figure 1, where the vapor pressure of isopentane vs. temperature and the gas law are plotted. In this case with 18.2 grams of isopentane and a sphere volume of $5.24 \cdot 10^{5} cm.^{3}$, we have:

$$P = 0.04\ T \text{ mb}$$

For equilibirum temperatures greater than $208^{o}K$ all of the isopentane is evaporated and the sphere internal pressure is determined by the gas law. For temperatures less than $208^{o}K$, some isopentane is liquid and the sphere

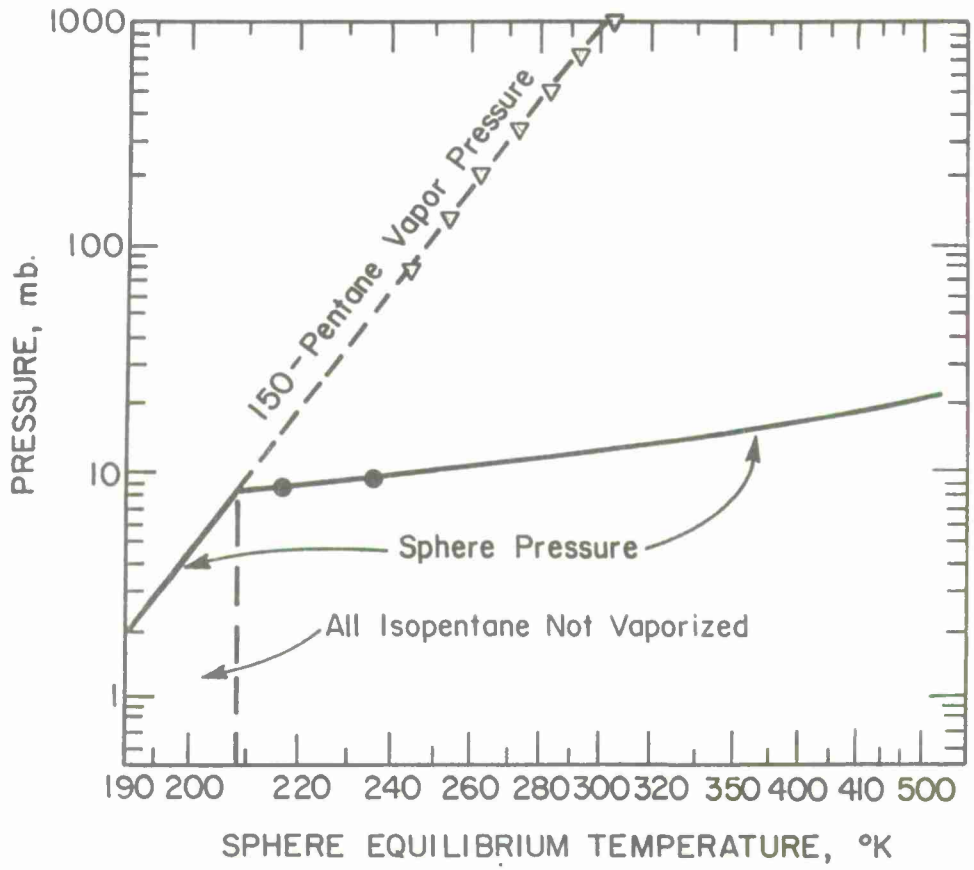

Figure 1 Sphere Internal Pressure vs Equilibrium Temperature

internal pressure is determined by the isopentane vapor pressure. Note that at a sphere equilibrium temperature of 190°K the sphere internal pressure would be about 1.7 mb. The lower temperature range of about 210°K or below presents a problem for continued sphere inflation.

The equilibrium adiabatic orifice flow rate can be estimated with the use of an equation which applies when the downstream pressure is less than the critical pressure, i.e. is less than 0.53 times the capsule pressure (see ref. 41, p. 4-61). The weight of fluid flowing through the orifice, $\dot{m}$, is given by:

$$\dot{m} = C_f A_{orifice}\, p_{capsule} \sqrt{\frac{g}{RT}\,\gamma\,\left(\frac{2}{\gamma+1}\right)^{(\gamma+1)/(\gamma-1)}} \qquad (1)$$

where C_f is the discharge coefficient (empirically determined) and the other terms are the conventional gas parameters (see list of symbols).

Assuming: $T = 300^{\circ}K$

$P_{sphere} = 5$ mb

$P_{capsule} = 1000$ mb

$C_f = 0.6$

$= 1.11$ (for isopentane)

$A_{orifice} = \frac{\pi}{4}(.025)^2\,\dot{m}^2 = \frac{\pi}{4}(.01)^2 cm^2$

$= 7.86 \cdot 10^{-5} cm^2.$

we find:

$$\dot{m} = 0.6 \cdot 7.86 \cdot 10^{-5} \cdot 10^6 \quad \frac{980.6 \cdot 72.15}{8.3143 \cdot 10^7 \cdot 300} \quad 1.11 \left(\frac{2}{2.11}\right)^{19.18}$$

$= 5.0\ 10^{-2}$ gr./sec.

If 50% of the isopentane has been expelled in liquid form the remainder will issue as vapor in a length of time equal to:

$$t = \frac{0.5 \cdot 18.6}{5.0 \cdot 10^{-2}} = 1.86 \cdot 10^2 \text{ sec} = 3.1 \text{ min}$$

In about 3 minutes the remaining isopentane would be expelled as vapor from the Robin capsule, providing only that the temperature remain reasonably high.

D. Radiation Effects (by F. L. Bartman)

The radiation balance of a mylar falling sphere can be calculated approximately if the radiative properties of the material are known. Other studies, published in the literature, which shed some light on this topic are: studies of the temperature distribution of spherical satellites (ref. 33), studies of the radiative heat transfer for high altitude balloons (ref. 34) and methods of analysis of the spherical satellite sensors which were used for earth albedo and earth radiation balance measurements (ref. 35).

The calculations which follow are calculations of the mean temperature of the thin wall of:

a) A transparent mylar sphere

b) An aluminized mylar sphere

c) A transparent Robin mylar sphere with corner reflector inside.

Radiation is the only mechanism of heat transfer considered. The mean temperature is found by equating the energy absorbed by the sphere to the thermal energy that it radiates back out into space.

TRANSPARENT SPHERE

The radiation balance for a transparent sphere is expressed as follows:

$$\pi R^2 \sum_{\lambda} \left[\alpha_\lambda \left(2 - \frac{\alpha_\lambda}{1 - r_\lambda}\right) H_{s_\lambda} + \beta\alpha_\lambda \cdot \left(2 - \frac{\alpha_\lambda}{1 - r_\lambda}\right) I_{E_\lambda} \right] = 4\pi R^2 \cdot \sum \epsilon_\lambda \left(2 - \frac{\epsilon_\lambda}{1 - r_\lambda}\right) W_\lambda(T) \quad (2)$$

where: πR^2 is the cross sectional area of the sphere

$\alpha_\lambda \left(2 - \frac{\alpha_\lambda}{1 - r_\lambda}\right)$ is the effective absorbtivity of the mylar at wavelength λ

$\epsilon_\lambda \left(2 - \frac{\epsilon_\lambda}{1 - r_\lambda}\right)$ is the effective emissivity of the mylar at wavelength λ

β is the solid angle of the earth as viewed from the sphere

$H_{s\lambda}$ is the spectral solar irradiance

$I_{E\lambda}$ is the spectral intensity of radiation leaving the earth, including the thermal radiation and reflected solar radiation

$W_\lambda(t)$ is the radiant emittance of the mylar material at mean temperature T.

α_λ is the spectral absorptivity of the mylar

ϵ_λ is the spectral emissivity of the mylar

r_λ is the spectral reflectivity of the mylar

Two additional equations which apply are:

$$\alpha_\lambda + r_\lambda + \tau_\lambda = 1 \tag{3}$$

and

$$\alpha_\lambda(T) = \epsilon_\lambda(T) \tag{4}$$

The effective absorptivity of the mylar sphere was determined as follows. If the gas inside the sphere is considered to be transparent then the sequence of encounters of a beam of radiation causes the effective absorptivity to be:

$$\begin{aligned}
\alpha_\lambda(\text{eff}) &= \alpha_\lambda + \alpha_\lambda \tau_\lambda + \alpha_\lambda \tau_\lambda r_\lambda + \alpha_\lambda \tau_\lambda r_\lambda^2 + \cdots \\
&= \alpha_\lambda (1 + \tau_\lambda + \tau_\lambda r_\lambda + \tau_\lambda r_\lambda^2 + \cdots) \\
&= \alpha_\lambda \left[1 + \tau_\lambda (1 + r_\lambda + r_\lambda^2 + r_\lambda^3 + \cdots)\right] \\
&= \alpha_\lambda \left(1 + \frac{\tau_\lambda}{1 - r_\lambda}\right) \\
&= \alpha_\lambda \left(2 - \frac{\alpha_\lambda}{1 - r_\lambda}\right)
\end{aligned} \tag{5}$$

The effective emissivity of the mylar sphere is determined in a similar fashion. In this case the radiation is emitted by the outer and inner surfaces of the fabric. The sequence of encounters of the inner plus the outer beam then causes the effective emissivity to be:

$$\begin{aligned}
\epsilon_\lambda\ (\text{eff}) &= \epsilon_\lambda + \epsilon_\lambda - \epsilon_\lambda \alpha_\lambda - \epsilon_\lambda r_\lambda \alpha_\lambda - \epsilon_\lambda r_\lambda^2 \alpha_\lambda - \cdots \\
&= \epsilon_\lambda \left[2 - \alpha_\lambda (1 + r_\lambda + r_\lambda^2 + \cdots)\right] \\
&= \epsilon_\lambda \left[2 - \frac{\alpha_\lambda}{1 - r_\lambda}\right] \\
&= \epsilon_\lambda \left[2 - \frac{\epsilon_\lambda}{1 - r_\lambda}\right]
\end{aligned} \tag{6}$$

provided the sphere surface is considered to be all at the same temperature

The term in the radiation balance equation which represents the radiation received from the earth is obtained as follows. The rate of transfer of energy from an element of area da, on the earth to an element of area da_2 on the mylar sphere at wavelength λ is given by:

$$dq_\lambda\ (1\text{-}2) = \alpha_\lambda\ (\text{eff}) \cdot I_{E\lambda}\ \frac{da_1 \cos\theta_1 \cdot da_2 \cos\theta_2}{r^2_{1\text{-}2}} \qquad (7)$$

where da_1 is an element of area on the earth and da_2 is an element of area on the mylar sphere (see figure). We must integrate over da_1 and da_2.

$$q_\lambda\ (1\text{-}2) = \int_{da_2} \int_{da_1} \alpha_\lambda\ (\text{eff})\ I_{E\lambda}\ \frac{da_1 \cos\theta_1\, da_2 \cos\theta_2}{r^2_{1\text{-}2}} \qquad (8)$$

For the radiation from a given element of area da_1 the beam of radiation arriving at all elements of area da_2 is the same . ˙ . we can separate the integrals:

$$q_\lambda(1\text{-}2) = \alpha_\lambda\ (\text{eff}) I_{E\lambda} \int_{da_1} \frac{da_1 \cos\theta_1}{r^2_{1\text{-}2}} \int_{da_2} da_2 \cos\theta_2$$

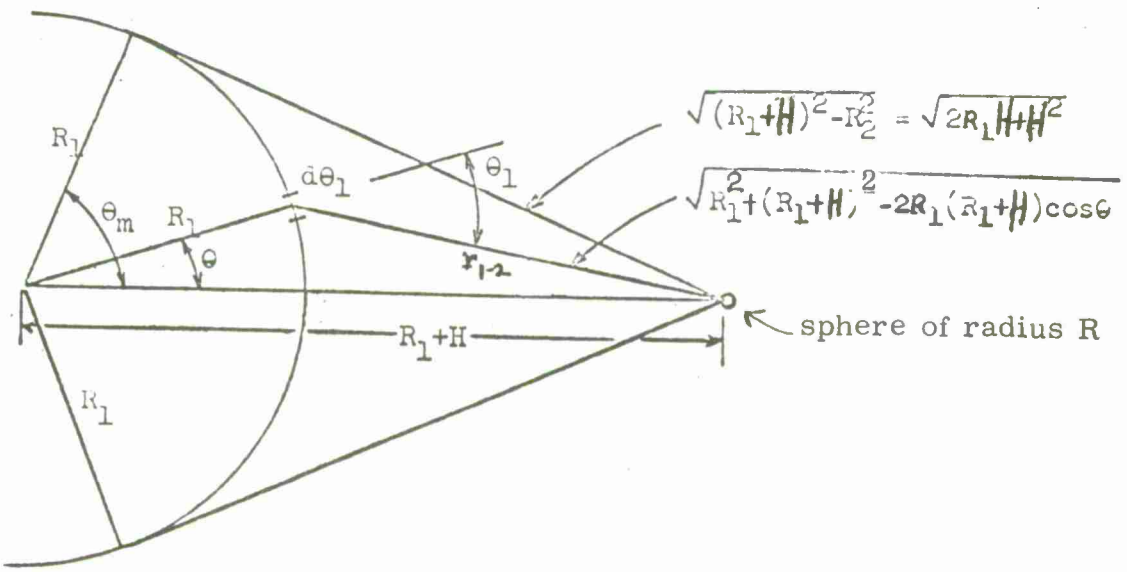

where we have assumed that a_λ (eff) is the same for all elements of area da_2 and the intensity of radiation emitted by the earth is the same for all elements of area da_1.

it can be seen that:

$$\int_{da_2} da_2 \cos\theta_2 = \int_0^{2\pi} \int_0^{\pi/2} \cos\theta_2 \cdot R \sin\theta_2 \, d\phi_2 R d\theta_2$$

$$= R^2 \cdot 2\pi \cdot \frac{\sin^{-2}\theta_2}{2} \Big|_0^{\pi/2} = \pi R^2 \qquad (9)$$

also $$\int_{da_1} \frac{da_1 \cos\theta_1}{r_{12}^2} = \int_0^{\theta_m} \int_0^{2\pi} \frac{R_1 \sin\theta \, d\phi \cdot R_1 d\theta \cdot \cos\theta_1}{r_{12}^2}$$

$$= 2\pi R_1^2 \int_0^{\theta_m} \frac{\cos\theta_1 \sin\theta d\theta}{r_{12}^2} \qquad (10)$$

If we note that:

$$r_{12}^2 = R_1^2 + (R_1+H)^2 - 2R_1(R_1+H)\cos\theta$$

and

$$\cos\theta_1 = \frac{(R_1+H)\cos\theta - R_1}{r_{12}} \qquad (11)$$

and integrate by parts, we find:

$$\int_{da_1} \frac{da_1 \cos\theta_1}{r_{12}^2} = 2\pi \left[1 - \frac{\sqrt{2R_1H+H^2}}{R_1+H}\right] = \beta$$

and

$$q_\lambda (1-2) = \alpha_\lambda (\text{eff}) \, I_{E\lambda} \cdot \pi \cdot R^2 \cdot \beta \qquad (12)$$

The intensity of radiation from the earth is the sum of the reflected solar radiation and the emitted thermal radiation:

$$I_{E\lambda} = \frac{\rho_\lambda}{\pi} H_{s\lambda} + I_{T\lambda}$$

$$\pi \cdot I_{E\lambda} = H_{E\lambda} = \rho_\lambda \cdot H_{s\lambda} + H_{T\lambda} \qquad (13)$$

where $\rho H_{s\lambda}$ is the flux of solar radiation reflected from the surface of the earth and $H_{T\lambda}$ is the flux of thermal radiation emitted by the earth. Thus the radiation balance equation can be written as:

$$\sum_\lambda \left[\alpha_\lambda \left(2 - \frac{\alpha_\lambda}{1-r_\lambda}\right) H_{s\lambda} + B \cdot \alpha_\lambda \left(2 - \frac{\alpha_\lambda}{1-r_\lambda}\right) H_{E\lambda}\right] = 4 \cdot \sum_\lambda \epsilon_\lambda \left(2 - \frac{\epsilon_\lambda}{1-r_\lambda}\right) W_\lambda / T)$$

$$\text{where } B = \frac{\beta}{\pi} = 2 \left[1 - \frac{\sqrt{2R_1 H + H^2}}{R_1 + H}\right] \qquad (14)$$

and the remainder of the symbols have been defined above. Finally we can simplify the equation by factoring to obtain:

$$\sum_\lambda \alpha_\lambda \left(2 - \frac{\alpha_\lambda}{1-r_\lambda}\right) (H_{s\lambda} + BH_{E\lambda}) = 4 \cdot \sum_\lambda \epsilon_\lambda \left(2 - \frac{\epsilon_\lambda}{1-r_\lambda}\right) W_\lambda (T) \qquad (15)$$

Absorptivity data for 0.5 mil mylar has been obtained from several sources which do not agree with one another. Curves of transmissivity for 1 mil Mylar are shown in figures 2 a and 2 b, covering the spectral range 0.3-2.6 μm and 8-15 μm, respectively. Reference 1, from which these data were taken, does not identify the source from which they were obtained. Transmissivity data for 1.5 mil Mylar have been obtained in the University of Michigan High Altitude Engineering Laboratory for the range 1.5-15.0 μm These three sets of data have been used to obtain a set of data for the transmissivity of 0.5 mil Mylar for the range 0.2-15.0 μm. Assuming that Beer's law holds for the transmissivity of Mylar, we have, that for a thickness x :

$$\tau_x = \exp(-Kx) \qquad (16)$$

Figure 2a Absorption Spectrum for Mylar (Low Range)

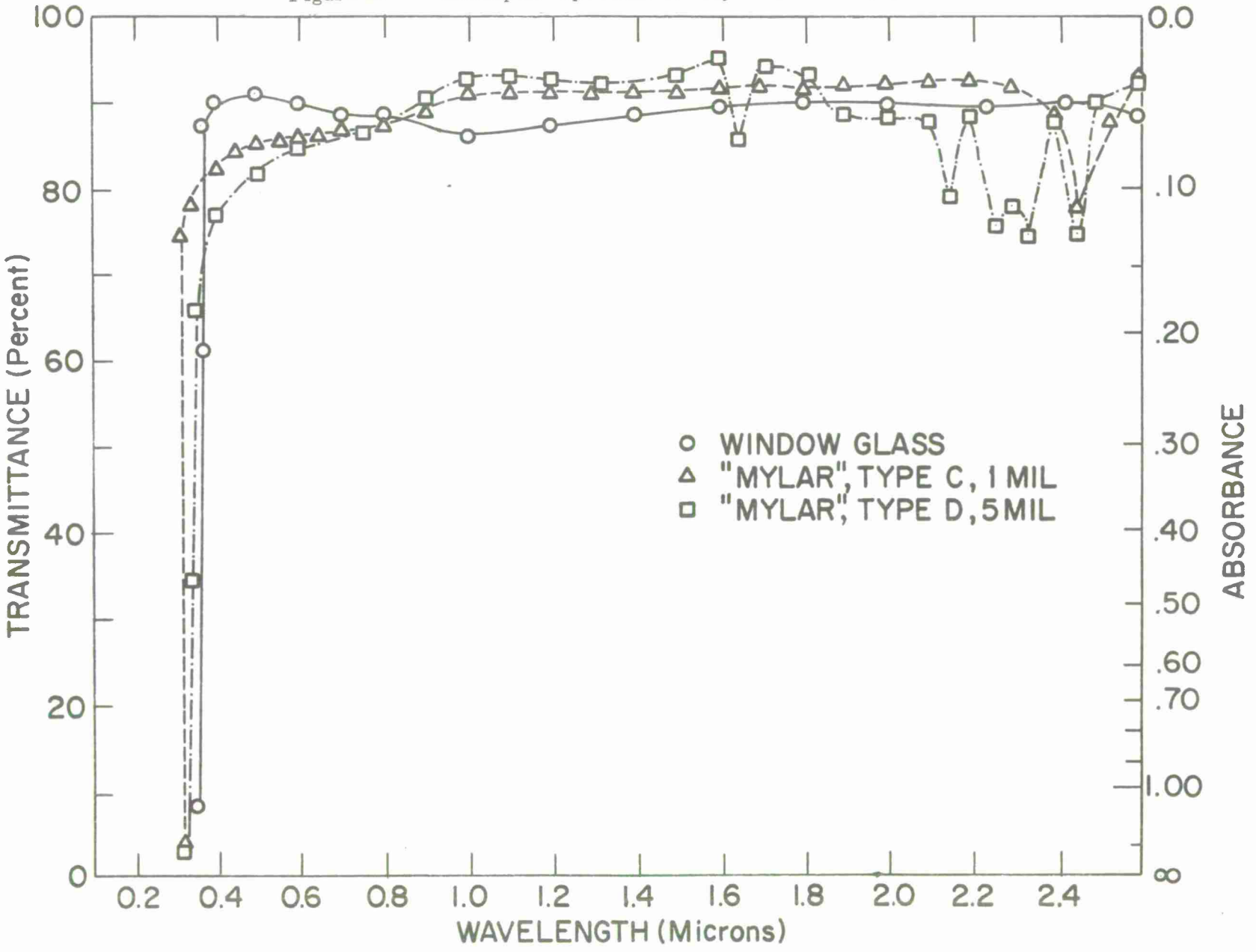

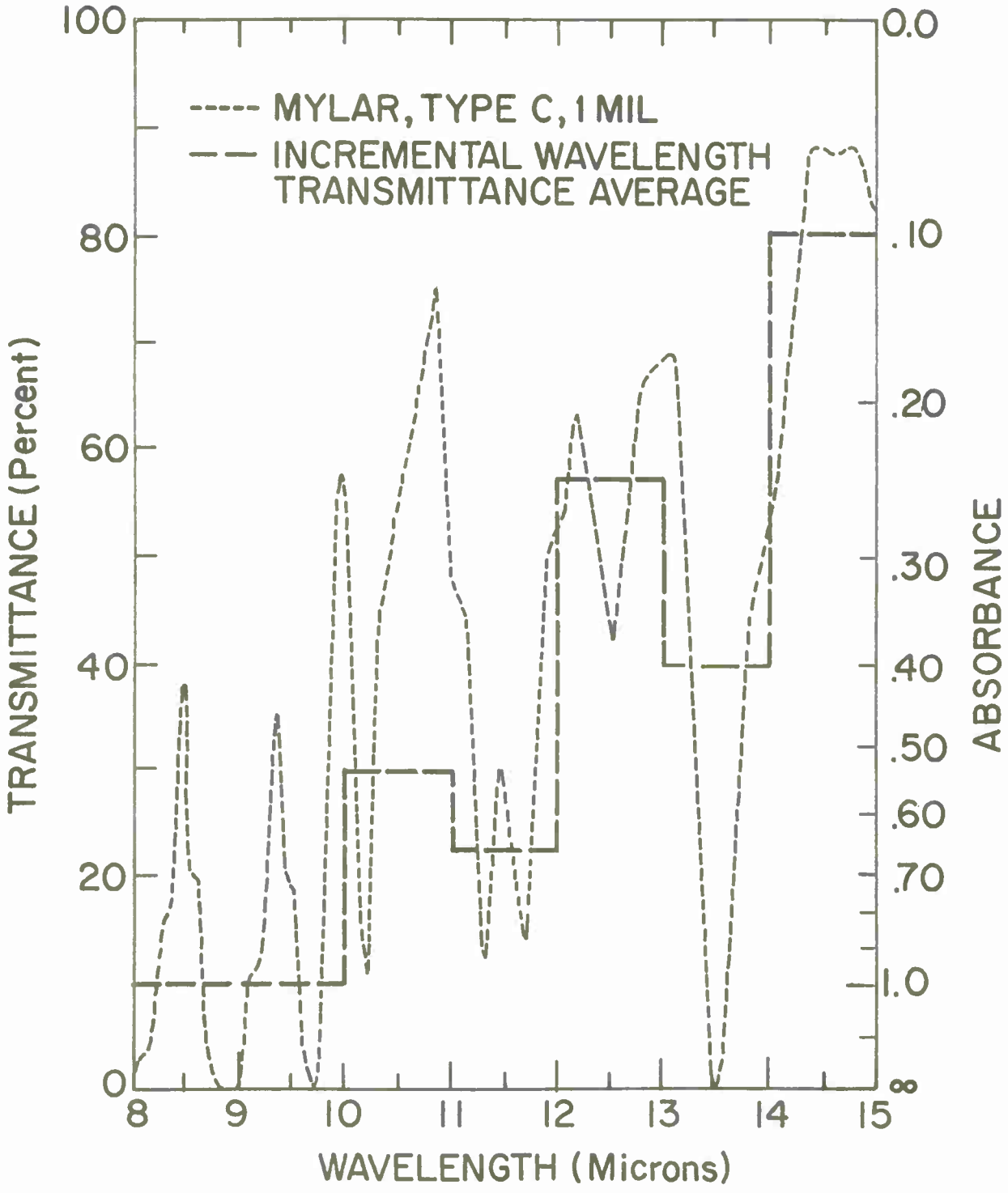

Figure 2b Absorption Spectrum for Mylar (High Range)

from this basic law we find that the transmissivity of 0.5 mil Mylar is:

$$\tau_{0.5} = \tau_{x}^{0.5/x}$$

Using this relationship we have derived the $\tau_{0.5}(\lambda)$ data for 0.5 mil Mylar from the 1.- mil. and 1.5 mil. Mylar data. The reflectance of such Mylar material is said to vary between 0.04 and 0.05 for the wavelength range of interest. Using the relationship that

$$\tau_{\lambda} + a_{\lambda} + r_{\lambda} = 1 \qquad (3)$$

a set of values of a_{λ} were calculated. This set of data is said to be set #1 of Mylar data.

Additional Mylar transmissivity data (set #2) was obtained from the Infrared and Optics Laboratory of the U. of Michigan Institute of Science and Technology. The curves of $\tau_{0.5}$ for the wavelength ranges 1-25 μm and 4-13 μm respectively, shown in figures 3 a and 3 b differs somewhat from the data of set #1. This set of data has also been used to derive a second set of a_{λ} data for 0.5 mil Mylar. The two sets of a_{λ} data, along with a_{λ}(eff) data calculated as outlined above are shown in table 5.

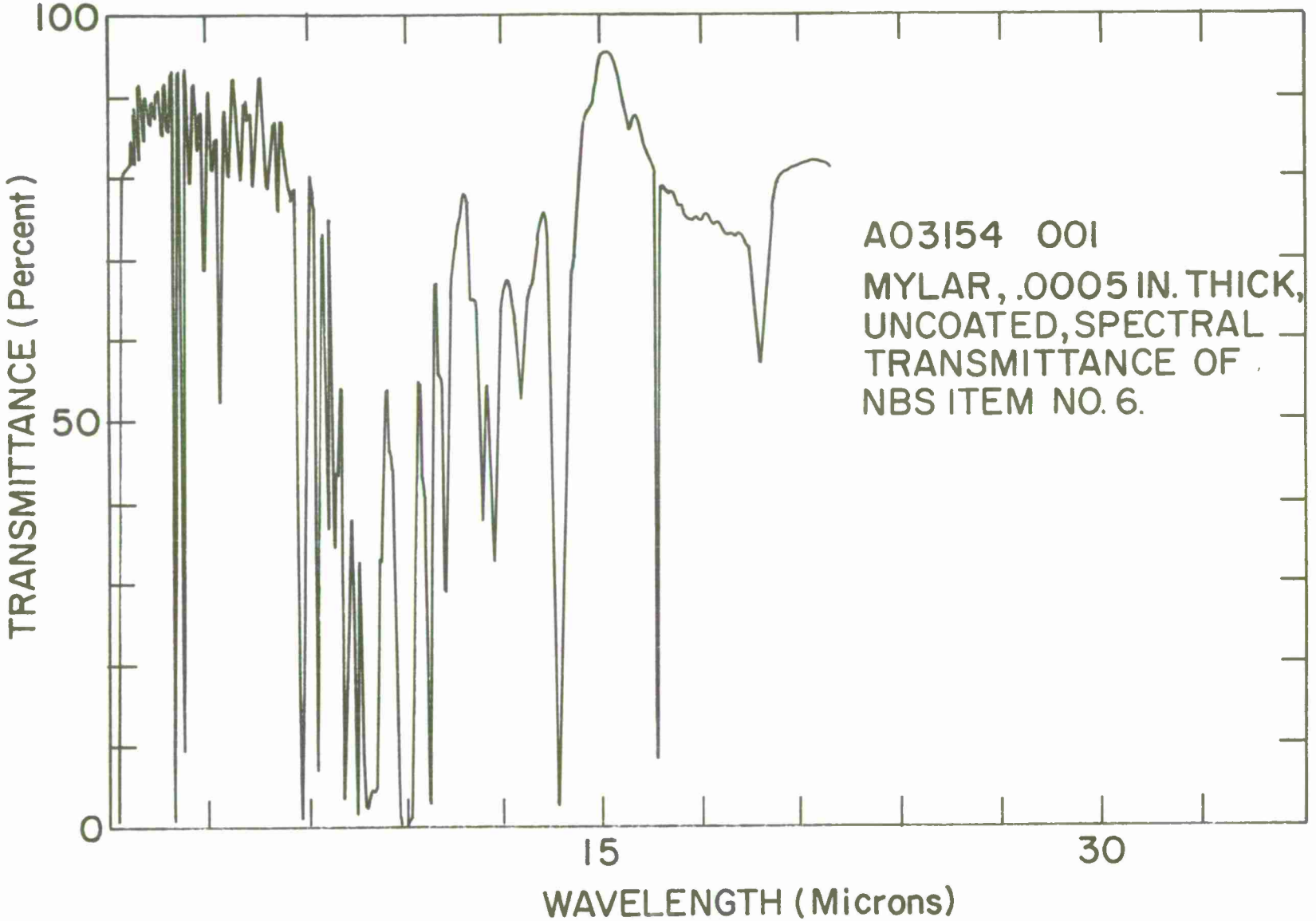

Figure 3a Spectral Transmittance for Uncoated Mylar 0.0005 inch Thick

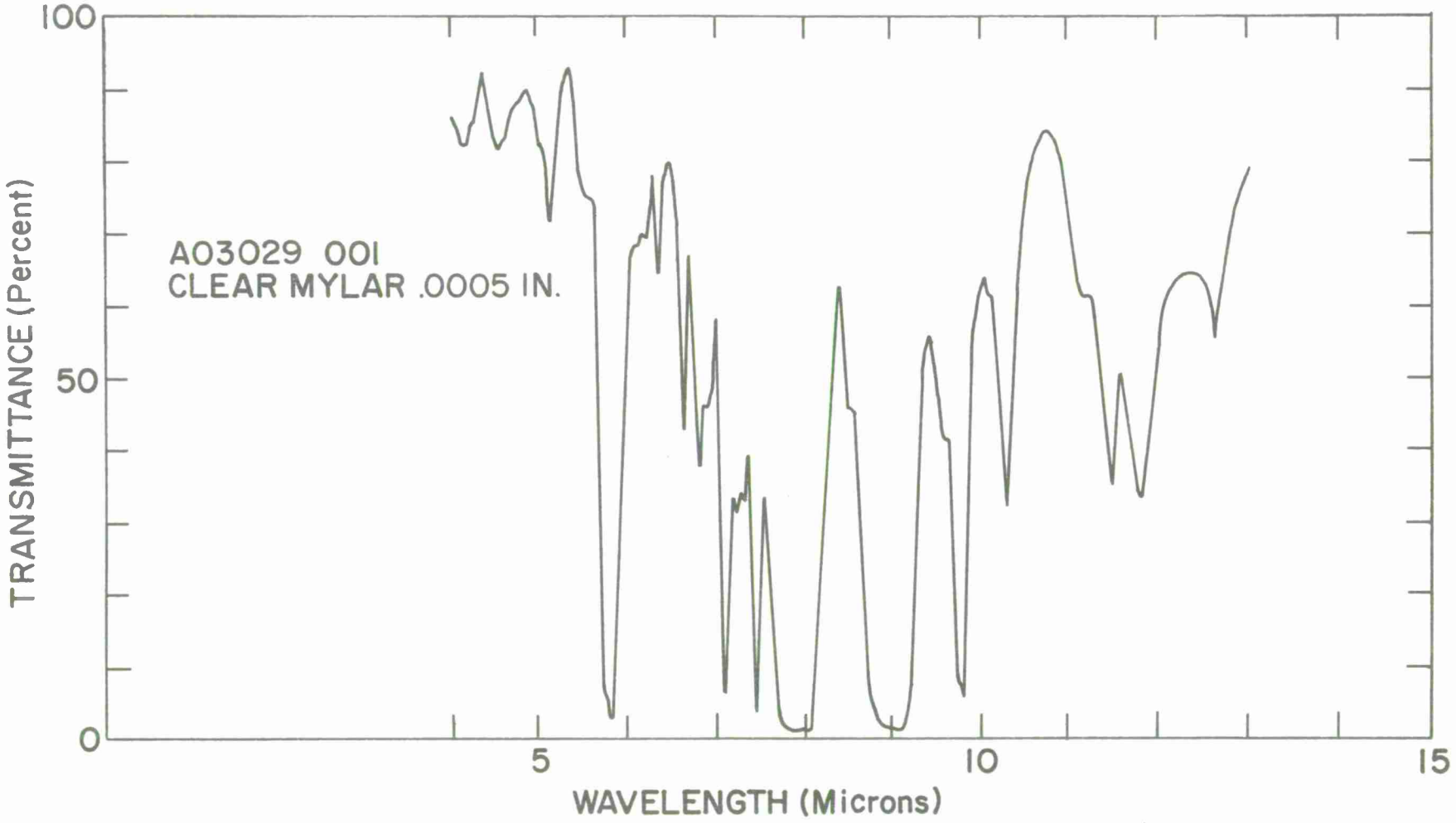

Figure 3b Spectrance Transmittance of Clear Mylar 0. 0005 inch Thick

Table 5. Thermal Characteristics of 0.5 mil Transparent Mylar

	Set #1				Set #2			
λ (μm)	τ_λ	r_λ	α_λ	α_λ(eff)	τ_λ	r_λ	α_λ	α_λ(eff)
0.2	--	0.04						
0.3	0.77		0.19	0.34				
0.4	0.91		0.05	0.10				
0.5	0.92		0.04	0.08				
0.6	0.93		0.03	0.06				
0.7	0.93		0.03	0.06		Same as		
0.8	0.94		0.02	0.04		Set #1		
0.9	0.95		0.01	0.02				
1.0	0.95		0.01	0.02				
1.1	0.96		--	--				
1.2	0.96		--	--				
1.3	0.96		--	--				
1.4	0.96		--	--				
1.5	0.95		--	--	0.88	0.04	0.08	0.15
2.0	0.94		0.02	0.04	0.86		0.10	0.19
2.5	0.92		0.04	0.08	0.84		0.12	0.23
3.0	0.87	0.05	0.09	0.17	0.83	0.05	0.12	0.23
3.5	0.92		0.03	0.06	0.82		0.13	0.24
4.0	0.92		0.03	0.06	0.80		0.15	0.28
4.5	0.92		0.03	0.06	0.81		0.14	0.26
5.0	0.88		0.07	0.14	0.78		0.17	0.31
5.5	0.60		0.35	0.57	0.33		0.62	0.84
6.0	0.77		0.18	0.33	0.65		0.30	0.51
6.5	0.65		0.30	0.51	0.48		0.47	0.71
7.0	0.41		0.54	0.77	0.23		0.72	0.89
7.5	0.34		0.60	0.82	0.09		0.86	0.94
8.0	0.52		0.43	0.67	0.30		0.65	0.86
8.5	0.41		0.54	0.77	0.20		0.75	0.91
9.0	0.46		0.49	0.73	0.20		0.75	0.91
9.5	0.55		0.40	0.63	0.30		0.65	0.86
10.0	0.66		0.30	0.51	0.50		0.45	0.69
10.5	0.80		0.15	0.28	0.70		0.25	0.43
11.0	0.66		0.29	0.49	0.50		0.25	0.69
11.5	0.57		0.38	0.61	0.40		0.55	0.78
12.0	0.76		0.19	0.34	0.57		0.38	0.61
12.5	0.76		0.19	0.34	0.62		0.33	0.55
13.0	0.84		0.11	0.21	0.43		0.52	0.76
13.5	0.44		0.51	0.75	0.35		0.60	0.82
14.0	0.83		0.12	0.23	0.77		0.18	0.33
14.5	0.91		0.04	0.08	0.90		0.05	0.10
15.0								

Aluminized Sphere

Data for the spectral reflectivity of aluminized mylar was obtained from reference 36. The spectral absorptivity was found by assuming that $\tau_\lambda = 0$ and that

$$\alpha_\lambda = 1 - r_\lambda \qquad (17)$$

Data obtained this way for the aluminum coating inside of the sphere (looking at mylar) and outside of the sphere (looking at aluminum) are given in table 6.

The thickness of the mylar material for the data of table 6 was 0.25 mil. The U. of Michigan aluminized spheres were of 0.5 mil. mylar flown with the aluminum coating facing outwards. No attempt has been made to estimate the absorptivity of such a sphere. Calculations were carried out only for the 0.25 mil aluminized sphere.

In this case the equation of radiation balance can be written as

$$\sum_\lambda \alpha_\lambda (H_{s\lambda} + B\, H_{e\lambda}) = 4 \cdot \sum_\lambda \epsilon_\lambda W_\lambda(T) \qquad (18)$$

where the values of α_λ were taken from table 6 and

$$\alpha_\lambda = \epsilon_\lambda$$

Table 6 Thermal Characteristics of Aluminized Mylar (0.25 Mil)

λ	Looking at Mylar		Looking at Aluminum	
	r_λ	α_λ	r_λ	α_λ
0.2	0.12	0.88	0.95	0.05
0.3	0.69	0.31	0.94	0.06
0.4	0.87	0.13	0.92	0.08
0.5	0.85	0.15	0.91	0.09
0.6	0.82	0.18	0.89	0.11
0.7	0.79	0.21	0.88	0.12
0.8	0.78	0.22	0.87	0.13
0.9	0.83	0.17	0.90	0.10
1.0	0.87	0.13	0.92	0.08
1.1	0.88	0.12	0.93	0.07
1.2	0.91	0.09	0.93	0.07
1.3	0.92	0.08	0.94	0.06
1.4	0.93	0.07	0.94	0.06
1.5	0.94	0.06	0.95	0.05
2.0	0.93	0.07	0.96	0.04
2.5	0.92	0.08	0.96	0.04
3.0	0.87	0.13	0.97	0.03
3.5	0.92	0.08	0.97	0.03
4.0	0.90	0.10	0.97	0.03
4.5	0.90	0.10	0.97	0.03
5.0	0.84	0.16	0.96	0.04
5.5	0.50	0.50	0.96	0.04
6.0	0.74	0.26	0.96	0.04
6.5	0.60	0.40	0.96	0.04
7.0	0.28	0.62	0.97	0.03
7.5	0.22	0.78	0.95	0.05
8.0	0.37	0.63	0.96	0.04
8.5	0.28	0.72	0.96	0.04
9.0	0.28	0.72	0.96	0.04
9.5	0.35	0.65	0.96	0.04
10.0	0.62	0.38	0.96	0.04
10.5	0.85	0.15	0.96	0.04
11.0	0.84	0.16	0.96	0.04
11.5	0.83	0.17	0.96	0.04
12.0	0.82	0.18	0.96	0.04
12.5	0.81	0.19	0.95	0.05
13.0	0.60	0.40	0.95	0.05
13.5	0.50	0.50	0.95	0.05
14.0	0.71	0.29	0.96	0.04
14.5	0.85	0.15	0.96	0.04
15.0				

Transparent Sphere with Aluminized Corner Reflector

In the case of the transparent Mylar sphere with aluminized corner reflector, it is assumed that all of the radiation which passes thru the transparent sphere is then alternately reflected by the aluminized corner reflector and the inside of the transparent sphere. In this case the effective absorptivity is given by:

$$\alpha_\lambda(\text{eff}) = \alpha_\lambda + \tau_\lambda \alpha'_\lambda + \tau_\lambda r'_\lambda \alpha_\lambda + \tau_\lambda r'_\lambda r_\lambda \alpha'_\lambda + \tau_\lambda (r'_\lambda)^2 r_\lambda \alpha_\lambda + \tau_\lambda (r'_\lambda)^2 (r_\lambda)^2 \alpha'_\lambda$$

$$= \alpha_\lambda \left[1 + \frac{\tau_\lambda r'_\lambda}{1 - r'_\lambda r_\lambda}\right] + \alpha'_\lambda \left[\frac{\tau_\lambda}{1 - r'_\lambda r_\lambda}\right]$$

Where the primed quantities refer to the aluminized Mylar corner reflector and the unprimed quantities to the transparent sphere. The values of α_λ, τ_λ, r_λ, used for the transparent sphere were taken from set 1 of table 5. Values of α'_λ and r'_λ were taken from table 6 for aluminized mylar with the aluminum coating facing outwards. These data and the calculated values of α_λ(eff) for the transparent sphere with inside corner reflector are given in table 7.

Table 7 Effective Absorptivity of Transparent Mylar Sphere with Aluminized Mylar Corner Reflector

λ	τ_λ	r_λ	α_λ	r_λ'	α_λ'	$\frac{\tau_\lambda}{1-r_\lambda' r_\lambda}\alpha_\lambda$	$1+\frac{\tau_\lambda r_\lambda}{1-r_\lambda' r_\lambda}$	$\frac{\alpha_\lambda' \tau_\lambda}{1-r_\lambda' r_\lambda}$	α_λ(eff)
0.2		0.04		0.95	0.05				0.00
0.3	0.77		0.19	0.94	0.06	0.80	0.33	0.05	0.38
0.4	0.91		0.05	0.92	0.08	0.94	0.09	0.08	0.17
0.5	0.92		0.04	0.91	0.09	0.95	0.07	0.09	0.16
0.6	0.93		0.03	0.89	0.11	0.96	0.06	0.11	0.17
0.7	0.93		0.03	0.88	0.12	0.96	0.06	0.12	0.18
0.8	0.94		0.02	0.87	0.13	0.97	0.04	0.13	0.17
0.9	0.95		0.01	0.90	0.10	0.99	0.02	0.10	0.12
1.0	9.95		0.01	0.92	0.08	0.99	0.02	0.08	0.10
1.1	0.96		--	0.93	0.07	1.00	--	0.07	0.07
1.2	0.96		--	0.93	0.07	1.00	--	0.07	0.07
1.3	0.96		--	0.94	0.06	1.00	--	0.06	0.06
1.4	0.96		--	0.94	0.06	1.00	--	0.06	0.06
1.5	0.95		--	0.95	0.05	0.99	--	0.05	0.05
2.0	0.94		0.02	0.96	0.04	0.98	0.04	0.04	0.08
2.5	0.92		0.04	0.96	0.04	0.96	0.08	0.04	0.12
3.0	0.87	0.05	0.09	0.97	0.03	0.91	0.17	0.03	0.20
3.5	0.92		0.03	0.97	0.03	0.97	0.06	0.03	0.09
4.0	0.92		0.03	0.97	0.03	0.97	0 06	0.03	0.09
4.5	0.92		0.03	0.97	0.03	0.97	0.06	0.03	0.09
5.0	0.88		0.03	0.96	0.04	0.92	0.13	0.04	0.17
5.5	0.60		0.35	0.96	0.04	0.63	0.56	0.03	0.59
6.0	0.77		0.18	0.96	0.04	0.81	0.32	0.03	0.35
6.5	0.65		0.30	0.96	0.04	0.68	0.50	0.03	0.53
7.0	0.41		0.54	0.97	0.03	0.43	0.77	0.01	0.78
7.5	0.34		0.60	0.95	0.05	0.36	0.81	0.02	0.83
8.0	0.52		0.43	0.96	0.04	0.55	0.66	0.02	0.68
8.5	0.41		0.54	0.96	0.04	0.93	0.76	0.02	0.78
9.0	0.46		0.49	0.96	0.04	0.48	0.72	0.02	0.74
9.5	0.55		0.40	0.96	0.04	0.58	0.62	0.02	0.64
10.0	0.66		0.30	0.96	0.04	0.69	0.50	0.03	0.53
10.5	0.80		0.15	0.96	0.04	0.84	0.27	0.03	0.30
11.0	0.66		0.29	0.96	0.04	0.69	0.48	0.03	0.51
11.5	0.57		0.38	0.96	0.04	0.60	0.60	0.02	0.62
12.0	0.76		0.19	0.96	0.04	0.80	0.33	0.03	0.36
12.5	0.76		0.19	0.95	0.05	0.80	0.33	0.04	0.37
13.0	0.84		0.11	0.95	0.05	0.88	0.20	0.04	0.24
13.5	0.44		0.51	0.95	0.05	0.46	0.74	0.02	0.76
14.0	0.83		0.12	0.96	0.04	0.87	0.22	0.03	0.25
14.5	0.91		0.04	0.96	0.04	0.96	0.08	0.04	0.12
15.0									

Incident Radiation

Values of spectral solar irradiance $H_{s\lambda}$, the spectral flux of thermal radiation from the earth $H_{\tau\lambda}$, both for clear skies and overcast conditions, and values of spectral bi-directional reflectance for the earth for clear sky and for overcast conditions are shown in table 8.

The spectral solar irradiance data were obtained from the Handbook of Geophysics (ref. 37). The spectral flux of thermal radiation from the earth was taken from reference 38 for clear sky conditions. These data were measured on a high altitude balloon flight over Palestine, Texas. For cloudy (overcast) conditions the spectral distribution of thermal radiation from the earth was taken from reference 39 (measured from the NIMBUS satellite).

The spectral bi-directional reflectance of the earth for clear sky conditions (including scattering from the atmosphere) were estimated by the author from data published in the report "The Reflectance and Scattering of Solar Radiation by the Earth" (reference 40). Two sets of data are given, since widely varying conditions can be met over the earth's surface.

Spectral bi-directional data for overcast conditions were also taken from a curve in reference 40 of data due to Novoseltsev (reference 42). The equation for $I_{E\lambda}$ is:

$$I_{E\lambda} = \frac{\rho_\lambda}{\pi} H_{s\lambda} + I_{T\lambda}$$

or

$$\begin{aligned} H_{E\lambda} &= \pi I_{E\lambda} \\ &= \rho_\lambda H_{s\lambda} + \pi I_{T\lambda} \\ &= \rho_\lambda H_{s\lambda} + H_{s\lambda} \end{aligned}$$

Values of solar irradiance and bi-directional reflectance are given for the wavelength range of 0.2 to 5.0 μm., the flux of thermal radiation covers the wavelength range 5.0 to 15.0 μm.

Night time conditions were simulated by letting the solar flux be zero without changing the thermal flux from the earth.

Table 8 -Radiation Data Used In Radiation Balance Calculations
Units of $H_{s\lambda}$ and $H_{T\lambda}$ are Watts/m^2 in that spectral interval

		Clear Sky			Overcast	
λ	$H_{s\lambda}$	$\rho_{\lambda 1}$	$\rho_{\lambda 2}$	$H_{T\lambda}$	ρ_{λ}	$H_{T\lambda}$
0.2	17.65	--	--		0.72	
0.3	109.64	0.10	0.15		0.72	
0.4	200.07	0.10	0.15		0.72	
0.5	193.00	0.10	0.15		0.71	
0.6	162.65	0.10	0.15		0.70	
0.7	127.82	0.15	0.20		0.70	
0.8	100.59	0.20	0.25		0.68	
0.9	80.53	0.20	0.25		0.66	
1.0	66.45	0.20	0.25		0.64	
1.1	55.14	0.15	0.20		0.62	
1.2	45.23	0.10	0.15		0.52	
1.3	36.38	0.10	0.15		0.47	
1.4	29.34	0.10	0.15		0.55	
1.5	84.63	0.10	0.15		0.45	
2.0	36.02	0.10	0.15		0.50	
2.5	17.71	0.10	0.15		0.35	
3.0	9.65	0.10	0.15		0.10	
3.5	5.69	0.10	0.15		0.10	
4.0	3.45	0.10	0.15		0.10	
4.5	2.24	0.10	0.15		0.10	
5.0				1.72		0.57
5.5				0.96		0.48
6.0				1.21		0.54
6.5				1.73		0.97
7.0				4.78		3.14
7.5				6.52		3.70
8.0				10.23		5.95
8.5				11.64		6.68
9.0				11.30		6.21
9.5				8.16		6.15
10.0				12.67		7.92
10.5				12.24		7.50
11.0				12.25		7.66
11.5				12.44		7.86
12.0				11.61		7.30
12.5				10.91		7.25
13.0				9.50		6.25
13.5				7.21		5.50
14.0				4.60		3.54
14.5				3.11		3.49
15.0						

Calculations and Results

A Fortran 4 program (IBM 360) was written for these calculations. For each case, the total solar flux input (direct and reflected from the earth) and the total thermal flux input were calculated. The Planck function was used for $W_\lambda(T)$, a mean value $W_{\bar{\lambda}}(T)$ being used for each 0.1 μm spectral interval. The proper mean temperature was obtained by successive approximation to make the total flux radiated from the sphere equal to the total absorbed flux.

Mean values of the sphere effective absorptivity for solar and thermal radiation and of the sphere effective emissivity for thermal radiation were also calculated.

Calculations were made for values of β corresponding to 80, 100, 120, 140 km. altitude.

The results obtained are shown in table 9, where equilibrium temperatures for the Robin and other spheres are shown. The following conclusions are apparent.

1. Equilibrium temperatures decrease only slightly with increasing altitude.
2. Equilibrium temperatures are only slightly different for transparent spheres with the different sets of α_λ(eff) data.
3. Equilibrium temperatures are only slightly different for the two different sets of earth reflectance data.
4. The significant differences between the spheres of different designs can be seen in the results for 140 km shown in the matrix below.

			U of M	
	Transparent Data Set #1	Transparent Corner Reflector	Aluminized inside	Aluminized outside
Overcast, Day	270.3	298.9	314.9	446.3
Clear(ρ_1), Day	262.3	282.3	294.0	396.0
Clear, Night	234.7	234.5	233.9	231.6
Overcast, Night	217.9	217.7	217.5	214.8
$\frac{\bar{\alpha}_s \text{ (eff)}}{\bar{\epsilon}_T \text{(eff)}}$	0.135	0.283	0.425	2.25

a) For each sphere, temperatures are highest for daytime overcast and lowest for nighttime overcast conditions

b) Nightime temperatures are essentially the same for all spheres

c) Daytime temperatures increase with increasing ratio of average effective solar absorptivity divided by average effective thermal emissivity.

d) The U of M aluminized sphere has significantly higher daytime equilibrium temperature than any of the other spheres

e) The "Robin" spheres have equilibrium daytime temperatures lower than the U of M aluminized spheres, but in the range of normal room temperatures.

Table 9. Equilibrium Temperatures of Robin and Other Spheres

Mylar Data					Clear Sky			Overcast		Equilibrium Temperature				$\bar{\alpha}_S$ (eff)	$\bar{\alpha}_T$ (eff)	$\bar{\epsilon}_T$ (eff)
1	2	3	4	5	$\rho_{\lambda 1}$	$\rho_{\lambda 2}$	Night	Day	Night	80km	100km	120km	140km			
x					x					264.0	263.3	262.8	262.3	0.07	0.52	0.50
x						x				265.5	264.8	264.3	263.8	0.07	0.52	0.50
x							x			237.0	236.1	235.4	234.7	--	0.52	0.48
x								x		272.3	271.5	270.9	270.3	0.08	0.51	0.50
x									x	220.0	219.0	218.6	217.9	--	0.51	0.47
	x				x					261.6	261.0	260.4	260.0	0.09	0.71	0.68
	x					x				263.1	262.4	261.9	261.3	0.09	0.71	0.68
	x						x			236.7	235.7	235.0	234.3	--	0.71	0.67
	x							x		267.3	266.6	266.0	265.5	0.09	0.70	0.68
	x								x	219.5	218.7	218.0	217.4	--	0.70	0.66
		x			x					284.2	283.1	282.7	282.3	0.15	0.53	0.52
		x				x				286.0	285.4	285.0	284.5	0.15	0.53	0.52
		x					x			236.8	235.9	235.2	234.5	--	0.53	0.50
		x						x		301.0	300.2	299.6	298.9	0.16	0.53	0.53
		x							x	219.8	219.0	218.4	217.7	--	0.53	0.49
			x		x					295.3	294.8	294.4	294.0	0.17	0.40	0.41
			x			x				298.0	297.5	297.1	296.6	0.17	0.40	0.41
			x				x			236.2	235.3	234.6	233.9	--	0.40	0.38
			x					x		317.1	316.2	315.6	314.9	0.17	0.39	0.42
			x						x	219.5	218.7	218.1	217.5	--	0.39	0.37
				x	x					397.5	397.0	396.6	396.2	0.09	0.04	0.04
				x		x				403.4	402.8	402.3	401.8	0.09	0.04	0.04
				x			x			233.9	232.9	232.2	231.6	--	0.04	0.04
				x				x		450.0	448.5	447.4	446.3	0.09	0.04	0.04
				x					x	216.9	216.1	215.4	214.8	--	0.04	0.04

1. Transparent 0.5 mil mylar sphere, set 1 α_λ(eff)
2. Transparent 0.5 mil mylar sphere, set 2 α_λ(eff)
3. Transparent 0.5 mil mylar sphere, set 1 α_λ(eff), with internal corner reflector of 0.25 mil aluminized mylar, aluminum coating facing outward.
4. Aluminized 0.25 mil mylar sphere, aluminum coating inside
5. Aluminized 0.25 mil mylar sphere, aluminum coating outside

E. Aerodynamic Heating Of Falling Spheres (F. F. Fischbach and F. L. Bartman)

The aerodynamic flow conditions for the Robin falling-sphere are shown in figure 4. The aerodynamic flow regimes based on the criteria:

$$3\,R_e^{1/2} < \frac{M}{R_e^{1/2}} \qquad \text{Free molecular flow regime}$$

$$\frac{1}{10} < \frac{M}{R_e^{1/2}} \leq 3R_e^{1/2} \qquad \text{Transition flow regime}$$

$$\frac{1}{100} < \frac{M}{R_e^{1/2}} \leq \frac{1}{10} \qquad \text{Slip flow regime}$$

$$\frac{M}{R_e^{1/2}} \leq \frac{1}{100} \qquad \text{Continuum regime}$$

are also shown in the figure.

For the typical sphere trajectory with 130 km apogee the following altitude layers correspond to the various regimes:

Free molecule	130 km - 128 km
Transition	128 km - 82 km
Slip	82 km - 61 km
Continuum	Below 61 km

Figure 4 Robin Falling Sphere Aerodynamic Flow Conditions for Peak Altitudes of 130, 100, 85 and 70 Km

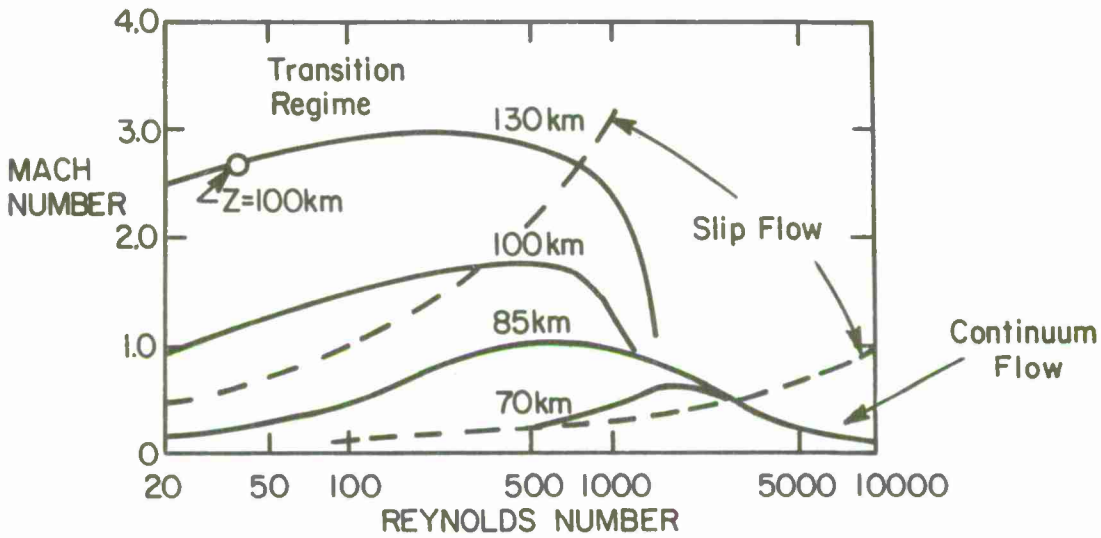

Continuum Regime

In the following, a discussion of continuum flow theory is used as a basis for consideration of the nature of heat transfer [Van Driest, 28] for application to falling spheres.

The Prandtl Number is defined as

$$Pr = c_p \mu / k$$

where

Pr = the Prandtl number

c_p = the specific heat at constant pressure

μ = the viscosity of the fluid

k = the thermal conductivity of the fluid

A value of Pr = 1 is assumed. This assumption implies that the total energy is constant throughout the boundary layer, even though the flow is not frictionless, and that the energy equation for adiabatic temperature changes applies. Laminar flow is also assumed (a condition most probably satisfied for the Reynolds number of the falling spheres).

Let ∞ indicate free-stream conditions behind the normal shock, w indicate wall, and a bar indicate mean conditions for a brief time period.

Under these conditions [Van Driest, 28] the continuity, momentum and energy equations are collected and integrated assuming that the temperature is a function of the velocity to find:

$$Cp\overline{T} = \alpha + \beta \bar{v} - \bar{v}^2/2 \qquad (20)$$

where α and β are integration constants, $\overline{T}$ is mean temperature and $\bar{v}$ is mean velocity.

The boundary conditions are

$$\overline{T} = T_w \text{ for } v = 0$$

$$\overline{T} = T_\infty \text{ for } \overline{v} = v_\infty \tag{21}$$

and, also:

$$\frac{v_\infty^2}{2c_p T_\infty} = \frac{\gamma-1}{2} M_\infty^2$$

where γ = the ratio of specific heats

M_∞ = the ratio of the free stream velocity to the velocity of sound in the free stream

therefore:

$$\frac{\overline{T}}{T_\infty} = \frac{T_w}{T_\infty} - \left(\frac{T_w}{T_\infty} - 1\right) \frac{\overline{v}}{\overline{v}_\infty} + \frac{\gamma-1}{2} M_\infty^2 \frac{\overline{v}}{\overline{v}_\infty} \left(1 - \frac{\overline{v}}{\overline{v}_\infty}\right) \tag{22}$$

and

$$\frac{q_w}{\tau_w} = c_p \frac{T_\infty}{v_\infty} \left[\left(1 - \frac{T_w}{T_\infty}\right) + \frac{\gamma-1}{2} M_\infty^2\right] \tag{23}$$

where q_w = the rate of heat flow at the wall

τ_w = the shear stress

For an insulated boundary layer $q_w = 0$ and equations (22) and (23) yield:

$$\frac{\overline{T}}{T_\infty} = \frac{T_w}{T_\infty} - \frac{\gamma-1}{2} M_\infty^2 \frac{\overline{v}^2}{v_\infty^2} \tag{24}$$

Equations (21) and (24) give:

$$\frac{\overline{T}}{T_\infty} = \frac{T_w}{T_\infty} - \frac{\overline{v}^2}{2c_p T_\infty} \tag{25}$$

and:

$$C_p T_w = C_p \overline{T} + \frac{\overline{v}^2}{2} = \text{constant} \tag{26}$$

Equations 24), 25), and 26) are for insulated walls.

Equations 23) and 26) yield, in the general case of heat transfer to or from the boundary layer.

$$q_w = (C_p \tau_w / v_\infty)(T_{w_{ins}} - T_w) \tag{27}$$

where $T_{w_{ins}}$ = the temperature the wall would acquire if the boundary layer were insulated.

We can define the heat transfer coefficient, h, as follows:

$$q_w = h\,(T_{w_{ins}} - T_w) \tag{28}$$

then

$$h = C_p\, \tau_w / v_\infty \tag{29}$$

The Stanton number is defined as a dimensionless heat-transfer coefficient

$$C_{H_\infty} = h / C_p\, \rho_\infty v_\infty \tag{30}$$

where ρ_∞ = the free stream mass density

If the local friction coefficient is taken to be

$$c_{f_\infty} = 2\, \tau_w / \rho_\infty v_\infty^2 \tag{31}$$

then

$$C_{H_\infty} = 1/2\; c_{f_\infty} \tag{32}$$

If we accept the von Karman and Tsien (Ref. 29) laminar flow analysis we can compute the skin-friction coefficient and the boundary layer thickness from empirical relations derived by Van Driest (Ref. 28):

$$C_{f_\infty}\left(R_\infty\right)^{1/2} = 1.33(1+.12\, M_\infty^2)^{\frac{z-1}{2}} \tag{33}$$

$$\frac{\delta}{x}\left(R_\infty\right)^{1/2} = 5.2(1+.09 M_\infty^2)^{\frac{z+1}{2}}. \tag{34}$$

where

$$R_{\infty} = \frac{\rho_{\infty} v_{\infty} x}{\mu_{\infty}}$$

and x is the coordinate along the surface in the direction of the free stream, measured from the leading edge.

And z is defined by the viscosity power law:

$$\frac{\mu_w}{\mu_{\infty}} = \left(\frac{T_w}{T_{\infty}}\right)^z \tag{35}$$

The classical theory has thus provided a complete solution except for the problem associated with the assumption of Prandtl Number=1.0. In actual fact, the insulated wall temperature will vary from the total free-stream temperature and Pr≠1.

This variation is defined in terms of a recovery factor, r.

$$r = \frac{T_{w_{ins}} - T_{\infty}}{T(1+.2M^2) - T_{\infty}} \tag{36}$$

Experiment shows $r = (Pr)^{1/2}$, thus

$$T_{w_{ins}} = T\left[1+.2(Pr)^{1/2}M^2\right] \tag{37}$$

Since Pr is actually about .75 at our temperature, $(Pr)^{1/2} = .87$, and,

$$T_{w_{ins}} = T(1+.17M^2) \tag{38}$$

This correction also applies to 33) and 34) which become, with z taken equal to .76.

$$c_{f_{\infty}} \left(R_{\infty}\right)^{1/2} = 1.33\ (1+.1M^2)^{-.12} \tag{39}$$

$$\frac{\delta}{x} \left(R_{\infty}\right)^{1/2} = 5.2\ (1+.078M^2)^{+.88} \tag{40}$$

The correction is thus negligible at low Mach numbers.

It remains to integrate Equation 28) with respect to surface area and time. This is difficult to handle since on a sphere the selection of appropriate free-stream Reynolds numbers, position of boundary-layer separation, and method of treating the wake are not straightforward.

For free-stream Reynolds numbers based on a characteristic length equal to the distance from the forward stagnation point along the sphere surface we require a mean distance for use in calculations. In the regime of sphere Reynolds numbers (based on diameter) of from 24 to 450 we shall assume an increase of wake separation angle of 0° to 72°. Above 450 we will assume a constant 72°. If the mean condition is assumed to occur one-third of the way between stagnation point and separation point, as on a cone, the characteristic length would be

$$\frac{180^{\circ}-0^{\circ}}{180^{\circ}} \frac{\pi d}{6} = .524d \quad (Re=24) \tag{41}$$

$$\frac{180^{\circ}-72^{\circ}}{180^{\circ}} \frac{\pi d}{6} = .315d \quad (Re\ 450) \tag{42}$$

It is readily seen that one-third the free-stream Reynolds number based on sphere diameter should furnish a close approximation for Re>450. The area of the portion of the sphere contiguous to the boundary layer will be

$$A = 4\pi r^2 - 2\pi rh$$

where

$$h=4(1-\sin 18^{\circ}) = .693r$$

Therefore $A = 2\pi r^2(2-.693)=2.05d^2$, and a simple approximation will be $A = 2d^2$

The remainder of the sphere surface area $0.693 \cdot 2\pi r^2$, is in contact with the vortical wake. The wake will be treated as a vortex consisting of a discrete mass of gas originating as the inner lamina of the boundary layer. It is reasonable to assume that the temperature of this gas approaches that of the sphere wall by the time of separation from the sphere surface. The vortex shedding frequency based on Strouhal Numbers between .2 and 2 2 ($Sr = Fd/v_\infty$, where F is shedding frequency) ranges from 60 to 180 cycles per second. This corresponds to Reynolds numbers from 10^3 to 10^4. This frequency is so high that no heat exchange is assumed effected between the sphere and the wake. The Strouhal numbers below Reynolds numbers of about 1000 are not known and the wake vortex is just periodic below the lower critical Reynolds number which is about 450. Therefore, in the region $Re<450$ we shall assume that the entire sphere area of πd^2 is subject to the same heat exchange given in Eq. 9 , and also that the characteristic length in the Reynolds number and heat transfer coefficient formulae for $Re<450$ is $\pi d/4$.

If we integrate Equation 28) with respect to surface area we get

$$\frac{1}{A}\frac{dq_w}{dt} = h \quad T(1+.17M^2) - T_w \tag{43}$$

where $h = C_{H\infty} \; c_p \; \rho_\infty \; v_\infty = 1/2 \, c_{f_\infty} \; c_p \; \rho_\infty \, v_\infty$

and $$c_{f_\infty} = \frac{1.33\,(1 + .12\,M_\infty^2)^{-.12}}{\sqrt{R_\infty}}$$

whence $$h = .67\,(1 + .12\,M^2)^{-.12} \; c_p \frac{\sqrt{\mu_\infty}}{\sqrt{x}} \sqrt{\rho_\infty v_\infty}$$

since $$Pr = c_p \mu / k = c_p \mu_\infty / k_\infty$$

$$h = .67\,(1 + .12\,M^2)^{-.12} \quad Pr \; k_\infty \sqrt{R_\infty} \quad x^{-1}.$$

Thus

$$\frac{1}{A}\frac{dq_w}{dt} = 1.33\,(1+.12M^2)^{-.12}\ \frac{Pr\,k_\infty\sqrt{R_\infty}}{2x}\,T(1+.17M^2)-T_w \tag{44}$$

We now investigate the empirical determination of mean characteristic length to use in equation 44). Measurements by Stine and Wanlass (Ref. 24) and by Crawford and McCauley (Ref. 22) are not completely applicable for the following reasons:

1. The bodies measured were hemispheres followed by cylinders,

2. The average value of Nusselt number is given where Nu=hx/k and x is the characteristic length. However $h=q/(T_r-T_w)$ therefore not only an average Nusselt number is required but an average recovery temperature. The authors fail to give such an average recovery temperature.

Measurements by Stalder and Nielsen (Ref. 23) are also subject to the first problem. Measurements by several authors which are compiled by McAdams (Ref. 27) are apparently based on heat transfer to a complete sphere but the methods are not specified and one assumes many of the data are from turbulent flows.

The theoretical methods of Sibulkin and Korobkin have also been investigated (Refs. 25, 26). Sibulkin has based his method on conditions at the stagnation point and experiment shows his method is applicable only within 45° of stagnation. Korobkin has modified this theory for incompressible flow but again only for hemispheres.

The method of attack which seems most satisfactory is as follows:

1. Knowing the laminar flow characteristics of the sphere at $Re > 1000$ (based on diameter) we shall extrapolate the measurements of Crawford and McCauley by the Stine and Wanlass theory to a position 108° from the stagnation point.

2. Integrate the parameter Nusselt number divided by the square root of Reynolds number along the surface of the sphere and find the mean $N_u / \sqrt{Re}$. The Nusselt number and Reynolds numbers here are based on a characteristic length equal to the distance around the perimeter of the sphere from the stagnation point.

3. Having found the mean $Nu/\sqrt{Re}$, determine the mean characteristic length.

4. Knowing the mean characteristic length, determine the ratio of the local temperature outside the boundary layer to the stagnation temperature at the point on the sphere one characteristic length from the stagnation point.

5. Using a recovery factor equal to the square root of the Prandtl number the recovery temperature, T_r, defined by

$$(Pr)^{1/2} = \frac{T_r - T_{local}}{T_{stagnation} - T_{local}}$$ can be determined.

The Prandtl number we use to determine the recovery temperature should be based on the local condition outside the boundary layer. This is in good agreement with experiment.

The above procedure has been carried out and the mean characteristic length has been found to be almost exactly 45° from the stagnation point. The ratio of local temperature outside the boundary layer to stagnation temperature at this point is 0.81

Putting $x = \frac{\pi d}{8}$ in equation 44) gives

$$\frac{dq_w}{A\,dt} = 1.33\,(1 + .12\,M^2)^{-.12}\,\frac{Pr}{2}\,k_\infty \left(\frac{\rho_\infty v_\infty \pi d}{\mu_\infty 8}\right)^{\frac{1}{2}} \frac{8}{\pi d}\,\left[T\,(1 + .17M^2) - T_w\right]$$

or, with Re based on sphere diameter,

$$\frac{dq_w}{A\,dt} = 1.33\,(1 + .12M^2)^{-.12}\sqrt{Re_\infty}\,\frac{k_\infty}{d}\sqrt{\frac{2}{\pi}}\,Pr\,\left[T\,(1 + .17\,M^2) - T_w\right] \tag{45}$$

Thus the mean Nusselt number based on sphere diameter is

$$Nu_{mean} = \frac{dq_w}{dt}\,\frac{d}{A k_\infty\,\left(T_{stag} - T_w\right)}$$

$$= 1.33(1+0.12M^2)^{-.12}\sqrt{Re_\infty}\sqrt{\frac{2}{\pi}}\,Pr \tag{46}$$

These equations require $Re > 450$. For $Re < 450$ we assume $x = \frac{\pi d}{4}$ and $A = \pi d^2$ and replace $\frac{2}{\pi}$ with $\frac{1}{\pi}$ in equations (45) and (46).

We shall now verify our solution with experiments at several Mach numbers. It must be borne in mind that our solution should give a smaller average heat transfer coefficient than any of the experiments on hemispheres because our reference area includes the region from 90^o to 108^o which has less heating than those regions nearer the stagnation point. On the other hand, our average heat transfer coefficient when multiplied by the reference area, $2d^2$, must yield more heat transfer than the hemisphere experimenters' heat transfer coefficients multiplied by $\frac{\pi}{2} d^2$. Therefore, our Nu_{sphere} must satisfy $\frac{\pi}{4}\,Nu_{hemisphere} < Nu_{sphere} < Nu_{hemisphere}$. The results are as shown in table 10.

TABLE 10

Comparison of Average Heat Transfer Parameters

Nusselt No. / Reynolds No.$^{1/2}$

Mach No.	Present Method (Spheres)	Korobkin Incompressible Theory Ref.26 (Hemispheres)	Stine & Wanlass Ref. 24 (Hemispheres) Exper.	Stine & Wanlass Ref. 24 (Hemispheres) Theory	Crawford & McCauley Ref. 22 (Hemispheres)	Stalder & Nielsen Ref. 23 (Hemispheres)	McAdams Summary Ref. 27 (Spheres)
	Reference Area is $2d^2$	Reference Area is $\frac{\pi d^2}{2}$ For All					Reference Area is πd^2
<0.3	.793	.940	--	--	--	.908	$.37\,Re^{0.1}$
1.75	.760	--	--	--	--	.948	FOR
1.97	.754	--	.760		.780	--	$17<Re<7x10^4$
2.67	.732	--	--	--	--	.920	At
5.04	.670	--	--	--	--	.819	All Mach Nos.
6.8	.634	--	--	--	.742	--	

These results show our method in very good agreement with experiments other than those quoted in McAdams. McAdams shows data which vary by 65% and also notes two other experiments which would have been 50% and 80% lower than the others if plotted. Also some experiments were based on irregular particle settling and others on mass transfer characteristics. Most are liquid flows with no reference to turbulence.

This method then is a theoretical method with the mean characteristic length determined by experiment. It is also Mach number dependent and applicable to subsonic as well as supersonic flow.

To summarize, then based on conditions behind a normal shock (or subsonic free-stream) and on sphere diameter:

$$\frac{dq_w}{dt}\,\frac{d}{k_\infty A\ T(1+.17M^2)-T_w} = N_u = 1.33(1+.12M^2)^{-.12}\sqrt{Re}_\infty\sqrt{\frac{2}{\pi}}\ Pr \qquad (46)$$

where

$$A = 2d^2 \text{ and } Re > 450$$

and

$$N_u = 1.33(1+.12M^2)^{-.12}\sqrt{Re}_\infty\sqrt{\frac{1}{\pi}}\ Pr \qquad (47)$$

where

$$A = \pi d^2 \text{ and } re < 450$$

Free-Molecular Flow

Although virtually none of the trajectory is in the free molecular flow region, free molecular flow theory can be used to provide an upper bound to the aerodynamic heating of the Robin sphere. The method we shall employ is to compute the aerodynamic heating in the free molecule region by use of the Newtonian impact theory, which for drag and lift at least has been proved very accurate for hypersonic flows. This theory gives an upper bound on heating, obtained from the assumption that all of the drag energy has been converted to heat on the sphere surface. The Newtonian theory says that the air is composed of inelastic particles which lose all momentum normal to a surface upon striking it and move with undiminished momentum tangentially.

The maximum energy which is available for aerodynamic heating for a sphere falling through a distance h with a change in vertical velocity of from V_1 to V_2 is:

$$\text{Available Energy} = mgh + \frac{1}{2} m(V_1^2 - V_2^2) \tag{48}$$

where

m = sphere mass

g = acceleration of gravity

h = vertical distance

V_1, V_2 = initial and final velocity

If the sphere falls through this distance in time t, then the average power available for heating is:

$$\text{Max Aero. Power} = \frac{mgh + \frac{1}{2} m (V_1^2 - V_2^2)}{t} \tag{49}$$

A calculation of the average power available for heating has been carried out for the trajectory of a 1 meter sphere. Results are shown in figure 5. The maximum power available for aerodynamic heating is shown as a function of altitude. It is assumed that this energy heats the sphere uniformly, as it might if the sphere rotates rapidly enough, and the temperature increase of the sphere as a function of time is calculated as follows.

Assuming that the sphere starts at 106 km with a temperature of 298.9°K (the radiative equilibrium temperature of a Robin sphere at 140 km under overcast day conditions), the temperature is determined from:

$$C\frac{dT}{dt} = \text{Max Aero. Power} + \text{Radiation Input} - \text{Radiation Loss}$$

At the start, under equilibrium conditons $\frac{dT}{dt} = 0$ and

Max Aero Power = 0, therefore:

$$(\text{Radiation Input})_{\text{Start}} = (\text{Radiation Loss})_{\text{Start}}$$
$$= \bar{\epsilon} \cdot \pi d^2 \cdot \sigma T_o^4 \qquad (50)$$

The radiation input is assumed to be constant at this value for the entire calculation. The radiation loss at any time t, with temperature T is:

$$\text{Radiation Loss} = \bar{\epsilon} \cdot \pi d^2 \cdot \sigma T^4$$

Thus:

$$C\frac{dT}{dt} = \text{Max Aero Power} + \bar{\epsilon} \cdot \pi d^2 \cdot \sigma T_o^4 - \bar{\epsilon} \pi d^2 \sigma T^4 \qquad (51)$$

For a given time interval, the change in temperature can be calculated by successive approximations. For the one meter sphere, the temperature vs. altitude curve is also shown in figure 4. Values of the parameters used in this calculation are:

Figure 5 Maximum Power Available for Heating Sphere, "Newtonian Sphere Temperature and Stagnation Temperature as a Function of Altitude

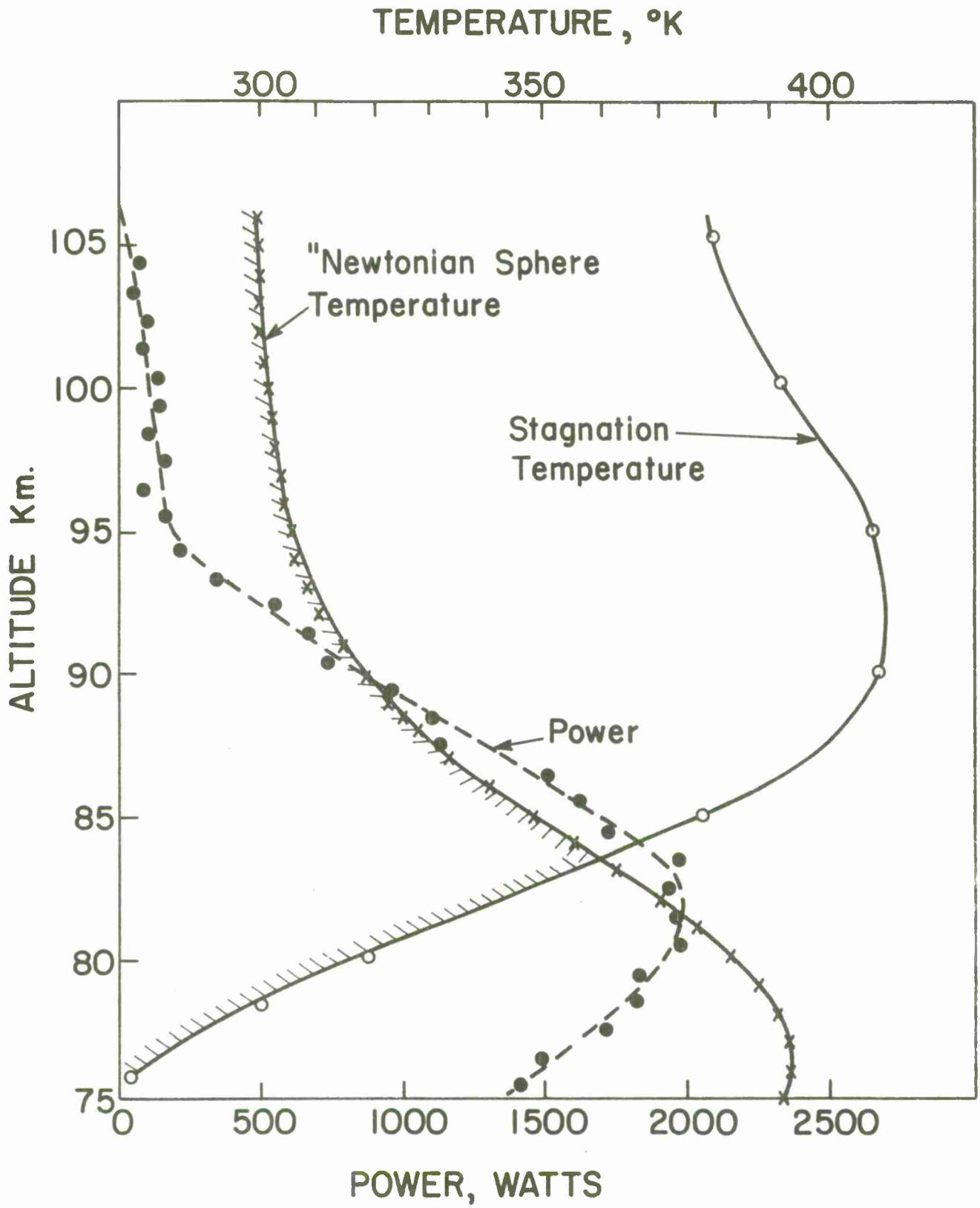

$\bar{\varepsilon} = 0.53$

$\sigma = 5.672 \cdot 10^{-8}$ watts$\cdot$ m.$^{-2}$ ^{o}K.$^{-4}$

$T_o = 298.9$

$C = 190.8$ joules/^{o}K.

Note that the max possible aerodynamic heating is a maximum at 80-84km and the maximum temperature is at 81-82km.

A maximum safe temperature for mylar is 423^{o}K. It can be seen that even with the maximum possible aerodynamic heating at all parts of the trajectory, this temperature is not approached. Actually, the heating is much less than this as predicted by the continuum theory developed above.

For the 80-81 km layer, according to the continuum theory, for example:

$$\frac{dq_w}{dt} = \frac{N_u \cdot K_\infty \cdot A}{d} \left[T(1+0.17M^2) - T_w\right]$$

and

$$N_u = 1.33(1+0.12M^2)^{-.12}\sqrt{Re_\infty} \cdot \sqrt{\frac{2}{\pi}} \cdot Pr \qquad (47)$$

Using Pr=0.75

$$Re_\infty = \frac{\rho \cdot V \cdot d}{\mu_\infty}$$

$$\frac{T_\infty}{T} = 1+0.17M^2 = 1+0.17(2.28)^2 = 1.89$$

$$\frac{\mu}{\mu_\infty} = \left(\frac{T}{T_\infty}\right)^{0.76} = \left(\frac{1}{1.89}\right)^{0.76} = 0.62$$

$$\frac{K}{K_\infty} = \frac{\mu}{\mu_\infty} = 0.62$$

$$A = 2d^2$$

d =1meter $\mu = 1.216 \cdot 10^{-5}$ kg-m$^{-1}\cdot$sec^{-1}

M=2.31 $K = 3.9 \cdot 10^{-3}$ cal$\cdot$ m$^{-1}\cdot$ sec$^{-1}\cdot$ ^{o}K^{-1}

V=625 m/sec. $T_w = 325^{o}$K (assumed)

$= 2 \cdot 10^{-5}$ kg$\cdot$ m^{-1} $T = 180^{o}$K

$$N_u = 1.33(1+0.12 \cdot 2.31^2)^{-.12} \sqrt{\frac{2 \cdot 10^{-5} \cdot 625}{1.96 \cdot 10^{-5}}} \sqrt{\frac{2}{\pi}} \cdot 0.75$$

$$= 1.55 \cdot 23.55 \cdot 0.712$$

$$= 20.7$$

$$T(1+0.17M^2) - T_w = 1.89 \cdot 180 - 325 = 15.0$$

$$\frac{dq_w}{dt} = 20.7 \cdot 6.3 \cdot 10^{-3} \cdot 2 \cdot 15.0$$

$$= 3.82 \text{ cal/sec} = 16.4 \text{ Watts}$$

The continuum theory with the data assumed above thus predicts aerodynamic heating of about 1% of the maximum possible aerodynamic heating given by Newtonian impact theory at this portion of the trajectory.

The aerodynamic heating will actually depend on the sphere temperature. As the sphere heats up, the heat transfer to the sphere decreases. An upper limit is set by the stagnation temperature.

$$T_s = T_\infty (1+0.17M^2) \qquad (52)$$

The stagnation temperature vs altitude is also shown in figure 5.

The combination of the two temperature curves in figure 5 define very nicely an upper bound for the sphere temperature. Above about 83 km, the upper temperature limit is set by the "Newtonian" impact theory (starting at 105 km. with a radiation equilibrium temperature of 298.9^{o}K. Below 83 km the upper temperature limit is set by the stagnation temperature.

Considering the very low value of aerodynamic heating predicted by the continuum theory at 81 km, and realizing that this is the region of maximum heat transfer so that the heating at all other altitudes is very much smaller, leads to the conclusion that the sphere will never rise significantly above the radiation equilibrium temperature.

F. Heat Transfer Within the Sphere (F. F. Fischbach and F. L. Bartman)

Heat transfer within the Robin sphere will take place by radiation, conduction and convection from the sphere and corner reflector surface to the liquid isopentane and to gaseous isopentane. This problem has not yet been considered in all necessary detail because an accurate model, suitable for analysis has not yet been formulated. Some consideration has been given to heat transfer from the sphere to liquid isopentane and from the sphere to gaseous isopentane.

One extremely simplified calculation can readily be carried out. This concerns the transfer of heat by conduction from the sphere to liquid isopentane. The total volume of 18.6 grams of liquid isopentane is

$$V = \frac{18.6}{162} = 30 \text{ cm}^3$$

If the liquid isopentane were uniformly distributed over the inside surface of a 1 meter sphere the layer thickness would be

$$\delta = \frac{30}{\pi 10^4} = 9.56 \cdot 10^{-4} \text{cm.}$$

The heat transfer by conduction across such a thickness would be extremely quick, for

$$q = KA \cdot \frac{\Delta T}{\Delta x} \qquad (53)$$

and for isopentane $K = 8 \cdot 10^{-3} \frac{TU}{\text{Hr. ft.}^{\circ}\text{F}}$

For each cm.^2 of surface the rate of heat conduction would be

$$q = \frac{8 \cdot 10^{-3} \cdot 1.076 \cdot 10^{-3}}{60 \cdot 9.56 \cdot 10^{-4} \cdot 3.281 \cdot 10^{-2}} \frac{9}{5} 17.58 \cdot \Delta T \text{ Watts}$$

$$= .125 \Delta T \cdot \frac{\text{joules}}{\text{sec.}}$$

The energy required to vaporize the liquid isopentane in each cm^2. of liquid would be.

$$q = \frac{18.6}{72.15} \cdot \frac{5878 \cdot 4.138}{\pi \cdot 10^4} = .202 \text{ joules}$$

The time required to transfer enough heat by conduction to vaporize the isopentane in this extremely simplified example is

$$t = \frac{.202}{.125\Delta T} = \frac{1.62}{\Delta T} \quad \text{seconds}$$

where ΔT is the temperature difference in $^{o}K.$ across the surface.

If only a fraction f of the sphere inside surface area were covered uniformly with liquid pentane, the time required to transfer enough heat to vaporize the isopentane would be:

$$\Delta t = \frac{1.61}{f \cdot \Delta T} \quad \text{seconds} \qquad (54)$$

The reader may determine the time Δt for the f and ΔT that he favors.

In most of the temperature history computation a great simplification obtains fromthe ability to consider the sphere, gas, and capsule to have no temperature gradients. To justify such a procedure it is necessary to calculate the rate of heat transfer within the sphere.

The Mylar sphere proper will probably have no strong gradients. The assumption is that all spheres during descent rotate randomly sufficiently to distribute the aerodynamic (and radiant) heating over the surface. We shall therefore neglect gradients in the skin.

The capsule in other than the Australian system rolls around the inner surface of the sphere at or near the stagnation point under the influence of drag deceleration and rotation of the sphere. Accordingly it is good contact with the surface. Since the capsule makes up only a small percentage of the specific heat of the sphere system, since aluminum has excellent thermal conductivity, and since it is in good contact with the skin the capsule is assumed to remain at the same temperature as the skin.

The isopentane gas contributes about 16% of the Robin mass and about the same portion of the system specific heat. The transfer of heat between Mylar and isopentane is to be calculated. The sphere rotation is assumed to have continued sufficiently long that all the gas is rotating with the same angular velocity as the sphere. There is no appreciable flow relative to the surface.

A portion of the isopentane is presumed to have evaporated as indicated in section C above. We are now concerned with heat transfer by conduction, convection, and radiation between the Mylar and the isopentane gas.

The conduction would be a simple and straightforward calculation except for the heat transfer coefficient between the Mylar surface and isopentane gas. If we assume no surface resistance that is, an infinite heat transfer coefficient we may use a Williamson and Adams graphical method, (reference 30) for conduction. Let

T_s = initial Mylar temperature

T_g = initial isopentane temperature

T = temperature of isopentane at center of sphere at time t

k = thermal conductivity of isopentane, .01 BTU/hr^{o}F ft (at 180^{o}F)

ρ = density of isopentane, 18.6x6/π gm. m^{-3}(Robin)

C_p = specific heat, isopentane, 0.5 cal/^{o}C-gm

r_s = radius of sphere, 0.5 m

We define X as a dimensionless time ratio:

$$X = kt/\rho c_p r_s^2 \qquad (55)$$

And define Y as the unaccomplished temperature change:

$$Y = \frac{T_s - T}{T_s - T_g} \qquad (56)$$

$$X = \frac{.01 \times \pi \times t(hr) \times 3.28 \times 9 \times 252}{18.6 \times 6 \times .5 \times .25 \times 5}$$

$$X = \frac{234}{69.8} \; t \; (hr) = .0558 \; t \; (min)$$

From the Williamson-Adams chart we now plot Y in % vs. time for the sphere center and do the same for the Gurney-Lure (reference 31) chart at the center and the 1/2 radius position. It is clear that an effective conduction occurs and no serious error will result if the skin and gas are considered isothermal.

Unaccomplished Temperature Change			Time
Williamson-Adams	Gurney-Lurie		
At Center	At Center	At 1/2 Radius	(min)
100%	100%	100%	0
91%	90%	--	1
62%	67%	31%	2
40%	42%	21%	3
21%	24%	12%	4
7%	7.5%	3.5%	6

However, this analysis assumed no surface resistance, an unconservative assumption. To obtain a measured heat transfer coefficient was not possible. If we assume surface resistance is the controlling factor, then by assuming no temperature gradient in the gas, we have:

$$-\log Y = 3 \; hr \; X/k \qquad (57)$$

where h is the heat transfer coefficient. Since r = 0.5 m, we have

$$\frac{hr}{k} = hx164 \quad \frac{ft^2 hr\,^oF}{BTU}$$

If h were as small as $\frac{1}{82}$ BTU/ft^2 -hr -^{o}F, the Gurney-Lurie chart gives:

Unaccomplished Temperature Change at Sphere Center (%)	Time (min)
100%	0
92%	1
84%	2
73%	3
60%	4
35%	6
24%	8

A comparable heat transfer coefficient in a flow of air with Re $\doteq$ 625 was h $\doteq$ .089 BTU/hr -ft^2 -^{o}F, an order of magnitude greater. It therefore appears safe to assume transfer by conduction of sufficient heat to hold the sphere isothermal for our present purposes. In all likelihood, the heat-transfer coefficient will be on the order of 0.1 BTU/ft^2 -^{o}F -hr or greater with consequent negligible surface resistance.

To be safer, we see if convection occurs as well. We wish to define the proper Grashof No. for enclosed spaces. The usual formulae for enclosed spaces do not apply in our case since we are interested in the heat transfer from a surface to a gas only, and not the transfer from the gas to a second surface.

As an approximation we consider the convection of vertical planes to gases. According to McAdams, data of King, Colburn and Jakob and Linke were all correlated and the results showed that the convective heat

transfer for various shapes, including spheres, could be stated by the one equation for vertical planes. The shape is unimportant. In the turbulent range the shape factor cancels out. In the laminar range the heat-transfer coefficient is inversely proportional to the fourth root of the shape factor. McAdams further states that the data for spheres fall in a range where the shape factor has substantially no influence.

The appropriate convective heat-transfer equation is:

$$N_u = c(G_r P_r)^n \tag{58}$$

where

$$N_u = h_c r/k \tag{59}$$

$$G_r = r^3 \rho^2 g\beta(T_s - T_g)/\mu^2 \tag{60}$$

$$P_r = C_p \mu / k \tag{61}$$

c and r are arbitrary constants

$$\beta = \frac{1}{T}$$

For: $G_r P_r = 10^{12}$ to 3.5×10^7, c=.13 n=.33

$G_r P_r = 10^4$ to 3.5×10^7, c=.55 n=.25

$G_r P_r \quad 10^4$ the Weise-Saunders curve is used.

When $G_r P_r \quad 10^3$ it may be assumed that convection is suppressed and conduction controls.

In our case:

$$k = 4.1 \times 10^{-5} \text{ cal/cm-sec-}^{o}\text{C}$$

$$\beta = \frac{1}{300} \quad {}^{o}\text{K}^{-1}$$

$$G_r = \frac{.5^3 \times 18.6^2 \times 6^2 \times 9.8 \ \Delta T}{2 \times 300 \times 3^2 \times 10^{-6} \ {}^{o}\text{K}} = 57.4 \times 10^4 \ \Delta T/{}^{o}\text{K}$$

$$P_r = \frac{c_p \mu}{k} = \frac{.5 \times 3. \times 10^{-5}}{41 \times 10^{-5}} = .366$$

Therefore the product of Grashof and Prandtl numbers is

$$G_r P_r = 2.1 \times 10^5 \ \Delta T/{}^{o}\text{K}$$

and convection is not suppressed, thus greatly aiding conduction in the transfer of heat between Mylar and isopentane. The constants for, say, a 10^{o} temperature difference are

$$G_r P_r = 2.1 \times 10^6$$

$$c = .55$$

$$h = .25$$

Then

$$h_c = \frac{k}{r} Nu = \frac{k}{r} \times .55 \times (2.1 \times 10^6)^{1/4} \qquad (62)$$

$$h_c = \frac{4.1 \times .55 \times 1.2 \times 31.62}{10^5 \times 50} \frac{cal}{cm^2 {}^{o}C\ sec} = 1.7 \times 10^{-5} \frac{cal}{cm^2 {}^{o}c\ sec}$$

Thus

$$q_c = h_c A \Delta T$$

or for the Robin sphere

$$q_c = 1.7 \times 10^{-5} \pi\ 10^4 \Delta T \text{ cal/sec}$$

$$q_c = .53 \Delta T \text{ cal/sec.}$$

Comparing this with conduction let us consider the result calculated for no surface resistance. In that case the average volume of gas lay at a radius $.8\ r_s$ (because $.8^3 = .5$). Returning to the Curney-Lurie chart we find that in 2 minutes at this radius the gas is heated to 84% of ΔT. Thus:

$$\Delta q = 18.6 \text{ gm } \frac{.5 \text{ cal}}{gm\ {}^{o}C} \quad \frac{.84\ T}{120 \text{ sec}} = .065\ \Delta T \text{ cal/sec}$$

which is an order of magnitude less than the convective transfer, and yet it is sufficient to allow us to neglect temperature gradients within the sphere.

The result is that convective transfer within the sphere is controlling, that the heat transfer between skin and gas is accomplished effectively in a

fraction of a minute, that convection is assisted by conduction which is at least an order of magnitude less, and that we may consider the entire sphere assembly isothermal.

In this analysis we have neglected entirely the radiative transfer of heat between Mylar and isopentane.

G. Chemical Reaction On Sphere Surface

The falling sphere will be heated due to the recombination of atomic oxygen when it occurs.

The energy of one molecular recombination is 5.1 eV. Since $1eV=3.826\times10^{-20}$ cal, the energy equals 19.5×10^{-20} cal/molecule.

The CIRA, 1965 atmosphere gives a curve of atomic oxygen number density versus altitude. Integration of this curve from 70 to 140 km gives

$$\int_{70}^{140} n(O_1)\,dz = 90\times10^{20} \text{ atoms/ } m^2. \qquad (63)$$

If the cross-sectional area of the sphere is A(meters^2), the time to traverse 140 to 70 km is 125 sec and the probability of an atom recombining is P, then the average heat input is:

$$\frac{Q}{t} = \frac{19.5}{2} \times \frac{10^{-20}}{125} \times 90\times10^{20} \times AP = 7.0\,AP\ \frac{cal}{sec}$$

(The 2 in the denominator arises because only one-half the recombination energy is from theimpinging atom.)

The probability has been estimated at .02 to 0.1. Let us assume P = .05

	Robin	Univ-Mich.	Australia
A (m^2)	$\pi/4$	$\pi/9$	π
$\frac{\overline{dQ}}{dt}$ (cal/sec)	.275	.122	1.1
ΔQ (cal)	34.4	15.2	138.

The peak concentration of atomic oxygen at 100 km is approximately 3 times the average concentration. The velocity at 100 km is close to maximum and is about 1 1/2 times the average velocity, thus the maximum heating due to atomic oxygen occurs at 100 km and is:

	Robin	Univ.-Mich.	Australia
$\frac{dQ}{dt}$max (cal/sec)	1.24	.55	4.95

These heating rates are, in general, negligible compared to other sources of heating.

V. Isopentane As The Inflatant

A. Discussion

Earlier studies reported in references 1 and 2 relative to the selection of an inflatant compound have been thoroughly reviewed. We consider the theoretical work to have been correct and the testing to have been pertinent and meaningful. Of the several chemicals evaluated, isopentane was chosen for a variety of reasons. We consider these reasons well founded.

There are two basic concerns stemming from the use of isopentane neither of which dictates a change. The first is its volatility under standard conditions which creates problems in sealing and storing capsules. This is fundamental to its required volatility at low pressures and potential substitute compounds can fare no better. Further, the Australian system has experienced satisfactory seals as has the Michigan 66-cm system (although a recent procurement of identical capsules by Sandia Corp. was partly defective), which indicates the problem can be surmounted. The second concern is whether sufficient heat was available for vaporization--in case previous temperature analyses were erroneously high. Flight histories have indicated that inflation usually is not a problem. However there is no justification for changing the inflation compound, and no substitute with improved overall qualities has been found.

Isopentane evaporation has been considered theoretically, but not in all necessary detail, in other parts of this report. There is some reason to believe that under some conditions not all of the isopentane is evaporated with the resulting loss of sphere pressure.

B. Isopentane Compendium

ISOPENTANE

There was no compendium of the chemical and physical properties of isopentane, hence the available information was collected and is published here.

ISOPENTANE $\equiv$ 2 - METHYL BUTANE

$$CH_3 \cdot CH_2 \cdot CH(CH_3)_2 = C_5 H_{12}$$

Molecular Weight = 72.15

Density:

$D_4^{20} = 0.61963$ gr cm.$^{-3}$ $D_4^{25} = 0.61455$ gr cm.$^{-3}$ $D_4^{20} = 0.61967$ gr cm.$^{-3}$

In the above the superscript refers to the temperature at which the density was determined, the subscript refers to the temperature of water to which the above density is referred.

$D = 0.6865$ (-50°c) gr cm.$^{-3}$

$D = 0.6146$ ($+30^{\circ}$c) gr cm.$^{-3}$

Mole Volume: (20°K)

Supercooled state 85.1 cm^3

Crystallized state 82.7 cm^3

Freezing Point:

-159.9°C. (113.1°K)

Melting Point:

112.6°K [Parks]

Boiling Point:

@760 mm: 27.852°C

27.9°C

27.95°C

Heat of Fusion:

1226.3 cal/mol

1232.2 cal/mol

1222.1 cal/mol

16.94 cal/g [Parks]

Heat of Vaporization

(298.16°K) 5878$\pm$ 5 cal/mol

5937 cal/mol

Dew Point:

@624 mm 22.1°

@265 mm 0.24°

Critical Temperature:

187.0°C, 460.96°K

Critical Pressure:

32.9 atm, 25018 mm

Critical Density:

0.234 g/ml

Heat Capacity:

Solid:

13°K	1.07	cal/°K/mol
20°K	3.25	"
80.4°K	0.217	cal/°K/g
102.0°K	0.279	"
110°K	20.75	cal/°K/mol
110°K	20.99	"

Fluid:

115°K	29.46	cal/°K/mol
120°K	29.68	"
120.5°K	0.409	cal/°K/g
275.8°K	0.521	"
290°K	40.49	cal/°K/mol
300°K	39.55	"

Gaseous at Cp:

C_p^o	250°K	24.52	cal/°K/mol
	317.2°K	30.65	"
	454°K	40.49	"
	487.05°K	43.00	"
C_p^o	1500°K	78.55	"

Vapor Pressure:

183.33°K	0.74 mm	
221.67°K	15.14 mm	
217.21°K	10.95 mm	"Bad measurements of Schumann" - Aston '64
295.2 °K	620.98 mm	

$\left\{\begin{matrix} 240^{o}K & 0.066 \text{ atm} \\ 443^{o}K & 25.1 \text{ atm} \end{matrix}\right.$

$\left\{\begin{matrix} -56.9^{o} & 10 \text{ mm} \\ +57.6^{o} & 1500 \text{ mm} \end{matrix}\right.$

$\left\{\begin{matrix} 16.29^{o} & 500.74 \text{ mm} \\ 28.59^{o} & 779.48 \text{ mm} \end{matrix}\right.$

-22.8^{o} 86 mm

Pressure Dependence of Boiling Point:

$.03815^{o}$/mm [Lamb & Roper]

^{o}C	mm Hg
28.587	779.48
28.160	768.08
27.673	755.31
27.240	744.11
26.773	732.12
22.435	627.97
16.291	500.74

[Willingham]

$$H^{p}_{vap} = .002614\ T_b^2 \left[\frac{dp}{dT}\right]_{T_b}$$ (Clausius - Clapeyron)

$$(T_A/T_B)_{P_1} = (T^1_A/T^1_B)_{P_2}$$ (Ramsay-Young rule)

Also: $(dp/dT)_{T_b}$ = 26.31 mm/^{o} for C_5H_{12}
27 for similar compounds

Here H_{vap} assumed independent of T, thus

$$dp/dT = p\ H_{vap}/RT^2$$

combined with Trouton's Rule, we have:

$$\left[dp/dT\right]_{T_b} = \frac{7975}{T_b}$$

Viscosity:

-50°	.0055 g/cm-sec
$+30^{\circ}$	.00205 "
$+30^{\circ}$	.00208 "
0°	.00278 "
$+20^{\circ}$	00225 "

Surface Tension:

10°	16.10 dyn/cm
15°	15.54 dyn/cm
20°	15 00 dyn/cm

Enthalpy:

Ideal gas state	200°K 2888 cal/mol
	1500°K 77, 740 cal/mol

Entropy:

Ideal gas state	200°K 72.50 cal/$^{\circ}$/mol
	1500°K 168.61 cal/$^{\circ}$/mol
Liquid	291.16°K 62.24 ± .1 cal/$^{\circ}$/mol

Other Specific References:

Isothermal compressibility at 0°, 50°, 95°

at pressure 9000 kg/cm^2 - Meyer

Molecular strength of fluid isopentane - Meyer

Relative viscosity, pressure 30, 000 kg/cm^2 - Bridgman

Internal friction of vapor at various pressures

at 25° - Day

at 25° and 100° - Bleakey

Computation over the relation between vapor pressure, temperature,

and density of fluid isopentane - Meissner & Paddison

Equation of state - Su & Chang (2)

Joffe

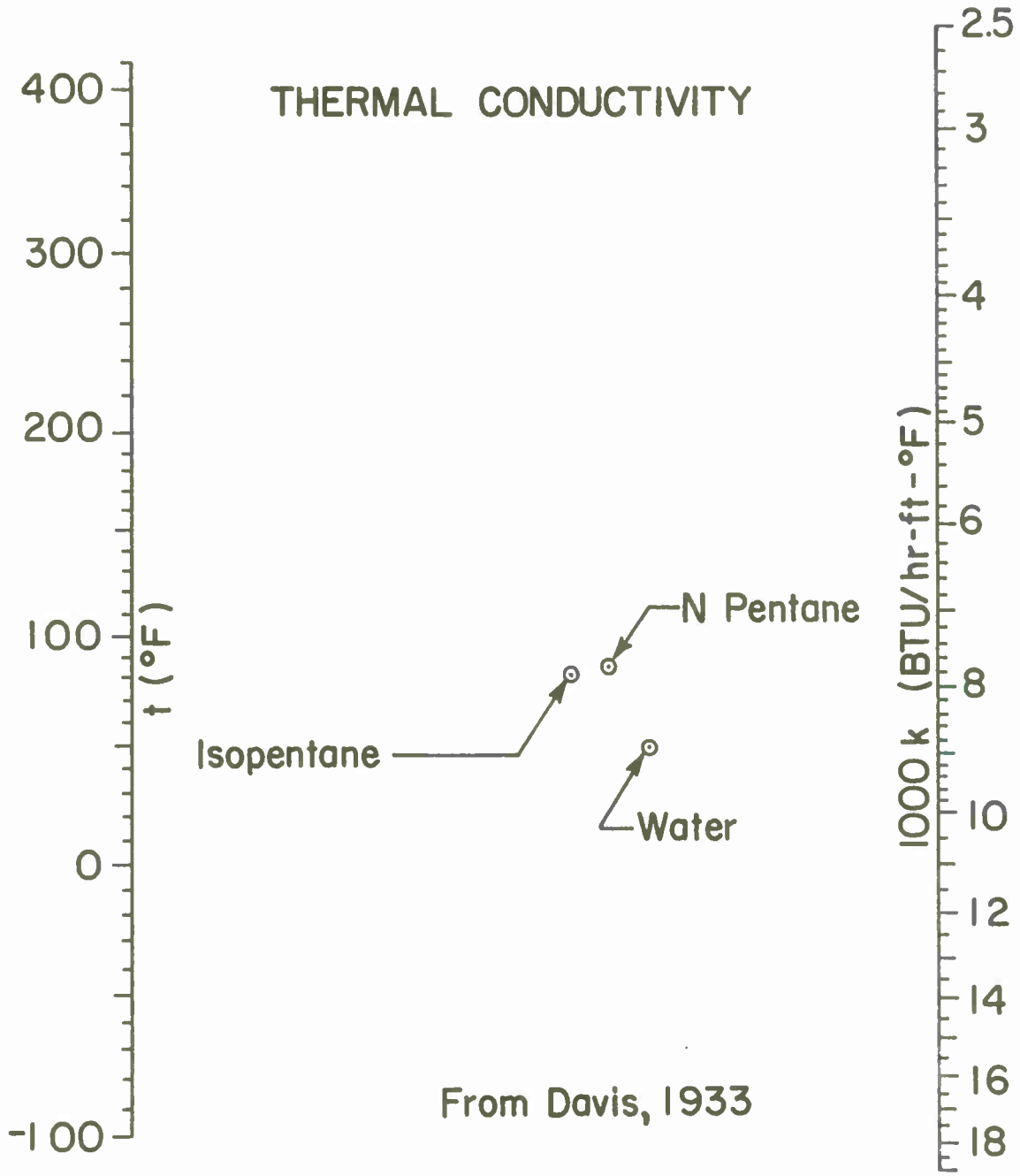

Figure 6 Thermal Conductivity of Isopentane

SPECIFIC HEAT RATIO:

The following graphical method of determining the specific heat ratio as a function of temperature and pressure is from Edmister, 1940:

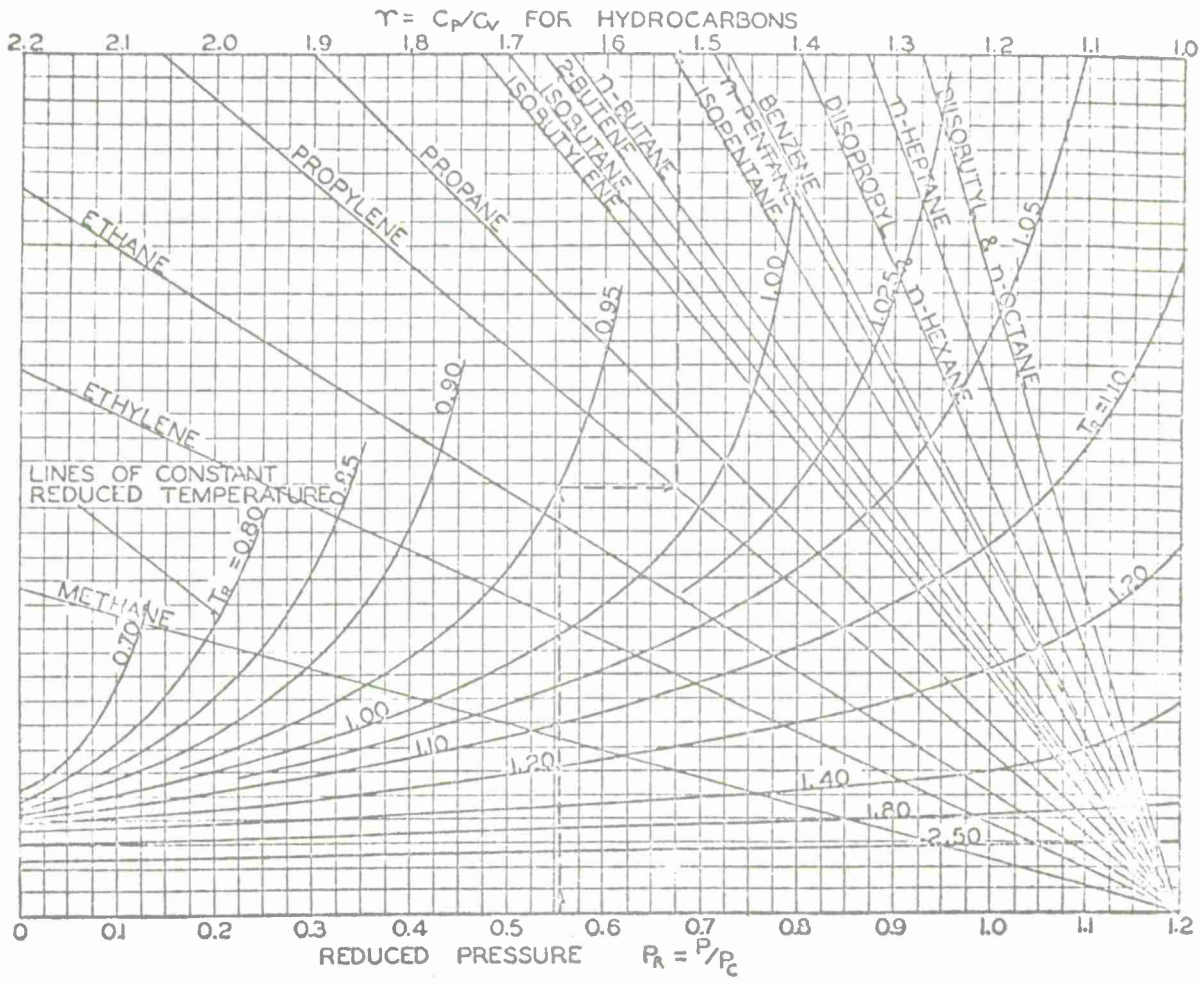

Figure 7 Specific Heat Ratio ($\gamma = C_p / C_v$) for Hydrocarbons

VAPOR PRESSURE FROM COX, 1936

If $\log_{10} P = A\,(1 - B/T)$

where P is pressure, atm.
B is boiling point, ^{o}K
T is temperature, ^{o}K
A is a function of T

Then for isopentane

$$\log_{10} A = 0.64079 + 0.19185\,(1 - T_R)\,(.85 - T_R)$$

where T_R = reduced temperature.

This formula fits the experimental data of Young which are shown in the curve of Copson and Frolich.

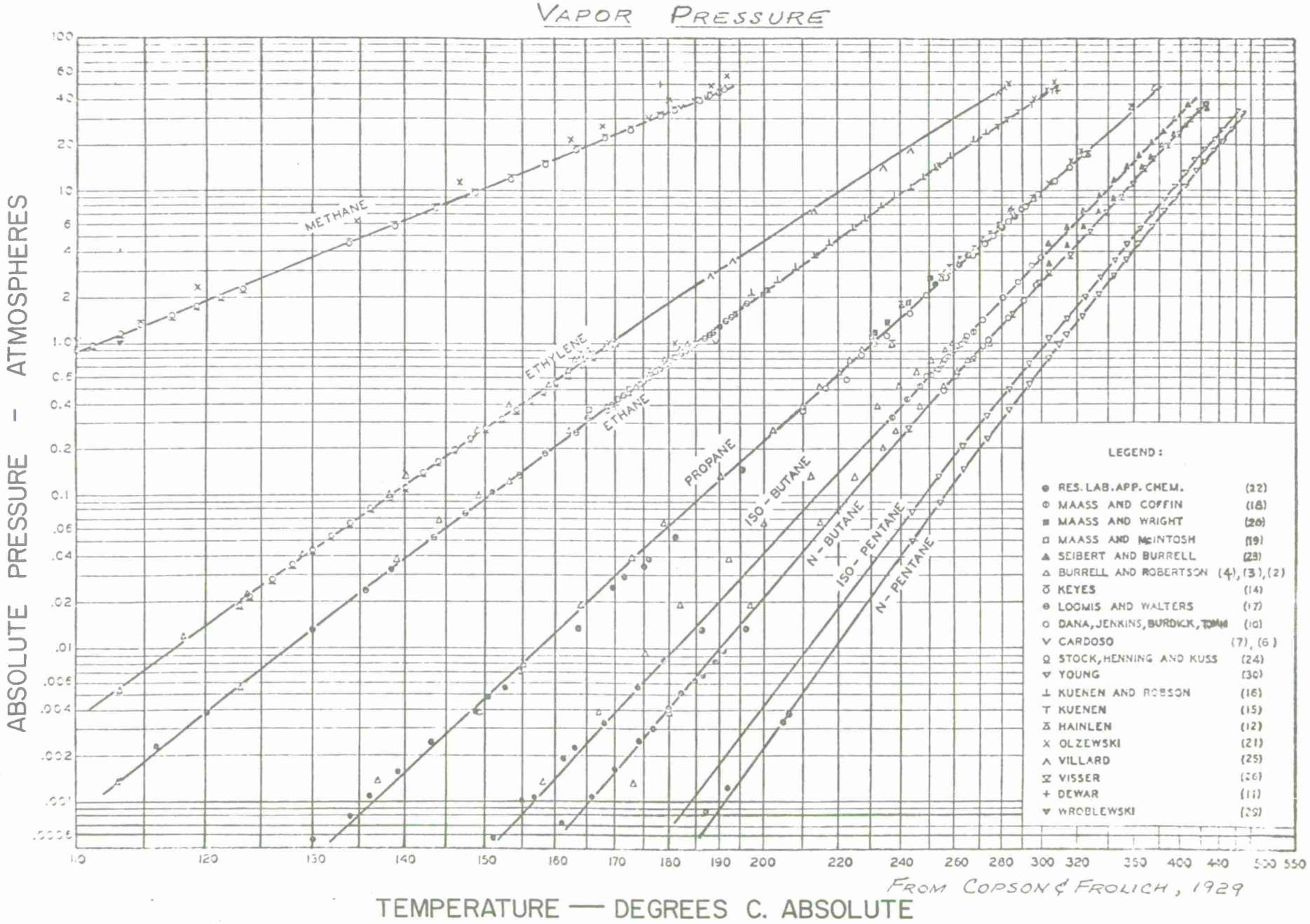

Figure 8 Vapor Pressure vs Temperature for Some Hydrocarbons

Bibliography

Aston, Am. Soc., 64.

Bleakey, Physics 3, 123, 1932, C. I, 180, 1933.

Bridgman, Proc. Am. Acad. Arts. Sci. 77, 123, C. A. 4069, 1949.

Copson and Frolich, Ind. Eng. Chem, 21, 1117, 1929.

Cox, Ind. Eng. Chem, 28, 615, 1936.

Davis, Ind. Eng. Chem, 33, 677, 1941.

Edmister, Ind. Eng. Chem, 32, 373, 1940.

Day, Phys. Rev. 2 40, 287, 1932.

Guthrie & Hu, Am. Soc., 65, 1141.

Joffe, Am. Soc., 69, 541, 1947.

Lamb & Roper, Am. Soc., 62, 8, 1940.

Meissner & Paddison, Ind. Eng. Chem, 33, 1191, 1941.

Meyer, Z. Physik. Chem. A, 173, 114, 1935.

Parks, et al, Am. Soc., 52, 1037.

Schumann, et al, Am. Soc., 64, 1041.

Scott, et al, Am. Soc., 73, 1707.

Su & Chang, Am. Soc., 68, 1081, 1946.

Su & Chang, Ind. Eng. Chem., 38, 805, 1946.

Willingham, et al, J. Res. Bur. Stds. 35, 239, 1945.

VI. Sphere Leak Analysis

A. Testing Considerations

Let
- d = sphere diameter
- T = temperature of gas, absolute
- m = mass of gas
- V = sphere volume
- $\mathcal{T}$ = Mylar thickness
- A = area of pin-hole orifice
- C = orifice coefficient
- s = hoop stress
- e = strain of mylar
- E = Young's Modulus, mylar = 550×10^3 psi
- v = velocity of gas in orifice
- p = pressure of gas
- ρ = density of gas
- γ = ratio of specific heats
- t = time
- M = molecular weight
- R = gas constant

subscripts
- o = initial (ambient)
- d = at deflation
- p = "performance requirement"
- g = ground test
- f = flight case

When the Viper-Dart Robin is ground tested in accordance with MIL-B-27373 A (USAF) it must meet the following performance requirement:

When filled with air at a pressure of atmospheric plus 35 mb, at a temperature of 213°K, the pressure loss shall not exceed 1 mb per hour.

Each sphere is subject to the following individual test:

When filled with air at a pressure of atmospheric plus 10 mb, temperature unspecified, the pressure loss shall be less than 0.5 mb in 30 minutes.

In flight the sphere is filled with isopentane weighing 18.6 gms. which should produce an average overpressure of approximately 10 mb. if the temperature-time history is suitable. The sphere should not lose more than 1 mb in 20 minutes.

We shall examine the adequacy of the ground testing, because the flow through an orifice on the ground will be radically different from that in flight.

We shall consider the expansion of the sphere as well as the gas compression. Our expansion will be considered isothermal in which case:

$$\frac{\rho}{\rho_o} = \frac{p}{p_o}$$

Since

$$\frac{m}{m_o} = \frac{\rho V}{\rho_o V_o} = \frac{\rho}{\rho_o} \frac{d^3}{d_o^3} = \frac{\rho}{\rho_o} (1+e)^3$$

then

$$\frac{m}{m_o} = \frac{p}{p_o} (1+e)^3 \qquad (64)$$

Differentiation of the logarithms yeilds

$$\frac{\dot{m}}{m} = \frac{\dot{p}}{p} + \frac{3\dot{e}}{1+e}$$

where $\dot{m} = \frac{dm}{dt}$

$$\dot{p} = \frac{dp}{dt}$$

$$\dot{e} = \frac{de}{dt}$$

Since

$$e = \frac{s}{E} = \frac{\pi d^2}{4} \frac{(p-p_o)}{\pi \tau d E}$$

$$e = \frac{\Delta p}{4 \tau E / d} \tag{65}$$

where

$$\Delta p = p - p_o$$

and

$$\dot{e} = \frac{\dot{p}}{4\tau E/d}$$

then

$$\frac{\dot{m}}{m} = \frac{\dot{p}}{p} \left(1 + \frac{3p}{4E\tau/d + \Delta p} \right) \tag{66}$$

In the above equation, the 1 in the brackets is the compressibility term and the $\frac{3p}{4E\tau/d + \Delta p}$ is the elasticity term.

Consider the three cases:

	p_o(mb)	p (mb)	$\frac{3p}{4E\tau/d + (p - p_o)}$	$\frac{\dot{m}p}{m\dot{p}}$
MIL-SPEC Performance Requirement	1013	1048	1.625	2.625
MIL-SPEC Individual Ground Test	1013	1023	1.607	2.607
Actual Flight Requirement	0	10	.0157	1.016

N. B: $\frac{\tau}{d} = \frac{.0005}{39.37} = 1.27 \times 10^{-5}$

$E = 550,000$ psi $= 37.4 \times 10^6$ mb.

Now consider the orifice mass flow:

$$\dot{m} = CvA\rho = Cv A \frac{m}{V}$$

$$\frac{\dot{m}}{m} = \frac{CvA}{V} \tag{67}$$

and write it in terms of pressure change for the three cases:

$$\frac{\dot{m}}{m}\frac{p}{\dot{p}} = \frac{C v A}{V}\frac{p}{\dot{p}} = 2.625,\ 2.607,\ 1.016 = x$$

$$\frac{\dot{p}}{p} = \frac{C v A}{V x} \tag{68}$$

Now consider the parameters associated with the three cases:

flow velocity, v, is determined below

orifice coefficient, C, is determined below

orifice area, A, is assumed equal and constant

$x = \frac{\dot{m}}{m}\frac{p}{\dot{p}}$ has been determined

p is given

The orifice flow velocity and coefficient must be determined. In the flight case we may assume that the low exhaust pressure makes the flow a sonic jet in which C is given by

$$C_f^2 = \frac{2}{\gamma + 1}^{\frac{\gamma + 1}{\gamma - 1}} \tag{69}$$

From the isopentane compendium $\gamma = 1.11$ and $C_f = .6$

The velocity, assuming an average temperature of 280° K, is given by

$$a^2 = v_f^2 = \gamma RT / M \tag{70}$$

$$v_f = \left(\frac{1.11 \times 8314 \times 280}{72.15} \right)^{1/2} = 215 \text{ m/sec}$$

In the ground test and performance requirement cases we assume that the flow is subsonic.

$$v_p^2 = \frac{2g\,(p - p_o)}{\rho} = \frac{2 \times 9.8 \times 35 \times 10.2}{1.225}\ \frac{m^2}{sec^2} = 5710$$

$$v_p = 75.5 \text{ m. sec}^{-1}$$

$$v_g^2 = \frac{2g(p - p_o)}{\rho} \quad \frac{2 \times 9.8 \times 10 \times 10.2}{1.225} \quad \frac{m^2}{sec^2} = (40.4 \text{ m/sec})^2$$

$$v_g = 40.4 \text{ m. sec}^{-1}$$

In the above 2 equations 10.2 is a factor used to convert mb to Kg. m^2.

The orifice coefficient is not easily obtained. For orifice flow, the Reynolds number is based on the orifice diameter, resulting in Reynolds numbers so small that values of orifice coefficient were not given in the handbooks consulted. Under standard conditions the usual coefficient is near 0.6, however, there is a trend to higher coefficients with lower Reynolds numbers. Our estimate in this case is thus a rather unusual 1.0.

$$Cp = Cg = 1.0$$

Utilizing the criteria above, let us determine the area of a pin-hole which allows exactly 1 mb drop in internal pressure in 20 minutes in the flight case

$$\frac{\dot{p}_f}{p_f} = \frac{C v A}{1.016 V} \qquad (71)$$

$$A = 1.016 \dot{p}_f V / p_f C v = \frac{1}{1200} \times \frac{4 \quad x .5^3 \quad x 1.016}{3 \quad x \quad 10 \quad x .6 \quad x 215} \quad m^2$$

$$A = .344 \text{ mm}^2$$

the orifice diameter is thus .66 mm.

The corresponding rate of pressure drop is now calculated in the performance requirement and ground test cases.

$$\frac{\dot{p}_p}{p_p} = \frac{1}{2.625} \times C_p v_p \frac{A}{V} = \frac{1 \qquad 1.0 \times 75.5 \times .344 \times 10^{-6} \times 6}{2.625} \qquad (72)$$

$$\frac{\dot{p}_p}{p_p} = .189 \times 10^{-4} / \text{sec}$$

$$p_p = 1048 \text{ mb}$$

therefore $\dot{p}_p = \frac{198}{10^4}$ mb/ sec or 23.8mb/ 20 min.

Similarly $\frac{\dot{p}_g}{p_g} = .102 \times 10^{-4}$ / sec

$p_g = 1023$ mb

$\dot{p}_g = 104 \times 10^{-4}$ mb/sec or 12.5 mb/20 min.

Thus we conclude that the performance requirement is very severe (about 24 times the actual flight requirement) and the ground test also, (being 12.5 times the flight requirement). There is some doubt of the actual number because of the assumption of orifice flow coefficient. However the lower limit for the coefficient would be 0.6 and since it enters linearly the requirements would still be considered a severe test, being respectively 14 and 7.5 times the flight requirement.

B. Corrections to Density for Leaking Spheres

Equation 67, from the mass flow analysis above, was:

$$\frac{\dot{m}}{m} = \frac{CvA}{V}$$

If we neglect sphere elasticity, $V = V_o$ and

$$\frac{\dot{m}}{m} = \frac{CvA}{V_o} = k \qquad (73)$$

where k is a constant to a first approximation.

Thus:

$$\frac{dm}{m} = k\,dt$$

$$\ell n(m) = kt + k'$$

$$m = e^{kt+k'}$$

Also, in this case $\frac{m}{m_o} = \frac{\rho V}{\rho_o V_o} = \frac{\rho}{\rho_o}$

Assuming an isothermal process:

$$\frac{\rho}{\rho_o} = \frac{p}{p_o}$$

Therefore: $$\frac{\dot{m}}{m} = \frac{\dot{\rho}}{\rho} = \frac{\dot{p}}{p}$$

Applying boundary conditions, letting sub o indicate ejection and sub d deflation:

$$m = m_o \quad \text{at} \quad t = t_o = 0$$

$$\frac{m}{m_o} = e^{kt} \qquad \text{also} \qquad \frac{p}{p_o} = e^{kt}$$

thus

$$\frac{p_d}{p_o} = e^{kt_d} \qquad \text{and} \quad kt_d = \log \frac{p_d}{p_o}$$

therefore $$\frac{m}{m_o} = \exp\left[\frac{kt}{kt_d}\ (kt_d)\right] = \exp\left[-\frac{t}{t_d}\ \log \frac{p_o}{p_d}\right]$$

We now have an equation which gives the mass of gas in the sphere as a function of time, deflation time, and deflation ambient pressure, all of which are required to correct the sphere mass. The times, t and t_d are of course measured from ejection since t_o was taken to be 0 (see reference 42 for examples of the application of this result).

C. Calculation of Design Deflation Altitudes

We base these altitudes on the pressures given in the U. S. Standard Atmosphere, 1962, and the equation of state applied to the gas within the sphere

$$p = \frac{mRT}{VM}$$

We assume that the sphere deflates when its internal pressure is equal to the outside ambient pressure.

If P is in mb, m in grams, t in ^{o}K, and V in meters^{3}, we find:

$$R = .08314 \text{ mb} - m^{3} / \text{mol} - {}^{o}K$$

$$M = 72.15 \text{ gm} / \text{mol}$$

$$P = 1.152 \times 10^{-3} \; mT / V \qquad (74)$$

Some sample deflation altitudes based on typical sphere temperatures:

	Robin	U - Michigan	Australia
m (gm)	18.6	8.0	74.4
V (m^3)	.524	.155	4.19
T (^{o}K)	225	225	240
P (mb)	9.2	13.4	4.91
Alt. (km)	31.8	29.3	36.1

VII. Logical Analysis, Results and Conclusions

The summary contained in this section is based on material discussed in detail in Part II and Appendices A, B and C of this report. The theoretical studies in Part II "Inflation Analysis of Mylar Falling Spheres" did not suggest any possible causes of failure. Positive clues to the possible failure modes come from the series of ground tests described in Appendix A.

A. Background and Test Philosophy

The overall inflation experience with the three systems studied was quite different. The 66 cm system failed in 6% of flights while the 2 m. system failed in 35% of flights and the 1 m. system failed in 55% of flights. These figures excluded flights in which rocket failure, gross ejection failure or radar acquisition failure was involved.

The reliability of the 66 cm system was justification for a goal of over 90% reliability for the future Viper-Dart Robin program. To attain this goal, it would have been easy simply to prescribe changing all components to those used in the 66 cm system. This could not be done for several practical and operational reasons:

1. The ROBIN system requires the use of the most attractive launch vehicle in the area of performance versus price, which is a Viper-Dart or similar combination.
2. The ROBIN system requires routine operational capability, with handling, storage, pre-flight checkout, launching, radar tracking, and data reduction by crews not possessing engineering or scientific background, or investigative motivation.
3. The ROBIN system must be launched from sites having FPS-16 as the highest quality precision tracking radar.
4. The ROBIN program requires relatively higher procurement rates.

Therefore, it was incumbent in the present investigation to analyze all possible sources of inflation difficulties. The investigators exhaustively

treated this listing of potential problems. It can be fairly stated that every suggestion raised by observers with or without falling sphere experience was scrutinized, regardless of its seeming plausibility. Also, there was no person or group involved in the falling sphere programs, past or present, whose views were not requested, discussed, and analyzed. We are aware that an analysis based on eliminating sources which are proved non-con tributory in order to pinpoint the one or more which are responsible suffers the danger of overlooking completely the one sought.

B. Analytic Method

All potential sources of inflation failure were considered. A potential source of failure was considered non-contributory if it was utilized identically in the 66 cm. system. A potential source of failure was considered non-contributory if identical usage was made in the 2 m. system and not used in the 66 cm. system. If not utilized in either the 66 cm. or the 2 m. system, a potential source was considered non-contributory if ground testing designed for the purpose revealed no fault. If flight testing comparison was impossible and ground testing had not been done and could not be undertaken within the scope of this investigation, theoretical proof, satisfactory in the opinion of the present investigators, was sufficient to lable a potential source non-contributory. If flight testing comparison was impossible and ground testing had not been done, but was possible within the scope of this investigation, ground tests were conducted. If ground tests were conclusive in the opinion of the investigators the source was labelled non-contributory.

If a potential source of inflation failure were demonstrated in laboratory test, or by theory, to be in fact a cause of failure, it would be labelled as such. In this case all other potential sources would nevertheless be examined.

If all potential sources were found non-contributory excepting one or more, and one or more sources were found definitely contributory, no prescription of the method of assessing the relative importance of those not eliminated with those definitely contributory was established before the fact.

If all potential sources were eliminated excepting one or more, these would be found to be the source or sources for 94% of inflation failures.

In addition the possible interaction of all potential sources was considered. However, the number of combinations was impossible to handle on other than a subjective basis. For example, the investigators consider relevant the interaction between the time of launch, the launch vehicle, and the evaporation rate of isopentane; while irrelevant is the interaction of the use of isopentane as an inflatant material with the use of a corner reflector versus an aluminized-surface sphere. The subtleties could be overwhelming and could be resolved only by the perspicacity of the investigating team. Failure by the investigators to consider each and every relevant combination must unfortunately be accorded some probability.

C. Results

1. No potential source of inflation failure was demonstrated to be an important actual source by objective tests, flight comparisons, or theory.

2. All potential sources were eliminated by flight test comparisons, prior ground tests, and theory, except:

a) Thermal damage to the sphere during ascent in the dart on a marginal basis.

b) Damage to the sphere at time of ejection by contact with sharp edges or hot surfaces of components of the dart.

c) Damage to the sphere due to the dynamics of unfolding the internal corner reflector

d) Loss of isopentane by the capsule subsequent to manufacture and before flight

e) Lack of sphere integrity due to quality control procedures in manufacture.

f) Lack of sphere integrity due to environmental conditions while in storage.

Approximately 150 potential sources were eliminated ranging from isopentane escape under various sized capsule orifices to the possibility of ambient atmospheric temperature cooling and condensing the isopentane gas. These are not listed.

3. Tests were conducted to eliminate as many as possible of sources 2a. through f. As a result, 2c, d, e, & f were eliminated. 2a and 2b were not possible to test.

D. Conclusions

1. The probable causes of more than 94% of Viper-Dart-Robin inflation failures are:

a) Thermal damage to the sphere during ascent in the dart. Some portions of the sphere may exceed 125°C. on a random basis depending upon construction and packaging.

b) Damage to the sphere at time of ejection by proximity to exceedingly hot dart parts, or by touching sharp surfaces.

2. Although a considerable effort has been spent on thermal studies of mylar spheres, it is our opinion that these studies are still incomplete. Additional effort should be directed to the goal of determining complete thermal-time histories of the Robin and U. of M. spheres with overall precision significantly better than the results presented in this report. The experience in the work done so far indicates that this goal can be achieved.

VIII. References

1. Welinski, B. R. "Robin System Inflation Reliability," Final Summary Report Contract No. AF 19(628) - 5538 G. T. Schjeldahl Co., May 30, 1968.

2. Slater, R. J., "Superpressure Balloons", Final Technical Report Contract AF 19(604) 4569, G. T. Schjeldahl Co., October 31, 1959.

3. Welinski, B. R., "Robin Meteorological Balloon Development", Final Technical Report Contract AF 19 (604) 6653, G. T. Schjeldahl Co., December 31, 1960.

4. Walker, R. L., Judi-Robin Balloon Dart Sounding Vehicle", Final Report Contract No. AF 19(628)-1624, Rocket Power, Inc., Dec. 1962.

5. Watson, C. W., "Judi-Robin Balloon Dart Sounding Vehicle", Final Report Contract No. AF 19(628)-2805, Rocket Power, Inc., AFCRL-64-471, May 1964.

6. Smalley, J. H. and L. R. Flink, "Modification of the Robin Meteorological Balloon-Volume I-Design and Test", Final Report Contract No. AF 19 (628) - 2945, Applied Science Division, Litton Systems, Inc., AFCRL-65-734 (I), Sept. 30, 1965.

7. Bollermann, B., and R. L. Walker, "Design, Development and Flight Test of the Viper Dart Robin Meteorological Rocket System," Final Report Contract No. AF 19(628) - 5911, Space Data Corp., AFCRL-68-0418, June 30, 1968.

8. Bollermann, B. and R. L. Walker, "Design, Development and Flight Test of the Viper Dart Robin Meteorological Rocket System Design Improvement," Final Report Contract No. F 19628-68-C-0393, Space Data Corp., AFCRL-70-0150, Jan. 1970.

9. Pearson, P. H. O., "Measurements of Atmospheric Density, Temperature and Pressure at Woomera on March 29, 1962, by the Falling Sphere Method, Australia Dept. of Supply, Weapons Research Establishment, Technical Note SAD 121, Salisbury, So. Australia, May 1963.

10. Pearson, P. H. O., "Two Falling Sphere Results for Woomera Extended to Include the Subsonic Region," Aust. Dept. of Supply, W. R. E. Technical Note PAD 87, Sept. 1964.

11. Pearson, P. H. O. and Curnow, R. J., "Basic Atmospheric Parameters as Measured by Four Falling Sphere Experiments at Woomera, April to July, 1964," Aust. Dept. of Supply, W. R. E. Technical Note PAD 81, Jan. 1965.

12. Pearson, P. H. O., "Basic Atmospheric Parameters as Measured by Four Falling Sphere Experiments at Woomera, Aug to Nov. 1964," Aust. Dept. of Supply, W. R. E., Technical Note PAD 99, April 1965.

13. Pearson, P. H. O., "Basic Atmospheric Parameters as Measured by Four Falling Sphere Experiments at Woomera, Dec. 1964 to March 1965," Aust. Dept. of Supply, W. R. E. Technical Note PAD 109, Dec. 1965.

14. Pearson, P. H. O., "Basic Atmospheric Parameters as Measured by Four Falling Sphere Experiments at Woomera, May to August 1965," Aust. Dept. of Supply, W. R. E. Technical Note PAD 113 March 1966.

15. Pearson, P. H. O., "Basic Atmospheric Parameters as Measured by Four Falling Sphere Experiments at Woomera, October 1965 to January 1966," Aust. Dept. of Supply, W. R. E. Technical Note SAD 166, Dec. 1968.

16. Pearson, P. H. O., "Basic Atmospheric Parameters as Measured by Four Falling Sphere Experiments at Woomera, Feb. to June 1966," Aust. Dept. of Supply, W. R. E. Technical Note SAD 211, February 1969.

17. Pearson, P. H. O., "Basic Atmospheric Parameters as Measured by Four Falling Sphere Experiments at Woomera, July to November 1966," Aust. Dept. of Supply, W. R. E. Technical Note SAD 219, February 1969.

18. Pearson, P. H. O., "Two Falling Sphere Results at Carnarvon on 22nd October, 1964," Aust. Dept. of Supply, W. R. E. Technical Note PAD 102, April 1965.

19. Pearson, P. H. O., " Falling Sphere Results for Woomera and Carnarvon During July 1964," Aust. Dept. of Supply, W. R. E. Technical Note PAD 103, April 1965.

20. Anonymous, "Status of Passive Inflatable Falling-Sphere Technology For Atmospheric Sensing to 100 km," Report NASA SP-219, 1969.

21. Peterson, J. W., et al., "Atmospheric Measurements Over Kwajalein Using Falling Spheres," NASA Contractor Report NASA CR-218, May 1965.

22. Crawford, D. H. and W. D. McCauley, "Investigation of the Laminar Aerodynamic Heat-Transfer Characteristics of a Hemisphere-Cylinder in the Langley 11-inch Hyperson Tunnel at a Mach No. of 6. 8," NACA Report 1323, 1957.

23. Stalder, J. R. and H. V. Nielsen, "Heat Transfer From a Hemisphere-Cylinder Equipped With Flow-Separation Spikes," NACA TN 3287, 1954.

24. Stine, H.A. and K. Wanlass, "Theoretical and Experimental Investigation of Aerodynamic-Heating and Isothermal Heat-Transfer Parameters on a Hemispherical Nose with Laminar Boundary Layer at Supersonic Mach Numbers," NACA TN 3344, 1954.

25. Sibulkin, M., "Heat Transfer Near the Forward Stagnation Point of a Body of Revolution," J. Aero Sci., 19, No. 8, 570-571, August 1952.

26. Korobkin, I., "Laminar Heat Transfer Characteristics of a Hemisphere for the Mach Number Range 1.9 to 4.9," NAVORD Report 3854, U.S. Naval Ordnance Lab., White Oak, Md., October 10, 1954.

27. McAdams, W.H., Heat Transmission, Third Ed., McGraw-Hill, 1954.

28. VanDriest, E.R., "Turbulent Boundary Layer in Compressible Fluids," J. Aero. Sci., 18, No. 3, 145-160, March 1951.

29. von Karman, T., and H.S. Tsien, "Boundary Layer in Compressible Fluids," J. Aero. Sci. 5, No. 6, 227, April 1938.

30. Williamson, E. D. and L. H. Adams, Phys. Rev., 14, 99-114, 1919.

31. Gurney, H. P. and J. Lurie, Ind. Eng. Chem., 15, 1170-1172, 1923.

32. Emmons, H W., Ed., "Fundamentals of Gas Dynamics," High Speed Aerodynamics and Jet Propulsion, Vol. 3, Princeton Univ. Press., 1958.

33. Skladany, J.T., "Temperature Distribution of a Thin-Walled, Transparent, Spherical, Earth Satellite", NASA Technical Note D-7035, March 1971.

34. Germeles, A. E., "Vertical Motion of High Altitude Balloons", Technical Report IV, Contract Nonr 3164(00), Arthur D. Little, Inc.) July 1966.

35. Suomi, V. E. K. J. Hanson and T. H. VonderHaar, "The Theoretical Basis for Low Resolution Radiometer Measurements from a Satellite", in Studies in Atmospheric Energetics Based on Aerospace Probings, Annual Report - 1966, Dept. of Meteorology, The University of Wisconsin, March 1967.

36. Wolfe, W. L., (Editor) Handbook of Military Infrared Technology", Office of Naval Research, Department of the Navy, Wash. D. C. 1965.

37. Valley, S. L., (Editor), "Handbook of Geophysics and Space Environments", Air Force Cambridge Research Laboratories, 1965.

38. Chaney, L. W., L. T. Loh, and M. T. Surh, "A Fourier Transform Spectrometer for the Measurement of Atmospheric Thermal Radiation," Univ. of Mich. Report 05863-12-T under contract NASr-54/03), Department of Aerospace Engineering, High Altitude Engineering Laboratory, May 1967.

39. Hanel, R. A., et. al., "The Nimbus 4 Infrared Spectroscopy Experiment, IRIS-D, Part I, Calibrated Thermal Emission Spectra, NASA Goddard Space Flight Center, Preprint X-622-71-272, July 1971.

40. Bartman, F. L., "The Reflectance and Scattering of Solar Radiation by the Earth," Univ. of Mich. Report 05863-11-T under contract NASr-54(03), Department of Aerospace Engineering, High Altitude Engineering Laboratory, Feb. 1967.

41. Marks, L. S. and T. Baumeister, "Marks Mechanical Engineer's Handbook," Sixth Edition, McGraw-Hill Book Company, Inc., 1958.

42. McWatters, K. D., and J. W. Peterson, "Adequacy of the Passive Inflated Falling Sphere Technique" in "Status of Passive Inflatable Falling-Sphere Technology for Atmospheric Sensing to 100 Km, NASA SP-219, A Symposium held at Langley Research Center, Hampton, Virginia, Sept. 23-24, 1969.

Appendix A. VIPER-DART SPHERE TEST PROGRAM

F. F. Fischbach and H. F. Allen

I. Recommendations

A. Material Required for Test Program

2 Production darts

2 Aerobee spheres

4 Spheres ordered from SDC

2 Sets of production staves

Misc. material for construction of dummy dart such as tubing, bar stock, O-rings, etc.

Plastic, for construction of dummy sphere.

Explosive material used in ejection charge.

B. Test Program

Test #1- Weight Determination and Jig Design

Step 1. Weigh darts and all sphere assemblies.

2. Disassemble darts by removing shear screws.

3. Weigh: a. Sphere-stave assemblies

b. Nose assembly.

c. Rear Assembly (mortar, piston, etc.).

4. Design test mortar, with replaceable ejection charge, Weighing same as item 3c.

5. Design test nose weighing same as item 3b.

6. Design dummy sphere to fit in production staves, the assembly to weigh same as item 3a.

7. Design horizontal support for test assembly, permitting free horizontal motion of all parts.

8. Construct all parts, including several ejection charges.

9. Reassemble production darts, with spheres replaced by 2 SDC spheres.

Test #2 - Ejection Tests - Dummy Spheres and Staves

Carry out several horizontal ejection tests. Redesign and rebuild support jig until it has been demonstrated that an actual sphere will not be damaged by an ejection test and subsequent recovery of the sphere. This may require several tests and subsequent revisions of test apparatus and procedure.

Test #3 - Ejection Test - Sphere Ordered from SDC

Step 1. Reweigh sphere-stave assembly, as a considerable amount of time will have elapsed since initial weighing.

2. Assemble dummy dart with sphere-stave assembly and ejection charge.
3. Carry out ejection test, with very careful recovery of sphere.
4. Weigh recovered sphere and staves.
5. Transport sphere to vacuum chamber.
6. Evacuate chamber, and determine altitude at which sphere inflates.
7. Continue evacuation to min. pressure. Hold at this pressure for 20 minutes.
8. Return chamber to atmospheric pressure, and determine altitude of deflation.
9. Reweigh sphere.

Test #4 - Ejection Test - Astrobee Sphere

Carry out same procedure as for Test #3, using Astrobee sphere-stave assembly.

Test #5 - Ejection Test - Production Sphere

Carry out same procedure using one of the production spheres removed from dart assembly.

Test #6 - Series of Ejection Tests in Large Vacuum Chamber

Step 1. Design and construct support to be used during tests in chamber. The design of this support including provision for protecting ejected sphere will evolve during the ejection tests at atmospheric pressure.

2. Transport the following equipment to Langley Research Center
   a. Dummy dart assembly.
   b. At least four ejection charges.
   c. 2 sphere assemblies obtained from SDC
      1 Astrobee sphere
      1 Production sphere previously removed from dart.
3. Assemble support jig in altitude chamber.
4. Assemble dummy dart, with sphere-assembly and ejection charge, and mount in support assembly.
5. Evacuate chamber to desired pressure.
6. Eject sphere.
7. If sphere inflates, hold chamber pressure for 20 minutes.
8. Return chamber to atmospheric pressure and observe altitude of deflation.
9. Reweigh sphere and staves.

Repeat above procedure for remaining three spheres.

The above test program leaves one of the four spheres ordered from SDC untested. Decision as to whether this sphere should be tested at atmospheric pressure or in the Langley chamber will be made during the series of atmospheric tests.

II. Viper-Dart Sphere Test Program (by H. F. Allen)

A. Introduction

The Viper-Dart test program comprised two parts: a series of ground ejection tests with dummy and actual spheres at the U of M, followed by a series of ejection tests in the 41 foot vacuum chamber at Langley Memorial Aeronautical Laboratory. For the purpose of these tests, six production sphere-stave assemblies, two pairs of staves, and several ejection charges were procured from Space Data Corporation. Two darts, complete except for ejection charges and fins, were obtained on loan from Patrick Air Force Base. The spheres in these darts were removed for test, and were replaced by spheres procured from S. D. C. Two sphere-stave assemblies were also obtained from Air Force Cambridge Research Laboratory.

Drawings of the dart assembly were made available by AFCRL, but weight information could not be obtained until the actual darts were received. These were disassembled and the parts were weighed. The ground test assembly was not an exact duplicate of the actual dart, as there was no need to streamline the nose or to provide fins. Consequently the assembly was designed with a cylindrical nose and breech, having the same external diameter as the mortar tube. The piston was an exact duplicate of the dart piston. The mortar tube was almost a duplicate of the actual dart mortar, except that the forward motion of the piston was stopped by a steel ring which was a heavy press fit (5 tons) into the bored-out forward end of the mortar tube. This easily machined arrangement had worked well with many types of spheres used by the U of M in previous projects. The aft portion of the nose piece, and

the forward portion of the breech, containing the ejection charge, were machined to the same contour as the corresponding parts of the actual dart, except that the ejection charge was fired by an instantaneous electric squib instead of a delay squib. The weights of all parts corresponded to those of the actual dart. The weight of the fins was included in the weight of the cylindrical breech.

B. Ground Tests at University of Michigan

Two series of tests were carried out at U of M. The first, using dummy spheres, was for the purpose of checking out the test assembly, and determining the procedure to be used in tests with live spheres. The second series of tests ejected four live spheres at ground level, after which the spheres were placed in a vacuum chamber to check the inflation altitude and the presence or absence of leaks.

The first two tests were carried out using a dummy sphere-stave assembly consisting of a properly ballasted metal tube, with the forward end machined to the stave contour. The tests were carried out with the test assembly mounted horizontally about 2'-3" above the ground, and not restrained in any way. The dummy sphere remained in contact with the nose during flight, and both struck the ground 22' to 25' from the center of the test mount. The breech, being somewhat lighter, struck the ground 27' to 30' behind the test mount. The dummy sphere stopped at initial ground contact, while the heavy nose bounced to a distance of 35'. The breech finally stopped 45' to 50' from the test mount. After each test, the ejection charge residue was readily cleaned from the mortar and other parts, using gasoline.

The various parts of the test assembly were not damaged except that the stop ring was moved forward about 1/4" by the impact of the piston, and had to be forced back into place after each test. Evidently the ejection charge is considerably stronger than those used with U of M spheres, as this problem had not been encountered in the past. The front end of the piston was peened out somewhat by the violent contact with the stop ring, so the forward edge was bevelled about 1/64", and the piston was then case hardened. After hardening, it was found that the staves would no longer slip easily into the

recess at the forward end of the piston, so in all subsequent tests, the aft end of each pair of staves was filed lightly so as to fit the recess in the piston.

Two more tests were carried out using staves procured from SDC and a roll of scrap polyethylene to simulate the sphere. The trajectories were essentially the same as in the previous tests. The dummy sphere stopped approximately at first ground contact, while the staves bounced to distances of 42' to 50'. It was apparent that ground contact of the sphere was rather forceful, and could result in damage to an actual sphere. All previous tests with U of M spheres had been carried out vertically from a stationary mortar, as the ejected parts were very light in comparison with the mass of the rocket carrying the mortar. In such tests, the sphere always fell very gently, and was never damaged.

In the case of the dart tests, the horizontal mortar position had been chosen because the ejected parts are actually heavier than the mortar and breech, so the breech assembly must be free to accelerate backward. In the next series of two tests, the assembly was lightly taped to a board which was mounted at an angle of 60^{o} with the horizontal, with the base of the breech about 18" above the ground. Breaking of the tape permitted the breech to accelerate freely backward until the ejected parts were well clear of the mortar. During each test, the nose section went an estimated 50' in the air, and landed 50' horizontally from the launch point. The breech was driven about four inches into the ground. The staves and dummy sphere separated from the nose in flight, and the sphere landed very gently. The tests were carried out facing a 5-10 knot breeze, so the sphere was blown backward somewhat, and landed well clear of the metal parts. It was considered that this procedure would not result in damage to an actual sphere.

The tests with the live spheres were carried out in the following manner. The sphere-stave assembly was weighed before insertion in the mortar, and the weight was compared with the nameplate data. The test ejection was carried out as described above, after which the ejected sphere and wrapper were weighed together. They were then placed in a 6'x6'x6' vacuum chamber, which was then pumped down at ambient temperature to a pressure corresponding to approximately 200 K feet. This pressure was held for 30 minutes, and the chamber was then returned to ambient pressure slowly enough so that deflation of the sphere could be observed. The deflated sphere and the wrapper were then weighed separately.

The first live sphere tested was one of the spheres procured from SDC. The nameplate data were as follows:

Serial No.	R-1262
Date of mfg.	5-13-71
Sphere-capsule wt.	110.8 gm.
Gross weight	467.5 gm.

The actual gross weight (sphere, capsule and staves) at U. of M. was 468 gm. so it was assumed that no isopentane had been lost during the storage period. After ejection, it was apparent that the capsule had been properly actuated, as liquid isopentane was visible inside the sphere envelope, which still remained tightly folded. Ambient temperatures were approximately 72^{o}F. The weight of the sphere after ejection was 110 grams, which checks the nameplate data as closely as can be expected, using a different balance. In the vacuum chamber, the sphere started to inflate first around the capsule, and as the pressure decreased, this area bulged more and more, but the tightly folded portion appeared reluctant to unfold. At an altitude of approximately 100K feet,

the sphere unfolded suddenly, and was completely inflated. One corner reflector spring tore loose from the sphere skin, but it is doubtful if this would cause much change in the radar cross section, as this portion of the corner reflector remained partially deployed. After 30 minutes, the pressure altitude in the chamber, which peaked at approximately 200 K feet, was slowly decreased. Small wrinkles appeared along the tapes connecting the gores at 110K. They were slightly deeper at 100K, but the sphere was still good, although there were small dents at the ends of the corner reflector springs. One small patch on the sphere distorted the surface very slightly, but it was considered that this would have no effect on the drag characteristics. At 96K, the wrinkles were much deeper, the dents at the corner reflector attachment points were about 4" or 5" across, and there was a noticeable flat spot on the bottom where the sphere rests. This was considered to be the deflation altitude. There was visible collapse at 95K. The temperature of the chamber was 72° F. The deflated sphere weighed the same as before the test, within the accuracy of the balance.

During all subsequent tests, the action of the sphere was essentially the same as described above, so only the inflation and deflation altitudes will be noted in this report. All weights corresponded to nameplate data, indicating no loss, or negligible loss of isopentane, both during storage and during the vacuum tests, so only nameplate data will be listed.

The second sphere tested was one of the two obtained from AFCRL. Nameplate data as follows:

Serial No.	R - 1255
Date of mfg.	9-16-70
Sphere - capsule wt.	113.0 grams
Gross weight	459.7 grams

This sphere inflated and deflated at 96K.

The third sphere tested had been removed from one of the darts, serial no. 390-448. Nameplate data as follows:

Serial No.	R 1160
Date of mfg.	10-8-70
Sphere-capsule weight	114.9 gm.

The gross weight is not listed, as this configuration is not reproducible once the sphere has been inserted in the dart. During the ejection test, the forward ends of the staves stuck in the nose section. However, the sphere fell separately, and was not damaged. This sphere also inflated and deflated at 96K. The chamber temperature was 50^{o}F to 55^{o}F. This sphere appeared to be slightly more "bumpy" than the first two, although the dimensions were probably well within the established tolerances.

The fourth test sphere was another of those procured from SDC. Nameplate data as follows:

Serial No.	R 1257
Date of mfg.	5-13-71
Sphere-capsule wt.	112.6 gm.
Gross weight	468.5 gm.

Again, inflation and deflation occurred at 96K. One spring tore loose from the corner reflector. This sphere appeared to be very smooth and spherical.

This sample of four spheres, two of which were procured from SDC directly, one of which was furnished by AFCRL, and one of which was removed from a production dart, showed no loss of weight during storage, indicating good capsule reliability. There was no damage during ejection, the spheres all inflated and deflated at the proper altitude, and showed negligible loss of weight during vacuum testing. This indicates excellent sphere integrity, and no difficulty with the ejection and capsule actuation system. Breakage of

two corner reflector supports is considered to be a minor problem, which may be related to the severe folding and compression required to fit the sphere into the small space available for the staves and sphere. Within the limits of the small number of tests carried out, the problem of sphere reliability appears to be narrowed to possible dynamic inflation damage, or to thermal problems. The question of possible dynamic inflation damage was investigated during subsequent ejection tests in the altitude chamber at LMAL.

C. Altitude Chamber Tests at Langley Memorial Aeronautical Laboratory

The four spheres tested at Langley comprised a parallel sample to the four tested at U of M. Nameplate data are as follows, including weights at Ann Arbor as of Sunday, 25 July, 1971:

#1 Procured from SDC

Serial No.	R 1260
Date of mfg.	5-13-71
Sphere-capsule wt.	111.9 gm.
Gross wt.	459.1 gm.
Present wt.	459 gm.

#2 Procured from SDC

Serial No.	R 1258
Date of mfg.	5-13-71
Sphere-capsule wt.	112.9 gm.
Gross wt.	462.5 gm.
Present wt.	463 gm.

#3 Removed from dart, serial no. 390-447

Serial No.	R 1159
Date of mfg.	10-7-70
Sphere-capsule wt.	112.6 gm.
Gross wt.	not reproducible

#4 Obtained from AFCRL

Serial No.	R 1261
Date of mfg.	9-16-70
Sphere-capsule wt.	113.7 gm.
Gross wt.	461.4 gm.
Present wt.	461 gm.

Spheres procured from SDC were installed in the two darts to replace the spheres removed for testing. Nameplate data on the darts were changed accordingly. The replacement spheres showed no loss of weight during storage prior to installation in the darts.

Serial No.	R 1243
Date of mfg.	3-10-71
Sphere-capsule wt.	113.4 gm.
Gross wt.	471.9 gm.
Gross wt. as of 7/25/71	472 gm.
Installed in dart, serial no.	390-447
Serial No.	R 1244
Date of mfg.	3-10-71
Sphere-capsule wt.	116.4 gm.
Gross wt.	471.6 gm.
Gross wt. as of 7/25/71	472 gm.
Installed in dart, serial no.	390-448

This makes a total of nine spheres manufactured between 9-16-70 and 5-13-71 which showed no loss of weight during storage. This indicates good leak-proof capsule construction for the sample tested.

After each test at U of M, the stop ring in the test mortar had been moved forward by the inertia of the piston and the pressure of the ejection charge, and had to be pushed back into place before the next test. The force required to install the ring initially was 5 tons. After the last test, the force required to push the ring back into place was 3 1/2 tons. The advisability of pinning the ring in position for the tests at LMAL was discussed, and it was decided that this would be unnecessary, as a press of sufficient capacity would probably be available at Langley, and the same procedure could be followed as in earlier tests.

During the ejection tests in the 41' spherical vacuum chamber at LMAL, the test assembly was supported in a trough consisting of a 6"x6"x1/2" aluminum alloy angle about 5 1/2 ft. long, mounted radially and slanting slightly upward from a point below one of the equatorial observation ports. A target, comprising a 4' x 4' piece of plywood, overlain by several alternating layers of matting and cardboard served as a backstop to decelerate the nose section of the test assembly. A flexible cable was clamped to the nose at its center of gravity, which was located at the end of the trough, about 5 1/2 ft. from the chamber wall. The cable was stretched to a support point at the top of the spherical chamber. This permitted the nose to fly on a parabolic trajectory across the chamber until it reached a point about 5' from the opposite wall, where the cable became taut and pulled the nose upward on an arc away from the path of the inflatable sphere. The target for the nose was therefore mounted about on the equator of the tank. Below the target was a net, covered with polyethylene sheet, which formed a backstop to decelerate the inflatable sphere. The net hung vertically below the target, and then sloped downward to form a basket, or pocket, to catch and hold the sphere. The ground test assembly was placed in the trough with the forward part of the nose piece extending a few inches beyond the end of the trough. A sheet metal angle covered the trough and prevented the breech from bouncing out. A small backstop of plywood, matting, and cardboard against the chamber wall at the aft end of the trough decelerated the breech, which was restrained from rebounding out the end of the trough by a short length of flexible cable. Motion pictures at 400 frames per second were taken from a port on the equator above and behind the trough, from a second port on the equator at 90^{o} to the right of the first, and from a third port in the top of the chamber. Still photographs of the test set up were taken, but later proved to be badly underexposed,

due to the use of a faulty light meter.

The test procedure was to evacuate the chamber at ambient temperature to as high an equivalent altitude as time permitted, (usually about 250K feet), fire the ejection charge, and then steadily reduce the chamber altitude, at a rate such that 100K would be reached in 20 minutes. This rate was continued until deflation took place, after which the chamber was rapidly returned to sea level.

During the first test, which was carried out 8-16-71, on sphere #1, the sphere appeared to be fully inflated as it struck the top of the net and fell back into the pocket, but it deflated immediately, so the chamber was returned to sea level. It was found that the stop ring had been forced completely out of the mortar tube, releasing the hot ejection charge combustion products, which burned several holes in the sphere. In addition, there was a rip in the sphere skin several inches long, with no burn marks, and the inflation capsule was found outside the sphere. This indicated that the capsule tore the sphere by inertia as it struck the net, and that the sphere would have deflated at once, even if the stop ring had not been forced out.

The target for the nose was too low, and the steel nose struck the chamber wall, with negligible damage to the nose and a small patch of paint chipped off the wall. For the next test, the backstop and the net were raised. The stop ring was pressed back into the mortar, and six 1/4-20 bolts were installed, the bolt ends being flush with the inside of the stop ring. The ejection charges, as received from SDC, were contained in small plastic bottles, which had been placed loosely in a box, and were free to rattle around during transportation to LMAL by U of M station wagon. After the first test, these

were examined carefully, and the pellets appeared to have a light coating of dust, which was assumed to consist of charge material which had been eroded from the pellets by vibration. This dust would burn very rapidly, raising the pressure behind the piston, thereby causing the pellets to burn more rapidly, thus raising the pressure still further. Malfunction of some early rocket grenades had been traced to a similar problem, so it was considered possible that higher pressure behind the piston, coupled with the decreased ambient pressure, (corresponding to 250K feet altitude) may have contributed to failure of the stop ring. For subsequent tests, when the ejection charges were built up, each individual pellet was carefully wiped off with tissue paper.

The second test, with sphere #2, was carried out 8-17-71, and was completely successful. The ejection charge was fired with the chamber at 250K, the sphere inflated immediately, and struck the net about two to four feet below the top. It then fell back into the pocket and remained inflated. As the chamber altitude approached 100K ft., about 20 minutes after ejection, small wrinkles appeared along the tapes on the sphere, and also, to a slight extent, in the skin. Below 100K, the usual dents began to appear at the ends of the corner reflector. At 97K, deflation was well underway. The chamber temperature was 85^{o}F. The nose hit the top of the target, glanced off, and hit the chamber wall again, so both target and net were raised another two feet.

The third test, 8-18-71, was carried out on sphere #3, which had been removed from a production dart. The chamber altitude at ejection was 235 K, temperature 74^{o}F. This time, the nose hit the center of the

target board. The sphere appeared to be inflated as it hit the net, but deflated at once, and the chamber was returned to sea level. The capsule was found in the pocket, outside the sphere, which had a rip in the surface several inches long. The rip was straight except for about three quarters of an inch at the center, which formed a semicricle. It is assumed that the capsule hit the sphere surface head-on as the sphere was stopped by the net, forcing the capsule through the sphere skin. This is a chance which must be taken during an altitude chamber ejection test.

The last test, using sphere #4, was completely successful. The sphere was ejected at 215K, as the pumping system was urgently required by a higher priority test in another chamber. The sphere inflated, fell back into the pocket, and remained inflated as the chamber altitude was slowly decreased. Deflation occurred between 100K and 98K.

After the motion pictures of the tests, taken at 400 frames per second, had been received at the U of M early in October, 1971, they were examined frame by frame during sphere ejection and inflation. Detailed notes taken during this examination are appended, and these contain much information not apparent during visual observation of the tests. During the first test, one bank of lights failed, so the pictures are very dark. However, the sphere, staves, and nose are visible clearly enough to convey nearly as much information as the more highly illuminated pictures of the other tests. The following paragraphs comprise a summary of information contained in these notes.

When the ejection charge was fired, the mortar, being the lighter part, moved rapidly rearward, so that the sphere and staves were completely freed while still in the trough. This required about .02 second. The sphere began to expand immediately at the capsule (aft) end, in a manner analogous to the

action which occurred slowly during the vacuum chamber portion of the tests at Ann Arbor. By the time the sphere and staves were clear of the trough, the capsule end of the sphere had expanded to several inches in diameter. This expansion while still in the trough undoubtedly gave all spheres an upward thrust. However, the action of the staves during release and inflation, which is not always predictable, modified this effect.

The initial expansion of the sphere at the aft end pushes the aft ends of the staves apart, while the forward ends remain together until they are free of the cavity at the rear of the nose. The time at which this occurs varies, and the relationship of the staves to the unfolding forward portion of the sphere varies, so that the behavior of the staves is different from test to test. In general, the staves are forced apart by the expanding sphere, whose center tends to remain near the leading edges of the staves as the forward part of the sphere unfolds. This tends to push and rotate the staves backward and to push the sphere forward toward the nose, thus tending to counteract the initial forward motion imparted to the stave when the capsule end of the sphere first expands. The final motion of the sphere relative to the nose can thus be forward or backward, depending on which of the stave motions predominates. Lateral motion may also be present. During an actual flight the high spin rate, not duplicated in chamber tests, would affect stave motion also.

The motion just described was observed in the case of test #1, when a stave was visible with its leading edge approximately above the center of the sphere. For a few frames the light was just right to show that the stave caused an indentation in the surface of the sphere for a short time just before complete inflation, as the inflating sphere pushed the stave upward and rearward while the stave pushed the sphere in the opposite direction. This action caused

the sphere to move forward, but was not quite enough to overcome the initial upward thrust imparted to the sphere during its initial expansion at the capsule end, so that in this case, the resultant sphere motion was forward and slightly upward with respect to the nose. A similar action was visible for a few frames during test #3, except that this time the stave moved slightly forward, and the sphere moved rearward relative to the nose. The sphere can thus be caused to move in almost any direction with respect to the nose. The heavy nose itself appeared to travel in a straight line until the cable became taut and pulled the nose up out of the way of the sphere.

In all cases, even during test #1, where several holes were burned in the skin, the sphere appeared to be completely inflated about .14 to .16 sec, after release, or .16 to .18 sec. after initiation of the ejection charge. However, in all cases, dents were visible at the ends of the corner reflector whenever the light was right. These must have disappeared very soon, as they were not noted during visual observation, until the initial stages of deflation of the two spheres which remained inflated. In the case of sphere #3, the capsule could be seen outside the sphere as it rebounded from the net. In the case of #1, the light was not sufficient to show small parts. Both spheres #1 and #3 appeared to be still inflated as they landed in the pocket below the net, but both were partly deflated before the camera film ran out. The correct inflation of all four spheres appears to rule out any dynamic inflation problems. Such damage as occurred in two cases can be attributed to other causes.

D. Conclusions

A total of eight spheres were tested, four by the U. of M. ground test technique, and four in the altitude chamber at LMAL, and nine were weighed after storage. The number of tests were therefore not very large, but some tentative conclusions may be drawn.

1. None of the nine spheres weighed had lost weight during storage, indicating that the inflation capsules were properly constructed, and no leaks were present.

2. Eight spheres inflated properly, although two which inflated upon ejection in the altitude chamber were damaged by causes inherent in the test technique, and deflated at once. This confirms proper activation of the capsule in all tests.

3. There was no damage to any of the four spheres tested in the LMAL chamber which could be attributed to dynamic unfolding, or to the method of ejection used in the dart, although it is our opinion that the ejection charge could probably be reduced somewhat. Mechanical damage due to contact of the sphere with the staves after ejection appeared to be unlikely, although hot staves might have a melting effect.

4. All six undamaged spheres deflated at altitudes ranging from 96K ft. to 98 K ft. after remaining above 100K ft. for 20 to 40 minutes, so the spheres were properly constructed, and no leaks were present.

The above test results and conclusions appear to indicate that flight failures may be attributed principally to thermal problems. There are several possibilities:

1. The overall temperature of the inside of the staves during flight may be high enough to reduce the strength of the mylar to the point where normal overpressure at inflation can cause damage to the sphere. There is little room for additional insulation, so the best solution to this problem appears to be an ablative coating on the exterior of the dart, at least in the forward portion.

2. The metal tabs which center the staves in the mortar tube can conduct heat directly from the inside of the mortar, and may result in hot spots and local damage to the sphere. These tabs could be replaced by insulating blocks, lightly cemented to the exterior of the staves. The blocks will shear off against the forward stop ring during ejection and permit the staves to pass freely out of the muzzle. Possibly some experiments should be carried out using a reinforced plastic stave material.

3. The dart nose, which is the hottest part of the dart, remains in close proximity to the inflated sphere during at least the first part of the vacuum trajectory, and there is some probability of contact. The manner in which the staves separate can cause the sphere to move toward or away from the nose, as shown by the films of the LMAL tests. Contact with the nose could result in immediate deflation of the sphere. A light touch, or possibly even a close approach, with radiation heat transfer, might cause a small leak, so that the sphere might not deflate at once, but would do so well above the design deflation altitude. Possibly some means of positively separating

the sphere and nose can be designed, but a better solution to the problem appears to be rearward ejection. If the fins are attached directly to the mortar tube, the only ejected parts will be the boat tail, the staves, and the sphere. These are very light, so a much smaller ejection charge will be required. The boat tail may be the coolest part of the dart, so the danger of damage to the sphere by contact is reduced. The delay squib will be located ahead of the sphere and staves, moving them rearward, and slightly reducing the heat transfer to the sphere before ejection. The c. g. of the dart will be moved forward, resulting in a small increase in stability.

4. The fact that all spheres weighed showed no loss of weight during storage, and that all successfully inflated spheres deflated at the correct altitude indicates that loss of isopentane prior to ejection of the sphere is not likely. This can always be checked by installing the sphere just before the dart is launched, and weighing it before installation. Deflation of flight spheres at altitudes above the design altitude is very probably due to damage which occurs at the time of ejection. In such cases, if a useful altitude range is covered, the data reduction procedure can be corrected by making the assumption that the loss of weight occurs during descent, as the isopentane leaks out through small holes.

Appendix I

Motion Picture Film Notes

The following notes were made during a frame-by-frame study of 16 mm motion picture film taken at 400 frames per second during the LMAL tests in the 41 foot spherical altitude chamber. Cameras were located on the equator of the tank above and behind the test mortar, on the equator at 90^{o} to the right of the first, and on top of the tank.

Test #1

Camera at 0^{o}

Films of this test were too dark for projection, but yielded considerable information during a study of individual frames. A flash is visible at ejection for several frames; after this, for several more frames, sparks are seen striking and bouncing off the inflating sphere, which is itself invisible. The sphere becomes better illuminated, and a stave is visible against the surface of the sphere, inclined to the right, its center slightly above, behind, and to the right of the sphere center. This stave is seen to be in contact with the sphere as a few frames before complete inflation, the light is right to show a depression in the surface of the sphere around the stave. The depression rapidly grows smaller as the inflating sphere pushes against the stave and separates sphere and stave. A dent at one end of the corner reflector is also visible at the same time, and is still visible, about six inches across, when the sphere becomes otherwise fully inflated, about 60 frames after ejection. It remains inflated until it passes out of the visible field. The sphere is seen in the pocket of the net near the middle of the roll of film, still inflated. It is visible again near the end of the film, partly deflated.

Camera at 90°

The sphere appears fully inflated when it comes into the field of view. Nose is visible behind sphere, (to sphere's left), about half of it visible. It may be in contact with the sphere. Sphere gains on nose until nose is completely hidden. One stave visible about half a sphere diameter behind sphere. Sphere moves out of bright area, so is not visible when it hits the net. Sphere center and stave both slightly above nose. Sphere fully inflated as it lands in pocket about mid-film and rebounds. Partly deflated as it lands a second time near end of film.

Camera at top

Too dark to show details of inflation, but the sphere is visible crossing a bright area and appears to be fully inflated except for a dent visible at an end of the corner reflector. Sphere is slightly to right of center line of ejection, and is overtaking the nose. It appears to be in contact with the nose, and when it disappears from the field, its leading edge is even with the leading edge of the nose, and the trailing edge of the nose appears to be in contact with the left side of the sphere, whose center is slightly less than one radius to the right of the nose. One stave is visible above the sphere, a little behind, and very slightly less than one radius to right of nose. The other stave not clearly seen except for a few frames, when it appears at least one diameter behind and about the same distance to left. It may have struck the net at this point, as it dissappeared from sight in a bright area, and motion of the net in this area was observed afterward. In this case, it would be well below the sphere, accounting for the upward momentum of the sphere and its movement to right in spite of the action of the other stave. Both staves tend to cause forward motion of the sphere relative to the nose, as both are lagging.

Test #2

Camera at 0^{o}

When the ejection charge is initiated, the lighter mortar moves rearward very rapidly, so the sphere and staves are still in the trough when released from the mortar. Eight frames (at 1/400 second per frame) required from first detectable motion of parts until sphere is clear. No flash this time. The sphere starts to expand immediately, and by the time it has cleared the trough, thirteen frames after release, the capsule (aft) end of the sphere has expanded to about a foot in diameter. The upper stave is pushed upward and to the right. The lower stave is prevented by the trough from moving downward, which results in an upward thrust to the sphere. The unfolding sphere rises above the nose, and appears completely inflated after 54 frames, except for a small corner reflector dent. The sphere moves to left of the nose, and strikes the top of the net. One stave moves well to right, the other very slightly to left, almost straight, and either well behind or below the sphere.

Camera at 90^{o}

The sphere is already above the nose, and appears to be fully inflated as it comes into the field of view. The leading edge of the sphere is nearly above the center of the nose, so the sphere would overlap the nose if both were on the same level. The leading edge of one stave, which is rotating upward, is about even with the aft end of the nose, and may be gaining slightly on the nose, until the cable pulls the nose upward. The sphere is about 1 1/2 diameters above the nose at the center of the field, and the second stave is two diameters to rear and below. The sphere is not well illuminated as it strikes the top of the net. The nose strikes the target out of the field of view. The sphere rebounds

from net a few inches, and then drops into pocket. Nose rebounds from target after sphere is well down in the clear. At one point, the sphere catches the light just right to show a corner reflector dent. The sphere is otherwise fully inflated.

Camera at top

Approximately eight frames from first motion to release. Sphere expands to spherical shape about a foot across at capsule end before rest of sphere unfolds. It appears to remain in contact with and partially surround the nose at first, and moves to the left. One stave moves to right, with its leading edge nearly even with the trailing edge of the nose, so it is travelling at about the same speed as the nose. The other stave is well behind and very slightly to right, almost straight. The sphere is completely inflated in about 56 frames. Stave out of field before striking net.

Test #3

Camera at 0^{o}

Ten frames from first motion until staves are clear of mortar. The capsule end of the sphere expands at once, pushing one stave upward, while the sphere itself is pushed upward by the other stave and the trough. At the instant the assembly is clear of the trough, the sphere is expanding mostly to left of staves. The expanding sphere moves upward, rotating one stave forward and upward until it is hidden by the sphere. Soon one stave is visible above the sphere, one below. Both staves are moving straight in the vertical plane of the trough, while the sphere moves to the left. Two felt pads are visible behind the sphere, one black and one white. The sphere looks round at 61 frames after release, but there a few wrinkles around the pole piece until 68 frames. A corner reflector dent is visible in the top of the sphere. The upper stave disappears out of the field, the lower stave moves very slightly

to right until it hits the net well below the sphere. The sphere hits the net about five feet below the top. The sphere is still inflated as it lands in the pocket and bounces. A small elongated object the size of the capsule is visible in the net below the sphere and slightly to right for a few frames. The sphere begins to deflate as it lands the second time, and is partly deflated at the end of the film.

Camera at 90°

The sphere is inflated as it comes into the field, above the level of the nose. When the sphere is in the center of the field, one stave is one diameter above, the other is one diameter below and aft. The leading edge of the sphere is about even with the trailing edge of the nose, and nearly half a diameter above. At the edge of the field, the sphere appears to be lagging the nose slightly. The upper stave appears to be gaining on the nose, the lower stave moves aft and downward, striking the net about two and one half diameters below the sphere. The sphere remains inflated as it strikes the net and rebounds, but a small dark spot appears on or close to its surface about at the point of contact with the net. This spot appears to be elongated, and about the size of the capsule. It is visible in several frames, after which it separates from the sphere. It then becomes indistinct, and appears to fall below the sphere. After a few more frames it is no longer distinguishable. The sphere is still inflated as it lands in the pocket, about the middle of the film. Only part of the sphere is visible after this, indistinctly, but it appears wrinkled, as though partly deflated.

Camera on top

Nine frames from first motion until sphere is released. As usual, the aft end of the sphere expands to about a foot in diameter before the rest

of the sphere unfolds. The sphere appears round about 63 frames after release, about 73 frames until wrinkles are all gone from surface. Shortly before complete inflation, one stave is visible on top of sphere, causing an indentation in the surface of the sphere. The stave is slightly to right of the sphere center, with its leading edge about even with the trailing edge of the nose. The sphere overlaps the nose slightly. The indentation disappears rapidly as the sphere expands, and sphere and stave are pushed apart. When the sphere is directly below the camera, the center of the upper stave is about even with the trailing edge of the nose, so the stave is moving forward relative to the nose. The lower stave is about half a diameter aft. Both staves very slightly to right, almost in a straight line with nose and trough. The sphere is moving slowly to left. A corner reflector dent is visible about six inches across. The sphere is well to left of staves and nose as it strikes the net, out of the field. As the sphere reappears, still inflated, one stave is visible, apparently lying on the net, below and behind the sphere. Wrinkles in the net confuse the view of the staves. The sphere is not clearly visible during the last half of the film, but the surface appears wrinkled.

Test #4

Camera at 0^{o}

About nine frames from first motion until sphere/stave assembly is clear. As the capsule end of the sphere expands, both staves are pushed upward and rotated forward, with lower (forward) ends close together and upper ends separating. They are soon hidden by the expanding sphere. The sphere moves to right and downward, and soon both staves and nose are visible, nose moving in a straight line, as usual, one stave to left, one to

right and a little above. Sphere appears round after 55 frames. Sphere continues to move to right and downward, one stave stays above sphere and moves upward, other stave moves to left and slightly upward. Sphere strikes net about 10 ft. down from top of net, and 4 ft. to right of center line. One stave strikes the net two feet down and four feet to right, other strikes four feet down and five or six feet to left. Sphere only partly visible during last half of film, but appears to be fully inflated.

Camera at 90°

Sphere appears round as it comes into field. Leading edge of sphere below and slightly behind nose, both staves nearly vertical, about three feet above sphere. One stave slightly forward of nose trailing edge, other slightly aft, both rotating forward (clockwise). Sphere moves partly out of field downward as it passes center of field, staves separating, one is half a stave length aft of nose trailing edge, other about half a length forward, both about three feet above nose. Both staves at nearly same level, about eight feet above sphere center, and moving upward relative to the nose. Sphere strikes net with center at lower edge of field, staves strike net about 8 to 10 ft. above sphere. The sphere, still fully inflated, rebounds back into field, then drops into pocket out of sight.

Camera at top

Seven frames from first detectable motion until staves are clear of mortar. Aft end of sphere expands, both staves visible above sphere, nearly parallel, aft ends slightly farther apart. Sphere moves to right. Just before complete inflation, leading edge of sphere appears to be nearly even with leading edge of nose, a little more than half a radius to right, and trailing edge of nose

is almost touching left side of sphere, although sphere is probably below nose as indicated by 90° camera. One stave moves to left, other moves to right and is nearly above the sphere center. Indentation in sphere surface is visible around this stave for a few frames, as expanding sphere pushes against it. Sphere looks round after 65 frames. Sphere continues to move to right, and lags both nose and staves. One stave remaining with its leading edge about even with the trailing edge of the nose, as the stave moves to left. Other stave moves right, and appears to gain slightly on nose. Corner reflector dent about six inches across is clearly visible as sphere moves out of field of view, its center nearly a diameter to right of nose, and its leading edge a few inches aft of nose trailing edge. One stave above leading edge of sphere, with its leading edge slightly ahead of nose trailing edge. The other stave is same distance to left, and lagging by half a stave length. The sphere strikes the net out of the field of view, and comes to rest near the center of the pocket, fully inflated, and well clear of staves.

Appendix B. BALLOON SYSTEM COMPONENT IMPROVEMENT RECOMMENDATIONS (F. F. Fischbach).

I. Recommendations Applying to Viper-Dart-Robin Payloads Now in Inventory at Launch Sites

1. There are no interim recommended design changes for application to the procudtion Viper-Dart-Robin payloads now in the field. Operational changes are recommended in the inflation analysis report.

II. Recommendations Applying to Future Viper-Dart-Robin Procurements

1. The sphere and staves should be positively accelerated away from the dart with considerable velocity, preferably rearward.

2. Additional insulation should be provided in the form of ablative coating on the external surfaces of the rocket from nose to boat tail, and/or on the interior wall surrounding the staves, and/or on the stave interior.

3. The quality assurance procedures in the purchase specification should be altered to include the following:

a) Add one atmosphere air pressure test of capsule prior to filling.

b) 100% Government Inspection of:

Capsule weight after filling

Temperature cycling of capsule

Capsule weighing after storage

Capsule longitudinal position at assembly with dart

4. Several spheres should be constructed of aluminized mylar without corner reflectors, 1 meter diameter, and tested under routine operational conditions, with standard radar personnel, without tracking aids, to determine if acquisition can be made. If successful, the adoption of the aluminized mylar sphere is indicated as atmospheric data output is not believed to be degraded.

5. If acquisition tests of the sphere in 4., above, are unsuccessful, the present sphere should be reatined. In that case, the corner reflector suspension spring should be replaced by an elastic band as was originally used.

6. After packing the sphere in staves the staves should be held together by two aluminum alloy rings having inside diameter equal to the staves nominal outside diameter plus. 020, having wall thickness of about .031, and length .125. The rings should have been sanded to a standard weight, such as .67 gram. The assembly including rings should be weighed and weight recorded to an accuracy of 0.5 gram or better. Similar rings should be supplied all field personnel to permit ready reweighing as conditions dictate.

7. Drawings of the following items will be furnished as provided for in Form 1423:

a) Cross-section of rearward-sphere-ejecting dart showing ejection components. (Para. 1)

b) Acceleration actuated capsule (Para. 2)

It should be noted that the authors feel that recommendations 1 and 2 are urgent because they have been found to dramatically affect the system reliability. Recommendations 4 and 5 are desirable though less urgent. The present investigation did not prove that the dynamics of unfolding the corner reflector caused problems with sphere integrity but the limited number of tests did not permit the opposite conclusion. Further, all persons involved, manufacturers, designers, and experimenters, were polled and agreed they would prefer to eliminate the reflector and believed higher reliability would result. The present investigation did prove that manufacture, packaging, transportation, and storage of the sphere with spring-supported

corner reflectors was being accomplished without damage.

Recommendations 3 and 6 are not urgent but are believed to be desirable safeguards.

III. Recommendations Applying to Future 1 5/8" O.D. Dart Designs

1. The sphere and staves should be accelerated rearward from the dart with considerable velocity.

2. The quality assurance procedures in the purchase specification should be altered to include the following:

a) Add one atmosphere air pressure test of capsule prior to filling.

b) 100% Government Inspection of:

Capsule weight after filling

Temperature cycling of capsule

Capsule weighing after storage

3. Several spheres should be constructed of aluminized mylar without corner reflectors, 1 meter diameter, and tested under routine operational conditions, with standard radar personnel, without tracking aids, to determine if acquisition can be made. If successful, the adoption of the aluminized mylar sphere is indicated as atmospheric data output is not believed to be degraded.

4. If acquisition tests of the sphere in 4. above, are unsuccessful a tracking aid consisting of a chemical cloud should be tested. If unsuccessful, mylar chaff should be used in minimum quantity required.

5. After packing the sphere in staves the staves should be held together by two aluminum alloy rings having inside diameter equal to the staves nominal outside diameter plus .020, having wall thickness of about .031, and length .125. The rings should have been sanded to a standard weight, such as .67 gram. The assembly including rings should be weighed and weight recorded to an accuracy of 0.5 gram or better. Similar rings should be supplied all field personnel to permit reweighing as conditions dictate.

Appendix C. AN APPRAISAL OF THE 1970 PROGRAM FOR ROBIN SPHERE DATA REDUCTION (by F. F. Fischbach)

I. Introduction and Background

The task reported here is an evaluation of the 1970 Robin Sphere Data Reduction Program. Part of the reason behind the evaluation is the fact that the Robin sphere data reduction had since its inception been performed in a considerably different manner from the data reduction of the University of Michigan 66cm sphere. Since both systems utilized the same basic payloads, spheres of the same mass/area ratio, and sometimes the same radar equipment it was evident that the optimum data reduction techniques were likely not being employed in both systems. The principal investigators, Mr. Engler of the University of Dayton and Mr. Peterson of the University of Michigan, for one reason or another never actually resolved the basic differences, although communication was frequent.

At least one reason for this state of affairs was the dissimilarity between the two systems, the likenesses notwithstanding. These differences included a radically different apogee, in many cases radically different radar equipment, and somewhat different motivation: the 66 cm. system being used for certain specialized investigations where the principals were personally involved in all phases of the data process whereas the Robin system was being aimed at automatic, routine, data reduction by personnel not specially trained in the techniques.

Mr. Peterson has departed from the sphere program and is not readily available for consultation. Mr. McWatters, an associate in the 66 cm. reduction program, is also employed elsewhere but is available for consultation,

and has assisted the present investigator. The present investigator was not connnected with the development of the 66 cm. program, and it is hopedthat what he lacks in experience is compensated for by a lack of bias toward the merits of either system.

II. Scope of Evaluation

The 1970 Robin Data Reduction Program *per se* was not available to the present investigation but, curiously, this was unimportant. Evaluation was performed by study of AFCRL-70-0366 by J. K. Luers which includes the basic concepts of the program as well as the simulation studies on which their optimum filter principle was based. Some additional information was obtained from NASA SP-219 and from conversation with the Robin program personnel.

The nature of this task was primarily a study of the Robin program with the following purposes:

1. Point out actual or possible errors in the basic method.
2. Point out any features which while not erroneous, might be performed in a simpler or more accurate manner.
3. Compare the dissimilarities in the two data reduction methods to determine if they are tantamount or if one is correct and one incorrect.
4. Furnish any constructive advice for improvement of the program.

III. Results and Conclusions

A. The process of taking raw data from an FPS-16 radar and converting it to a rapid printout of density, pressure, and temperature has been accomplished with considerable mathematical precision. The possible sources of error are all considered and comprehensively treated. The method of optimizing the smoothing parameters was pursued exhaustively. No mathematical errors were found in the formulations presented, although not every equation was checked.

B. The discussion of the determination of deflation altitude contained in AFCRL-70-0366 indicates that in some cases deflation altitude may not have been determined with as great a precision as possible. It is hoped that this was not so and that, if so, the procedure has been improved.

Great precision in the determination of deflation altitude allows an accurate correction to be made for loss of sphere mass throughout the entire flight and therefore it is important that the deflation altitude be made with as great a precision as possible.

A "simple and precise" method for the determination of deflation altitude and the correction for loss of sphere mass was discussed at the Langley Sphere Symposium and is presented in the proceedings of this symposium (see pp 149-51 and figs. 5-7 of NASA-SP 219).

C. While no errors in the program were found, there are areas that may be considered for improvement. The most important of these areas is the nature and the manner of smoothing out radar noise from the position data. Most of the "optimum filter" development by Luers is a computer exercise in showing the sum of bias and noise errors at each altitude with the following parameters varied:

Apogee

Degree polynomial fit to position data

Number of points fit

Often the smoothing was done to derive velocity and then done again to derive acceleration. In these cases of "double smoothing" the degree and number of points is determined twice.

A large amount of effort was apparently expended in this exercise for according to Luers "all possible combinations of N and M" (N= no. of points in velocity fit, M in acceleration fit) were tried for each of four polynomial degree combinations, 1-1, 1-3, 3-1, 3-3. Then a second degree polynomial was tried. For second degree polynomials only one fit is required, first derivative for velocity, second for acceleration. Luers does not say all possible numbers of points were used for the fit (although this would have been easy compared to double smoothing) but he determines that 31 points (1/2 sec each) is the best smoothing interval. The optimum double smoothing technique was determined to be a linear-cubic of 19-1/2 second position points and 21-one second velocity points.

Fortunately, Luers has plotted the bias and noise errors separately. This is important because although the total expected error on a given flight may be the RMS sum of the two errors, to minimize this sum may not be most desirable in choosing smoothing parameters.

The foregoing evaluation of smoothing parameters was done at 125 km apogee. After a choice was made, the apogee was varied and found to exert relatively little influence.

The present investigator comments as follows on the smoothing interval selection:

1. An extraordinary amount of attention seems to have been placed on the degree or degrees of the smoothing polynomials.

2. Constant-time smoothing was used in all trial examples.

3. It should have been evident a priori that a constant-time smoothing parameter in any form would be too short at the low end or too long at the high end.

4. With a properly varying number of points, any low degree polynomial could have been chosen. Thus instead of varying the constant-time time ("all possible combinations of N and M") it might have been more instructive to try many variations in the N and M versus altitude with a given polynomial.

5. In any case no bias error below 70 km need be entertained. This was recognized after the computer exercise was finished and the 1-3 degree double smoothing had been chosen. It was determined that the noise error would be held to 2% by arbitrarily expanding from 19 to 51 the number of position points smoothed to get velocity. It is not necessary to maintain 2% noise error and the smoothing interval may be further expanded without incurring bias error in the last ten kilometers or so, which will be shown for the quadratic.

The previous discussion of deflation altitude indicates that this region is very important.

6. Luers does not say so, but he may be attempting to compare the smoothing selection chosen (i.e., a 19-1/2 second point linear fit for velocity, followed by a 21 one-second velocity point cubic fit for acceleration arbitrarily expanding to 51 points for velocity) for the 1970 Robin program with the type of smoothing done at University of Michigan on the 66 cm program. The latter smoothing (shown below) was based on a quadratic fit, with the second derivative calculated in one step. The number of points was selected on the basis of vertical smoothing interval in kilometers,

which in trun was originally based on computer simulations and was modified over the years. Luers makes a point on page 16, "In comparing the optimum quadratic and the optimum linear-cubic smoothing techniques, it is easily seen that the 19-21 linear cubic produced significantly better results in the 70-100 km region." He goes on to speculate about the reasons. The errors inherent in the 1970 Robin and University of Michigan 66 cm programs will be compared below. The 66 cm program quadratic with variable smoothing will be seen to fare considerably better than Luers' "optimum quadratic," which indicates little more than that smoothing interval as a function of altitude is important and polynomial degree is not.

7. A comment or two must be made here concerning radar noise simulation. From carefully reading the Luers report it seems that an arbitrary figure of σ_2=15 m, t=0.5 sec, where σ_2^2 is the variance of a normally distributed variable, was input throughout all error analyses as the noise figure of FPS-16 radar. (The method of best smoothing for radar noise will be discussed in section 9, below.) In attempting to compare results of the two methods, we find the Luers' theoretical noise error very large for a normally distributed variable with <u>independent</u> 1/2 second samples. He has plotted it correctly - it just doesn't jibe with experience in using the FPS-16. The 15 meter figure may be responsible and will be mentioned below. The noise error of most consequence that appears in using the 66 cm program is confined to regular functions of long wavelength. These are akin to Luers' vertical wind errors and will be compared in that context. This investigator has understood that radar noise error (excepting thermal noise) is apt to have very low frequency.

8. The present investigator has prepared the following for consideration:

a) A table of smoothing intervals used by both programs in terms of time interval and altitude layer. They should be comparable below 70 km. Above 70 km the Univ-Mich interval in seconds should be increased slightly, up to 30% at 100 km because it was based on a 150 km apogee. There is no change in the km values for varying apogees. (see fig. 9 and Table 11)

b) Plots of bias error for the smoothing equation: (fig. 10)

$$x = x_o + \dot{x}_o \, t + 1/2 \, \ddot{x}_o \, t^2$$

where x is any coordinate, $t = t - t_o$.

If f is the frequency of points, N is the total number of points used, equally spaced in time and centered at t_o, $N = 2M+1$

$$\ddot{x}_o = \frac{30f^2}{2N^3 - 7N + 2} \sum_{n=-M}^{n=M} \left[\frac{3n^2}{M(M+1)} - 1 \right] x_n$$

$$\dot{x}_o = \frac{12f}{N^3 - N} \sum_{n=-M}^{n=M} n x_n$$

x_o = radar raw coordinate.

The plots are for various smoothing intervals which are functions of altitude and are given in a separate figure.

c) Plots of noise error plus bias error for sinusoidal error inputs of several wavelengths and amplitudes for the same equation as b). (fig. 11)

Table 9. Smoothing Intervals

Alt. (km)	U-M Smoothing Interval (km)	Robin Smoothing Interval (km)	U-M Smoothing Interval (Sec)	Robin Smoothing Interval (Sec)
100	10	22.3	11.1	30.0
99	10		11.0	
98	10		10.9	
97	10		10.8	
96	10		10.8	
95	10	23.8	10.75	
94	10		10.7	
93	10		10.7	
92	10		10.7	
91	10		10.7	
90	10	24.0	10.8	
89	9.4		10.2	
88	9.1		10.0	
87	8.6		9.60	
86	8.3		9.47	
85	7.9	23.2	9.26	
84	7.5		9.08	
83	7.2		9.08	
82	6.9		9.01	
81	6.5		9.11	
80	6.3	19.8	9.37	
79	6.0		9.67	
78	5.7		10.0	
77	5.5		10.5	
76	5.2		10.1	
75	4.9	13.5	11.7	
74	4.7		12.5	
73	4.5		13.6	
72	4.3		14.6	
71	4.1		15.6	
70	4.0	9.0	16.3	
69	3.8		17.0	
68	3.6		17.4	
67	3.4		17.4	
66	3.3		17.75	
65	3.2	6.45	18.0	
64	3.0		17.9	30.0
63	2.9		18.5	
62	2.8		18.9	
61	2.6		18.4	
60	2.5	5.0	18.7	
59	2.4		18 8	
58	2.3		19.2	
57	2.2		19.6	
56	2.1		19.7	
55	2.0	3.75	19.8	
54			20.9	
53			22.1	32.0
52			23.1	
51			24.2	
50		2.9	25.5	
49			26.7	34.0
48			28.0	
47			29.6	
46			31.6	36.0
45		2.2	33.9	
44			36.9	
43			40.5	38.0
42			44.2	
41			48.3	40.0
40		1.6	52.7	
39			56.4	42.0
38			60.0	
37			63.7	44.0
36			67.8	
35		1.24	74.1	46.0
34			82.6	
33			92.6	
32			100.0	
31			107.5	
30		0.8	129.0	
29			168.0	

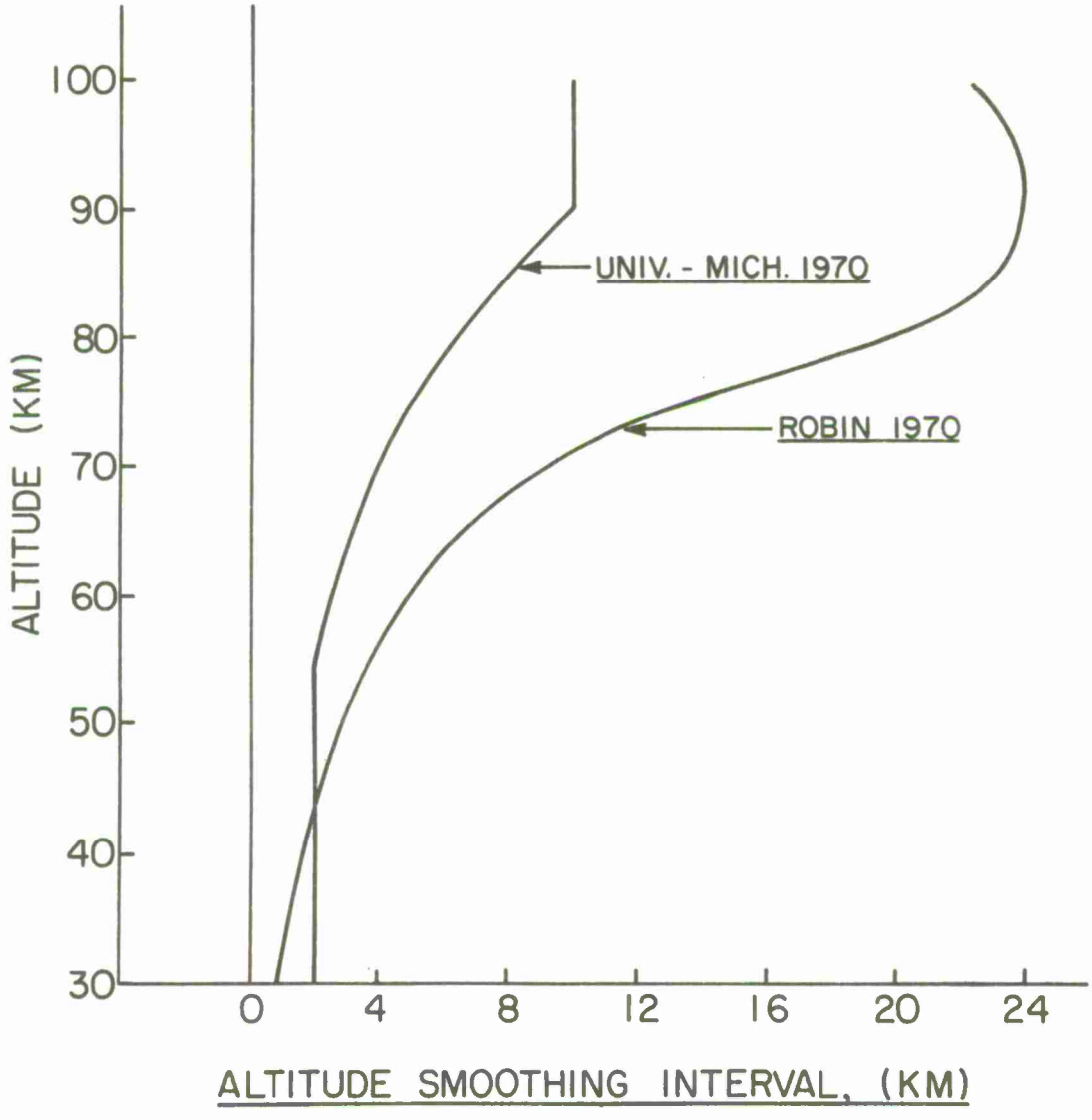

Figure 9 Altitude Smoothing Intervals used in University of Michigan and in Robin Data Analysis

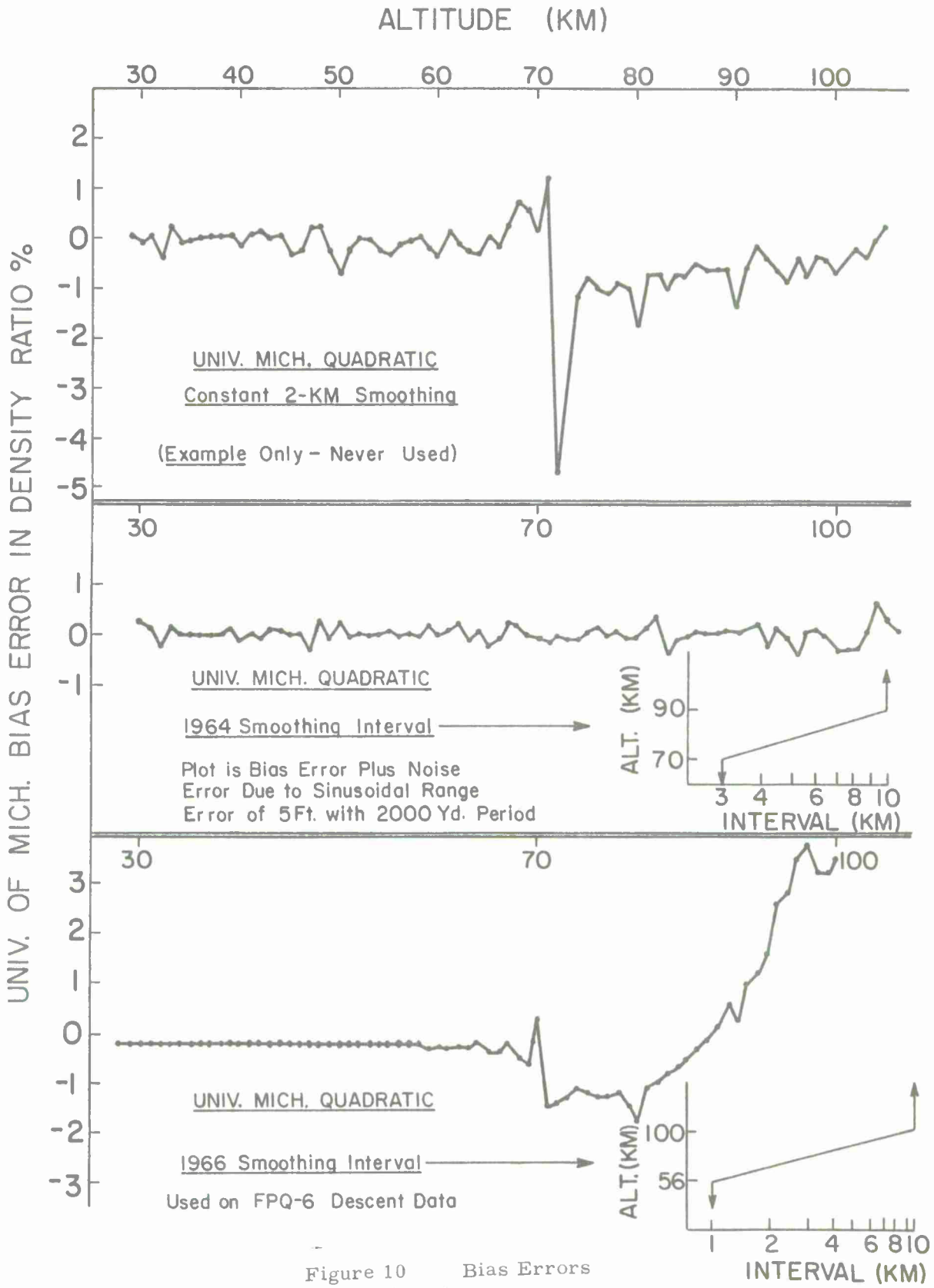

Figure 10 Bias Errors

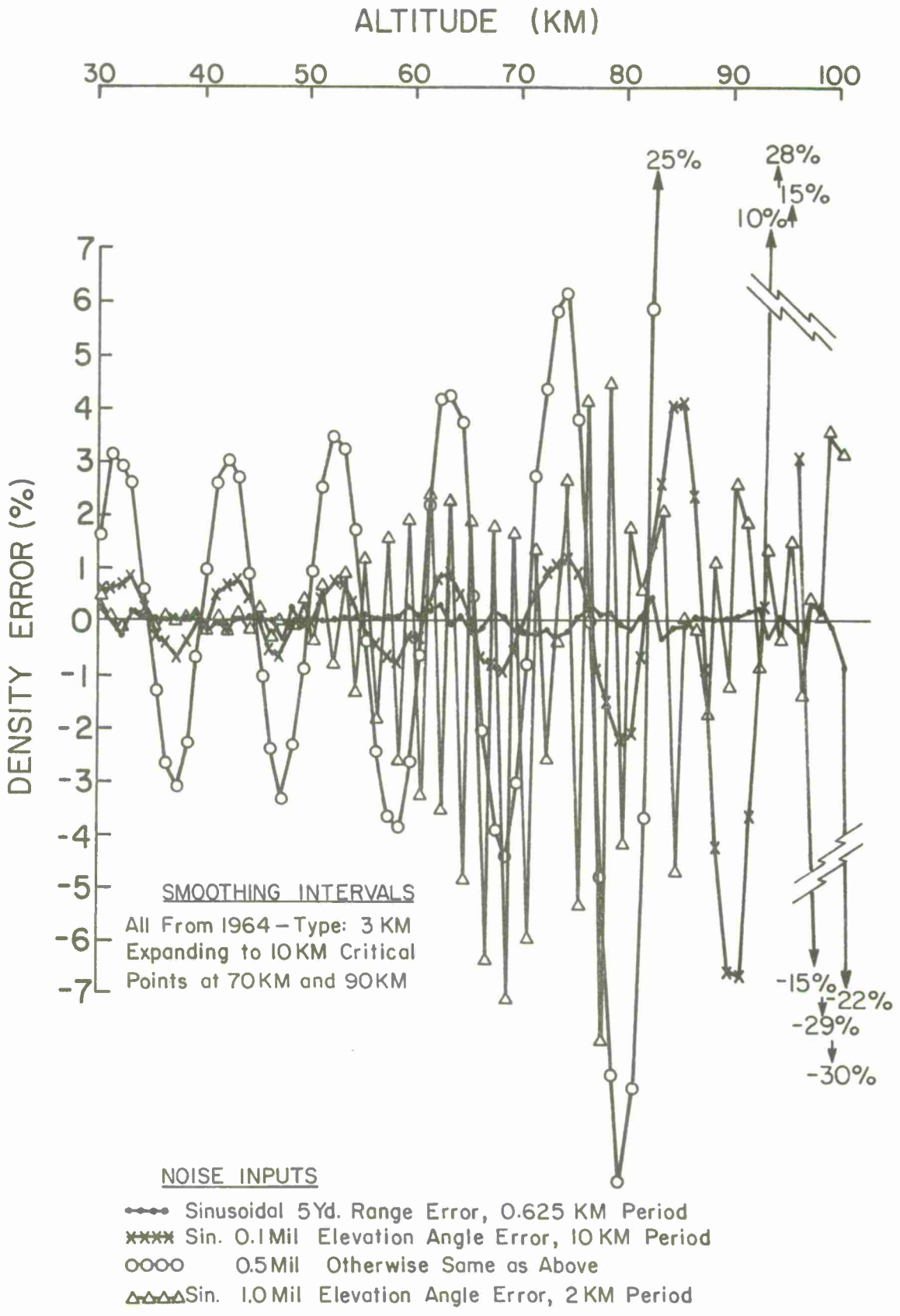

Figure 11 Noise Error plus Bias Error

9. The choice of coordinate system makes a difference in the smoothing. The 1970 Robin program uses radar raw data (range, azimuth angle, elevation angle vs. time) converted by the radar's computer to x, y, z vs. time as its input. The spherical coordinates of range, azimuth, and elevation are used in the 66 cm program so that different smoothing functions may be used for different coordinates. (In working with upleg data or with FPQ-6 and Tradex radars which have range-rate capabilities this is a large advantage.) The FPS-16 range accuracy is quoted as $\pm$ 5 yds., while angle accuracy may be deduced from such specifications as bearing accuracy, output noise error, other mechanical errors, etc. The angle accuracy cannot by specification be better than 0.2 mils (not normally distributed, either) and probably lies between 0.2 and 0.5 mils. These accuracies require S/N ratio greater than 20. It is elementary to note that if one coordinate can be measured much more accurately than the others, individual smoothing will provide the most accurate positioning. The exact amount of advantage in the FPS-16 sphere descent track cannot be easily deduced since the two operating programs vary widely in smoothing interval as well as coordinate systems.

At 100 km slant range, $\sigma_{\dot{\varepsilon},\, \alpha} \geq 20$ m. while $\sigma_r < 5$m. If spherical coordinates were utilized, the range smoothing might be reduced by one-half, and the bias error reduced at high altitudes. At high altitude the range component of $\dot{z}$ is still appreciable.

D. Conclusions

1. The deflation altitude and mass correction procedures should be made operational, if this has not already been done.

2. The program otherwise is free from major theoretical error, and the theory itself has been formulated with great energy, more than adequate detail, and exceptional care.

3. Improvement should be made by lengthening the smoothing interval at the very low end, to improve deflation determination, and perhaps the data.

4. Improvement might be gained by decreasing the smoothing interval at the very highest altitudes so to minimize bias error at the expense of noise error. Noise error is possibly overestimated, and at least susceptible to improvement, whereas bias error, once present, is a permanent degradation of data.

5. If the program is rewritten or given a major overhaul, consideration should be given to the use of spherical coordinates with separate smoothing parameters for range.

IV. References

Luers, J. K., AFCRL-70-0366, July 1970.

Bollerman, B., & R. L. Walker, AFCRL-70-0150, Jan. 1970.

Peterson, J. W., et al., Univ. Mich. Rpt. 05436-1-F, Jan. 1965.